

**IMPROVING NUTRIENT TRANSPORT SIMULATION IN SWAT BY  
DEVELOPING A REACH-SCALE WATER QUALITY MODEL**

by

**Femeena Pandara Valappil**

**A Dissertation**

*Submitted to the Faculty of Purdue University*

*In Partial Fulfillment of the Requirements for the degree of*

**Doctor of Philosophy**



Department of Agricultural & Biological Engineering

West Lafayette, Indiana

August 2019

**THE PURDUE UNIVERSITY GRADUATE SCHOOL  
STATEMENT OF COMMITTEE APPROVAL**

Dr. Indrajeet Chaubey, Chair

Department of Natural Resource and the Environment, University of Connecticut

Dr. Sara K. McMillan

Department of Agricultural and Biological Engineering

Dr. Antoine F. Aubeneau

Lyles School of Civil Engineering

Dr. Nicola Fohrer

Department of Hydrology and Water Resources Management, Christian-  
Albrechts-Universität zu Kiel

**Approved by:**

Dr. Nathan S. Mosier

Head of the Graduate Program

*To my mentors, family and friends*

## ACKNOWLEDGMENTS

I would like to thank all my teachers, family and friends for continuously motivating and supporting me throughout my academic career. I feel very fortunate to have had the opportunity to work with some great mentors during my time at Purdue University. My advisor, Dr. Indrajeet Chaubey, has played a huge role in bringing out the best in me as a researcher. Besides introducing me to several professional development opportunities, he taught me not just to think and work independently, but to always see the bigger picture of things, which I am sure will help my future career tremendously.

Many thanks to my committee members, Dr. Sara McMillan, Dr. Antoine Aubeneau and Dr. Nicola Fohrer for their reviews, encouragement and insightful suggestions. They proved to me that committee members can be as beneficial as one's own advisor in improving the quality of research. I am grateful to them and Dr. Paul Wagner for always finding time from their busy schedule to provide constructive comments on all my manuscripts. I specially thank Dr. Aubeneau and Dr. McMillan for introducing me to the world of tracer tests and in-stream modeling. Thanks are also due to Dr. Fohrer, Dr. Wagner and students/visiting scholars at Kiel University (Johannes Fischer, Oliver Tank, Jeba Princy and Cicily Kurian) for their help in carrying out my experiments. I extend my heartfelt gratitude to my Masters' advisor, Dr. K.P. Sudheer, for being the reason I started enjoying research and for identifying the potential in me to pursue PhD. I also thank my undergraduate advisor, Dr. Suja Nair, for being a great teacher and helping me choose my career in water research.

I am deeply indebted to my friends and family for serving as my emotional support system during my ups and downs in these past four years. My friends in US (Lakshmy, Aswathy, Jijo, Vishnu, KK, Anup, Rahul, Neel, Kingsly, Akhila, Sudheer) are one of the reasons this journey will have a special place in my heart. Special thanks to all my long-term friends from school and college (Sujaya, Neepa, Aadarsh, Alex, Anoop, Sruthi) for always cheering me up. I would also like to thank my colleagues (Garett, Fariborz and Sushant) and staff in ABE (Barb Davies and Becky Peer) for their personal and professional help and making my office a happy place.

Last, but certainly not the least, I am grateful to my husband (Cibin), parents, siblings and my in-laws for believing in me more than I believed in myself. Thank you to my husband for always putting up with me during my stress-filled days, for tolerating our long-distance relationship, for clearing all my modeling doubts and for being a mentor for life. Without you by my side, this PhD would not have been possible. Above all, I thank God, the almighty for His blessings and providing me strength and opportunity to successfully complete this research.

## TABLE OF CONTENTS

LIST OF TABLES .....	9
LIST OF FIGURES .....	10
ABSTRACT .....	12
1. INTRODUCTION .....	15
1.1 Overview .....	15
1.2 Research Objectives .....	18
1.3 Research Hypotheses .....	20
1.4 Thesis Organization .....	20
1.5 References .....	21
2. MERGING OTIS AND QUAL2E MODELS TO DEVELOP AN ENHANCED PHYSICALLY-BASED MODEL FOR NUTRIENT TRANSPORT IN STREAMS .....	23
2.1 Abstract .....	23
2.2 Introduction .....	23
2.3 Materials and Methods .....	26
2.3.1 Model Development .....	26
2.3.2 Study Area and Data .....	30
2.3.3 Experimental Data .....	31
2.3.4 Literature Data .....	32
2.3.5 Sensitivity Analysis .....	34
2.3.6 Model Calibration, Validation and Generalization .....	35
2.4 Results and Discussions .....	37
2.4.1 Experimental Tracer Test .....	37
2.4.2 Sensitivity Analysis .....	39
2.4.3 Model Validation for Literature Data .....	40
2.5 Summary and Conclusions .....	45
2.6 Acknowledgments .....	46
2.7 References .....	46
3. SIMPLE REGRESSION MODELS CAN ACT AS CALIBRATION-SUBSTITUTE TO APPROXIMATE TRANSIENT STORAGE PARAMETERS IN STREAMS .....	50

3.1	Abstract.....	50
3.2	Introduction.....	51
3.3	Methodology.....	55
3.3.1	The OTIS Model.....	55
3.3.2	Meta-Analysis.....	57
3.3.3	Experimental Instream Tracer Test .....	62
3.4	Results and Discussions.....	65
3.4.1	Meta-Analysis.....	65
3.4.2	Experimental Instream Tracer Test .....	68
3.5	Summary and Conclusions .....	74
3.6	Acknowledgments.....	75
3.7	References.....	76
4.	<b>AN IMPROVED PROCESS-BASED REPRESENTATION OF STREAM SOLUTE TRANSPORT IN THE SWAT MODEL.....</b>	<b>80</b>
4.1	Abstract.....	80
4.2	Introduction.....	81
4.3	Methodology.....	84
4.3.1	Study Area and Data.....	85
4.3.2	SWAT Model Calibration and Validation.....	86
4.3.3	Modified SWAT Model (Mir-SWAT) .....	88
4.4	Results and Discussions.....	94
4.4.1	Time Series Analysis .....	96
4.4.2	Reach-Scale Analysis .....	100
4.4.3	Point Source Load Scenario.....	103
4.5	Summary and Conclusions .....	104
4.6	Acknowledgments.....	106
4.7	References.....	106
5.	<b>SUMMARY, CONCLUSIONS AND RECOMMENDATIONS FOR FUTURE RESEARCH.....</b>	<b>111</b>
5.1	Research Summary .....	111
5.2	Major Research Findings .....	113

5.3	Limitations of current study and recommendations for future research .....	116
	APPENDIX A. CALIBRATED STORAGE PARAMETERS.....	119
	APPENDIX B. META-ANALYSIS PAPERS .....	121
	APPENDIX C. MODIFIED SWAT MODEL PERFORMANCE .....	130

## LIST OF TABLES

Table 2.1. Tracer test details of experimental data from Kielstau catchment (this study) and other published literature data. ....	33
Table 2.2. Typical ranges and default values for key reaction parameters in the model.....	35
Table 3.1. Reach data for tracer tests conducted in Kielstau catchment.....	64
Table 3.2. Pearson’s correlation coefficient between storage parameters and streamflow parameters. ....	66
Table 3.3. Model performance indicators for newly developed regression equations. ....	68
Table 3.4. TSM-calibrated transient storage parameters for tracer tests at Soltfeld and Freienwill .....	68
Table 4.1. Performance statistics of calibrated SWAT model for Kielstau catchment during calibration (2010-2014) and validation (2015-2016) periods.....	95

## LIST OF FIGURES

Figure 2.1. Modeling framework showing processes considered in this study. ....	29
Figure 2.2. Graphical User Interface for Enhanced OTIS Model created using MATLAB with separate sections for calibrating transient storage and reaction modules. ....	31
Figure 2.3. Study area (Kielstau Catchment in Northern Germany) with highlighted study reaches at Soltfeld and Freienwill where tracer injections were conducted. ....	32
Figure 2.4. Observed and modeled breakthrough curves for Kielstau phosphate tracer tests conducted at (a) Soltfeld and (b) Freienwill. ....	37
Figure 2.5. PO <sub>4</sub> -P concentration in main channel and change in PO <sub>4</sub> -P concentration in main channel and storage zone as simulated by new model for Freienwill data. ....	39
Figure 2.6. Sensitivity analysis plots for Freienwill test data, showing change in phosphate uptake rate with changing values of $\alpha_0$ , $\alpha_P$ and [A].....	40
Figure 2.7. Calculation of uptake rates from observed and modeled nutrient concentrations.....	43
Figure 2.8. (a) Scatter plot showing close match between modeled and measured uptake rates for different parameters from the whole data set (experiment and literature). (b) Box plot showing the range of uptake rates grouped into different studies .....	44
Figure 3.1. Conceptual representation of OTIS model showing main channel and transient storage zone processes (Runkel and Broshears, 1991). ....	56
Figure 3.2. Frequency distribution of discharge, velocity, width and depth values used in regression analysis on a log scale. ....	58
Figure 3.3. Ratio of storage zone area and stream cross-sectional area versus friction factor for tracer tests done on US reaches (Harvey and Wagner, 2000).....	61
Figure 3.4. Frequency distribution of $\log(\alpha)$ values for all meta-analysis data (n=517) shows an approximate normal distribution with a mean value of $\alpha=2.5 \times 10^{-4} \text{ s}^{-1}$ .....	61
Figure 3.5. Study area (Kielstau Catchment in Northern Germany) with highlighted study reaches at Soltfeld and Freienwill.....	63
Figure 3.6. Soltfeld (left) and Freienwill (right) streams showing meandering patterns and transient storage potential with deposited logs and vegetation.....	63
Figure 3.7. Transient storage parameters ( $A_s$ , $D$ and $\alpha$ ) calculated from new regression equations versus measured/calibrated values for the entire calibration and validation data from meta-analysis.....	67
Figure 3.8. Comparison of storage parameters obtained using different equations when compared with calibrated values. ....	70

Figure 3.9. Observed and modelled breakthrough curves for few tracer tests conducted by Hall et al. (2002) at Hubbard Brook Experimental Forest.....	73
Figure 3.10. Observed and modeled breakthrough curves for Kielstau tracer tests conducted at (a) Soltfeld and (b) Freienwill.....	74
Figure 4.1. Study area: Kielstau Catchment in Northern Germany with highlighted study reaches at Soltfeld and Freienwill where tracer injections were conducted. ....	86
Figure 4.2. Flowchart showing the Mir-SWAT model framework and modified routing algorithms .....	92
Figure 4.3. Simulated and observed time series data for (a) streamflow , (b) sediment, (c) nitrate and (d) phosphate at Soltfeld station (watershed outlet).....	95
Figure 4.4. Dissolved oxygen concentrations at the watershed outlet with SWAT and Mir-SWAT models along with discrete measured values during 2015-2016. ....	97
Figure 4.5. PO <sub>4</sub> -P concentrations at the watershed outlet with SWAT and Mir-SWAT models along with discrete measured values, enlarged to show the results during two storm events in 2015 and 2016.....	98
Figure 4.6. Average and maximum concentrations of Chl- <i>a</i> at the watershed outlet with SWAT and Mir-SWAT models for different months during 2015-2016.....	100
Figure 4.7. Algae, nitrate and phosphate concentrations (a) at the end of the stream reach within subbasin 1 over the 24-hour time period and (b) along the reach at the end of the day, on 01/30/2013 using Mir-SWAT model. ....	102
Figure 4.8. Dissolved Oxygen (bars) and PO <sub>4</sub> -P concentrations in the reach for days 28 to 31 of January 2013 using SWAT and Mir-SWAT models. ....	103
Figure 4.9. Concentration versus time plot for reach within subbasin 1 when a hypothetical point source load of 5 mg/L nitrate was discharge at the beginning of the reach for 2 hours. ....	104

## ABSTRACT

Author: Pandara Valappil, Femeena. PhD

Institution: Purdue University

Degree Received: August 2019

Title: Improving Nutrient Transport Simulation In SWAT By Developing A Reach-Scale Water Quality Model

Committee Chair: Indrajeet Chaubey

Ecohydrological models are extensively used to evaluate land use, land management and climate change impacts on hydrology and in-stream water quality conditions. The scale at which these models operate influences the complexity of processes incorporated within the models. For instance, a large scale hydrological model such as Soil and Water Assessment Tool (SWAT) that runs on a daily scale may ignore the sub-daily scale in-stream processes. The key processes affecting in-stream solute transport such as advection, dispersion and transient storage (dead zone) exchange can have considerable effect on the predicted stream solute concentrations, especially for localized studies. To represent realistic field conditions, it is therefore required to modify the in-stream water quality algorithms of SWAT by including these additional processes. Existing reach-scale solute transport models like OTIS (One-dimensional Transport with Inflow and Storage) considers these processes but excludes the actual biochemical reactions occurring in the stream and models nutrient uptake using an empirical first-order decay equation. Alternatively, comprehensive stream water quality models like QUAL2E (The Enhanced Stream Water Quality Model) incorporates actual biochemical reactions but neglects the transient storage exchange component which is crucial in predicting the peak and timing of solute concentrations. In this study, these two popular models (OTIS and QUAL2E) are merged to integrate all essential solute transport processes into a single in-stream water quality model known as 'Enhanced OTIS model'. A generalized model with an improved graphical user interface was developed on MATLAB

platform that performed reasonably well for both experimental data and previously published data ( $R^2=0.76$ ). To incorporate this model into large-scale hydrological models, it was necessary to find an alternative to estimate transient storage parameters, which are otherwise derived through calibration using experimental tracer tests. Through a meta-analysis approach, simple regression models were therefore developed for dispersion coefficient ( $D$ ), storage zone area ( $A_s$ ) and storage exchange coefficient ( $\alpha$ ) by relating them to easily obtainable hydraulic characteristics such as discharge, velocity, flow width and flow depth. For experimental data from two study sites, breakthrough curves and storage potential of conservative tracers were predicted with good accuracy ( $R^2>0.5$ ) by using the new regression equations. These equations were hence recommended as a tool for obtaining preliminary and approximate estimates of  $D$ ,  $A_s$  and  $\alpha$  when reach-specific calibration is unfeasible.

The existing water quality module in SWAT was replaced with the newly developed 'Enhanced OTIS model' along with the regression equations for storage parameters. Water quality predictions using the modified SWAT model (Mir-SWAT) for a study catchment in Germany showed that the improvements in process representation yields better results for dissolved oxygen (DO), phosphate and Chlorophyll-a. While the existing model simulated extreme low values of DO, Mir-SWAT improved these values with a 0.11 increase in  $R^2$  value between modeled and measured values. No major improvement was observed for nitrate loads but modeled phosphate peak loads were reduced to be much closer to measured values with Mir-SWAT model. A qualitative analysis on Chl-a concentrations also indicated that average and maximum monthly Chl-a values were better predicted with Mir-SWAT when compared to SWAT model, especially for winter months. The newly developed in-stream water quality model is expected to act as a stand alone model or

coupled with larger models to improve the representation of solute transport processes and nutrient uptake in these models. The improvements made to SWAT model will increase the model confidence and widen its extent of applicability to short-term and localized studies that require understanding of fine-scale solute transport dynamics.

# 1. INTRODUCTION

## 1.1 Overview

Impairments of water bodies caused by natural and anthropogenic factors are known to negatively impact the normal functioning of stream ecosystems. Pollutants originating from point and non-point sources continue to raise environmental and health concerns for both humans and aquatic life (USEPA, 2003). Within a stream reach, these pollutants in the form of chemicals and nutrients are carried forward simultaneously undergoing a range of biogeochemical processes. Managing stream water quality and ecosystem health requires understanding of biogeochemical processes affecting fate and transport of pollutants. Water quality models are useful tools often deployed to predict the extent and timing of water pollution. These models may operate at different spatial scales ranging from single reach-scales to large watershed scales, and vary in complexity ranging from simple regression models such as Spatially Referenced Regressions On Watershed attributes or SPARROW (Alexander et al., 2002) to complex mechanistic models such as Soil and Water Assessment Tool or SWAT (Arnold et al., 1998; Shrestha et al., 2008).

Ideally, there are four key processes influencing fate and transport of any water quality constituent- (1) advection, (2) dispersion, (3) transformations or reactions with other constituents, and (4) exchange with transient storage or the slow moving zones in the stream. Most of the existing models typically use only some of these processes to simulate solute transport. For instance, the widely popular solute transport model– One-dimensional Transport with Inflow and Storage model or OTIS (Runkel, 1998; Bencala and Walters, 1983) – is used to model reactive and non-reactive solute transport in individual stream reaches based on advection, dispersion, transient storage exchange and a simple first-order decay based reaction. Another model known as The Enhanced

Stream Water Quality Model or QUAL2E (Brown and Barnwell, 1987; Chapra et al., 2008) is commonly used as a water quality planning tool to simulate various water quality variables. QUAL2E is based on a one-dimensional advection-dispersion equation and includes numerous biochemical reactions involving nitrogen, phosphorus, sediment and algae, but neglects the strong influence of transient storage component which is especially crucial in studying unsteady pollutant input (Marsalek et al., 2003). The modeling framework and processes used in the existing water quality models is largely based on the context in which these models are typically used. While OTIS is primarily used for reach-scale studies in combination with experimental data, QUAL2E is mainly used for modeling long-term effect of conventional pollutants such as continuous waste loads in the form of industrial effluents. In order to accurately represent solute transport in streams and to use a single water quality model in different scenarios, it is therefore necessary to have a universal and comprehensive process-based model that includes all the key in-stream processes affecting stream solute transport.

One major drawback of using solute transport models in data scarce regions is the large number of model parameters that require calibration in order to be used for any given stream. Tracer studies are generally found effective in parameterizing and calibrating these models (Martin and McCutcheon, 1999). Continuous monitoring of conservative and non-conservative tracers along a stream reach can provide useful data to calibrate parameters that affect nutrient transport in streams. Whereas conservative tracer studies are mostly helpful in determining transient storage parameters, non-conservative tracers are mainly used to estimate biotic and abiotic nutrient uptake rates (Tank et al., 2008; O'Connor et al., 2010). OTIS, for example, relies on experimental tracer tests to calibrate model parameters affecting dispersion and transient storage exchange. QUAL2E model

either requires measured water quality data or precise knowledge of various reaction parameters to be able to effectively model in-stream nutrient dynamics. Since these model parameters are representative of a given reach, the calibrated parameters values may not be applicable to a different reach or even the same reach under different ecohydrologic conditions (Kelleher et al., 2013). When using such models for large-scale watershed level studies involving multiple streams with varying biophysical conditions, extensive field experiments and stream-specific calibration may be required, thereby increasing the cost and computational time associated with such studies. Alternate simple methods to estimate parameters in the water quality model would be beneficial in addressing these issues. Hence, research efforts are needed to develop a generalized water quality model that needs minimum or no calibration, and capable of making reliable water quality predications under varying biophysical stream conditions.

Watershed scale models often do not include a detailed fine-scale stream solute transport routine. For example, although SWAT has been successfully setup and calibrated for numerous watersheds around the world, effective calibration of water quality variables is challenging in SWAT, owing to limited data availability, input uncertainty or inaccurate representation of nutrient transport processes (Gassman et al., 2007). Additionally, researchers have reported that refining in-stream water quality algorithm in SWAT is essential for improved simulation of pollutant transport (Migliaccio et al., 2007). SWAT uses equations from QUAL2E for simulating the biochemical processes pertaining to water quality in stream reaches. However, a modified version of QUAL2E is implemented in SWAT at a daily scale without accounting for advection, dispersion and transient storage exchange. Hence, there is a need to improve the physical representation of solute transport in SWAT by including equations related to these in-stream processes. Additionally, by

incorporating the finite-difference solution approach used in OTIS and QUAL2E models, these processes can be represented at a finer time and distance-scale in SWAT model which is essential to capture the hydrochemical behavior of stream solutes (Kirchner et al., 2004). An improved and more generalized water quality model developed by using knowledge from existing models can therefore act as a stand-alone model or be further coupled to watershed scale models like SWAT to better represent stream solute transport and to enhance water quality predictions.

## **1.2 Research Objectives**

The overall goal of this study is to develop a reach-scale water quality model based on physical and biochemical stream processes and to incorporate the model into Soil and Water Assessment Tool (SWAT) for improved prediction of water quality variables. We aim to combine knowledge from two existing solute transport and water quality models to develop an enhanced model, and to further generalize the model parameters to be used in large-scale studies. Following are the specific objectives of this study:

Objective 1: Develop a reach-scale water quality model based on in-stream physical and biochemical processes and validate the model using experiment data collected from tracer studies

Tasks in Objective 1 were (1) to combine the advection-dispersion-transient storage processes used in OTIS (solute transport model) and reaction processes used in QUAL2E (water quality model) to develop an enhanced solute transport model, (2) to calibrate and validate the new model using both experimental and literature data and to assess its performance as a predictive tool without

calibration, and (3) to build an improved user interface for running the enhanced model and to provide users with better data visualization and modeling options.

Objective 2: Generalize the in-stream model by expressing transient storage parameters as a function of easily available stream parameters

Tasks in Objective 2 were (1) to develop regression equations for three transient storage parameters using readily available stream characteristics based on a meta-analysis approach, (2) to test their effectiveness in predicting parameter values and modeling solute breakthrough curves, and (3) to determine the accuracy and sensitivity of the parameter values based on expected ranges in stream characteristics.

Objective 3: Incorporate the developed water quality model into SWAT and evaluate the model performance

Tasks in Objective 3 were (1) to modify in-stream water quality algorithms in SWAT model by incorporating the newly developed solute transport model into the source code and (2) to run and evaluate the performance of modified SWAT model in predicting water quality conditions of the study catchment.

### **1.3 Research Hypotheses**

The specific hypotheses guiding this research are:

1. Simple regression equations relating transient storage parameters and easily available stream parameters can be reasonably used to approximate transient storage parameters in streams.
2. Inclusion of stream processes such as advection, dispersion and transient storage exchange processes at finer scales can enhance the prediction of water quality variables in SWAT by improving the representation of in-stream solute transport dynamics.

### **1.4 Thesis Organization**

The dissertation contains five chapters. Chapter 1: Introduction, provides an overview of issues caused by water pollution in streams/rivers and the need for an enhanced solute transport model to study fate and transport of in-stream pollutants. This chapter further discusses about some existing water quality models and research gaps in the field of water quality modelling, and finally focusses on the objectives of this study and accompanying hypotheses. Chapters 2-4 are written in journal manuscript format and focus on the three research objectives, respectively. These chapters are reformatted from the journal articles that are either accepted, submitted for review or in preparation for submission in various journals. Chapter 2 covers objective 1 and primarily discusses the modeling framework of our new solute transport model, along with calibration and validation results based on experimental and literature data. Chapter 3 focuses on objective 2 and proposes three new regression equations that can be used to estimate stream transient storage parameters. This chapter is based on the paper ‘*Simple regression models can act as calibration-substitute to approximate transient storage parameters in streams*’, published in *Advances in Water Resources Journal* (DOI: 10.1016/j.advwatres.2018.11.010). Chapter 4 discusses the application of the newly

developed model into SWAT hydrological model and its ability to predict long-term water quality conditions in a study catchment in Germany. Chapter 5: Summary and Conclusions, provides an overview of the key findings of the work along with its limitations and scope for future studies.

## 1.5 References

- Alexander, R. B., A.H. Elliott, U. Shankar, G.B. McBride. (2002). Estimating the source and transport of nutrients in the Waikato River Basin, New Zealand. *Water Resources Research*, 38 (2002), pp. 1268-1290
- Arnold, J.G., R. Srinivasan, R.S. Muttiah, J.R. Williams. (1998). Large area hydrologic modeling and assessment. Part I: Model development. *J. Am. Water Resour. Assoc.*, 34 (1), pp. 73-89.
- Bencala, K.E. and R.A. Walters. (1983). Simulation of solute transport in a mountain pool-and-riffle stream: A transient storage model: *Water Resources Research*, v. 19, no. 3, p. 718-724.
- Brown, L. C. and T. O. Barnwell, Jr. (1987). The enhanced stream water quality models QUAL2E and QUAL2E-UNCAS: Documentation and User Manual. Tufts University and US EPA, Athens, Georgia.
- Chapra, S.C., Pelletier, G.J. and Tao, H. 2008. QUAL2K: A Modeling Framework for Simulating River and Stream Water Quality, Version 2.11: Documentation and Users Manual.
- Gassman, P.W., M. R. Reyes, C. H. Green, and J. G. Arnold (2007). The Soil and Water Assessment Tool: Historical development, applications, and future research directions. *Transactions of the American Society of Agricultural and Biological Engineers*. 50(4), 1211-1250.
- Kelleher, C., T. Wagener, B. McGlynn, A. S. Ward, M. N. Gooseff, and R. A. Payn (2013). Identifiability of transient storage model parameters along a mountain stream, *Water Resour. Res.*, 49, 5290–5306, doi:10.1002/wrcr.20413.
- Kirchner, J. W., X. H. Feng, C. Neal, A. J. Robson (2004). The fine structure of water-quality dynamics: the (high-frequency) wave of the future. *Hydrological Processes* 18: 1353–1359.
- Marsalek J., Sztruhar D., Giulianelli M., Urbonas B. (2003). Enhancing Urban Environment by Environmental Upgrading and Restoration. *Nato Science Series: IV: Earth and Environmental Sciences*, vol 43. Springer, Dordrecht
- Martin, J.L. and S. McCutcheon (1999) *Hydrodynamics and Transport for Water Quality Modeling*. CRC Press, Inc., Florida.

- Migliaccio, K.W., I. Chaubey, and B.E. Haggard (2007). Evaluation of landscape and instream modeling to predict watershed nutrient yields. *Environ. Model. Softw.* 22:987–999. doi:10.1016/j.envsoft.2006.06.010
- Neitsch, S. L., J.G. Arnold, J.R. Kiniry, J.R. Williams (2005). *Soil and Water Assessment Tool Theoretical Documentation, Version 2005*, Springer, Berlin.
- O'Connor, B. L., M. Hondzo, and J. W. Harvey (2010), Predictive modeling of transient storage and nutrient uptake: Implications for stream restoration, *J. Hydraul. Eng.*, 136(12), 1018–1032
- Runkel, R.L. (1998), *One-Dimensional Transport with Inflow and Storage (OTIS): A Solute Transport Model for Streams and Rivers*: U.S. Geological Survey Water-Resources Investigations Report 98-4018, 73 p.
- Shrestha, S., F. Kazama & L. T. H. Newham. (2008). A framework for estimating pollutant export coefficients from long-term in-stream water quality monitoring data. *Environmental Modelling and Software* 23:182-194.
- Tank, J. L., E. J. Rosi-Marshall, M. A. Baker, and R. O. Hall (2008), Are rivers just big streams?: A method to quantify nitrogen demand in a large river, *Ecology*, 89(10), 2935 – 2945.
- U.S. Environmental Protection Agency. (2003). *National Management Measures for the Control of Non-point Pollution from Agriculture EPA-841-B-03–004* US Environmental Protection Agency, Office of Water, Washington, DC pp. 2–8

## **2. MERGING OTIS AND QUAL2E MODELS TO DEVELOP AN ENHANCED PHYSICALLY-BASED MODEL FOR NUTRIENT TRANSPORT IN STREAMS**

### **2.1 Abstract**

Growing need to address water pollution demands advanced tools that can predict fate and transport of water quality constituents. Existing stream solute transport models use simple first-order kinetics to evaluate N and P loss, which ignore biochemical reactions and interactions. This study aims to integrate the One-dimensional Transport with Inflow and Storage (OTIS) model and The Enhanced Stream Water Quality Model (QUAL2E) to develop a physically-based solute transport model. By using background algal concentration as the only calibration parameter, a generalized model was attained with  $R^2=0.97$  in more than 70% test cases evaluated in this study. The new model performed fairly well in predicting nutrient uptake for this study's experimental data and for several other published data ( $R^2=0.76$ ,  $NSE=0.47$  and  $\text{Percent Bias}=-4.3\%$ ). Inclusion of actual biochemical reactions from QUAL2E is expected to give extra confidence and opportunity for incorporating more realistic data which is unfeasible in existing first-order decay-based models.

### **2.2 Introduction**

Streams and rivers are complex ecohydrological systems under persistent human pressure (Carpenter et al., 1998; Johnson et al., 1997). Societies need clean water for their activities but use waterways to dispose of their waste, a costly dilemma requiring expensive engineering solutions. Solute transport models are frequently used to simulate transport of reactive and non-reactive solutes in streams, predicting the extent and timing of contaminant spills for example, or the export of pollutants during extreme events (Mueller Price et al., 2014; Ani et al., 2009). In these models,

advection, dispersion and reactions are the basic processes considered. Another key mechanism in stream solute transport is transient storage, when water is held back in slow moving areas of a stream, called transient storage zones, which can include pools, hyporheic flows, boundary layers, vegetation etc. (Runkel and Broshears, 1991). Transient storage models (TSM) quantify conservative and reactive solute transport with a one-dimensional advection-dispersion-reaction equation to route water and solutes downstream and capacity coefficients to store water in one or more transient storage zones, each characterized by a specific residence time distribution and biogeochemical activity. (Bencala and Walters, 1983; Stream Solute Workshop, 1990; Ward et al., 2017; Harvey et al., 1996).

The One-dimensional Transport with Inflow and Storage model (OTIS, Runkel, 1998) is one of the most commonly used implementations of TSMs (Bencala and Walters, 1983; Sheibley et al., 2014; Mueller Price et al., 2016). Originally OTIS was developed for small mountain streams, but it has been widely used in streams with small to moderate width and depth where one-dimensional transport can be assumed (Fischer et al., 1979). In OTIS, conservative solutes move by advection and dispersion and exchange with a single transient storage zone, while reactive solutes decay according to a first order reaction rate assigned to each domain. OTIS is primarily used in conjunction with field-scale tracer experiments where conservative or reactive tracers are injected into a given stream reach to monitor tracer concentrations over time. OTIS parameters are calibrated by fitting observed and simulated tracer concentration data and nutrient transport in streams is thus represented by two calibrated decay parameters. Therefore, some of the limitations of using OTIS are: (1) the need for calibration when field data is scarce, and (2) the empirical nature of first-order decay equations.

Watershed-scale models often do not include a detailed stream solute transport module owing to the large scale of simulation. For instance, studies have suggested the need for refining and improving nutrient transport representation in one of the most widely used watershed models- the Soil and Water Assessment Tool (SWAT) (Gassman et al., 2007; Femeena et al., 2018). In the context of large watershed-scale studies, it becomes challenging to use OTIS where uptake parameters should be calibrated separately for each stream reach. Another limitation is the use of first-order rate kinetics (Potter et al., 2010; O'Connor et al., 2010). The degree of nutrient limitation affects nutrient uptake in streams (Tank et al., 2017). The relationship between uptake and limiting nutrient concentration is frequently described by Michaelis-Menten asymptotic equation. O'Brien et al. (2007) emphasized the link between decreasing biological nitrogen uptake with increasing  $\text{NO}_3$  concentration. Subsequent studies also supported this concept by identifying a partial saturation effect in nutrient uptake (Mulholland et al., 2008, 2009; Hall et al., 2009). However, some studies also reported discrepancies, like Bernot et al. (2006) which showed that biological uptake of nitrate was saturated at higher concentrations, whereas ammonium and phosphorus uptake increased with higher concentrations. Nutrient uptake dynamics are complex and change in space and time, and it is inappropriate to assume a single first-order uptake rate can universally simulate nutrient transport. Hence, a comprehensive, process-based model that simulates nutrient uptake in streams should be preferred.

Stream water quality models such as The Enhanced Stream Water Quality Models-QUAL2E/QUAL2K (Brown and Barnwell, 1987; Chapra et al., 2008) and Water Quality Analysis Simulation Program-WASP (Di Toro et al., 1983; Connolly and Winfield, 1984; Ambrose, R.B. et al., 1988) are examples of process-based models that consider biochemical reactions in addition

to the advection-dispersion equations for transport. However, these models neglect the strong influence that transient storage can have on pollutant dynamics (Marsalek et al., 2003) and are used as water quality planning and management tools rather than solute transport models. An ideal nutrient/solute transport model should represent all four key processes: advection, dispersion, transient storage and in-stream biogeochemistry. To address this gap, we combined the advection-dispersion-transient storage processes used in OTIS (solute transport model) and reaction processes used in QUAL2E (water quality model) to develop an enhanced solute transport model. We calibrated and validated our new model using both experimental and literature data and assessed its performance as a predictive tool without calibration. As part of the study, an improved user interface for running OTIS and ‘Enhanced OTIS’ model has been built to provide users with better data visualization and modeling options.

## **2.3 Materials and Methods**

### **2.3.1 Model Development**

The proposed solute transport model was created in MATLAB<sup>TM</sup> by combining the algorithms of OTIS and QUAL2E. The OTIS model (Bencala and Walters, 1983) uses a finite-difference approach to calculate solute concentration at different times along the stream length. Advection, dispersion, transient storage and decay processes are modeled in OTIS using equations 2.1 and 2.2 below. The lateral flow component of OTIS is ignored in this study and therefore we recommend this model for stream reaches where negligible lateral inflow/outflow is observed. The five major calibration parameters in the OTIS model include dispersion coefficient ( $D$ ), stream cross-sectional area ( $A$ ), storage zone area ( $A_s$ ), storage exchange coefficient ( $\alpha$ ) and first-order decay parameters in main channel and storage zone ( $\lambda$ ,  $\lambda_s$ ).

$$\frac{\partial C}{\partial t} = D \frac{\partial^2 C}{\partial x^2} - u \frac{\partial C}{\partial x} + \alpha(C_s - C) - \lambda C \quad (2.1)$$

$$\frac{\partial C_s}{\partial t} = -\alpha \frac{A}{A_s} (C_s - C) - \lambda_s C_s \quad (2.2)$$

where  $A$  = stream channel cross-sectional area [ $m^2$ ],  $A_s$  = storage zone cross-sectional area [ $m^2$ ],  $C$  = in-stream solute concentration [ $mass/m^3$ ],  $C_s$  = storage zone solute concentration [ $mass/m^3$ ],  $D$  = dispersion coefficient [ $m^2/s$ ],  $Q$  = volumetric flowrate [ $m^3/s$ ],  $u$  = average flow velocity (m/s),  $\alpha$  = storage zone exchange coefficient [ $s^{-1}$ ],  $\lambda$  = main channel decay coefficient [ $s^{-1}$ ],  $\lambda_s$  = storage zone decay coefficient [ $s^{-1}$ ]

The QUAL2E Model (Brown and Barnwell, 1987) is a steady-state model that simulates up to 15 water quality parameters in branching streams and well-mixed lakes. It uses a finite-difference solution of advective-dispersive mass transport and reaction equations to compute steady state water profiles. The major water quality parameters simulated in QUAL2E include dissolved oxygen, algae, nitrogen (as organic N,  $NO_3^-$ ,  $NO_2^-$  and  $NH_4^+$ ) and phosphorus (as organic and inorganic P). Algal growth is the key process affecting nutrient transport in QUAL2E, which is further influenced by growth limiting factors such as light, nitrogen and phosphorus. Algal biomass concentration in the model is expressed in terms of Chlorophyll-*a* concentration using a simple relationship (equation 2.3). Major equations affecting nitrate and phosphate uptake by algae are given in equations 2.4 and 2.5 (see Brown and Barnwell (1987) for the complete set of equations and parameters).

$$Chl\ a = \alpha_0 A \quad (2.3)$$

$$\frac{dN_3}{dt} = \beta_2 N_2 - (1 - F)\alpha_1 \mu A \quad (2.4)$$

$$\frac{dP_2}{dt} = \beta_4 P_1 + \sigma_2/d - \alpha_2 \mu A \quad (2.5)$$

where  $Chl\ a$  = Chlorophyll-a concentration ( $\mu\text{g-Chla/L}$ ),  $\alpha_0$  = a conversion factor ( $\mu\text{g-Chla/mg-A}$ ),  $A$  = algal concentration ( $\text{mg-A/L}$ ),  $N_3$  = concentration of nitrate nitrogen ( $\text{mg-N/L}$ ),  $\beta_2$  = rate constant for oxidation of nitrite nitrogen ( $\text{day}^{-1}$ ),  $N_2$  = concentration of nitrite nitrogen ( $\text{mg-N/L}$ ),  $F$  = fraction of algal nitrogen taken from ammonia pool,  $\alpha_1$  = fraction of algal biomass that is nitrogen ( $\text{mg-N/mg-A}$ ),  $\mu$  = local specific growth rate of algae ( $\text{day}^{-1}$ ),  $P_2$  = concentration of dissolved phosphorus ( $\text{mg-P/L}$ ),  $\beta_4$  = organic phosphorus decay rate ( $\text{day}^{-1}$ ),  $P_1$  = concentration of organic phosphorus ( $\text{mg-P/L}$ ),  $\sigma_2$  = benthos source rate of dissolved phosphorus ( $\text{day}^{-1}$ ),  $d$  = mean stream depth (ft) and  $\alpha_2$  = fraction of algal biomass that is phosphorus ( $\text{mg-P/mg-A}$ ).

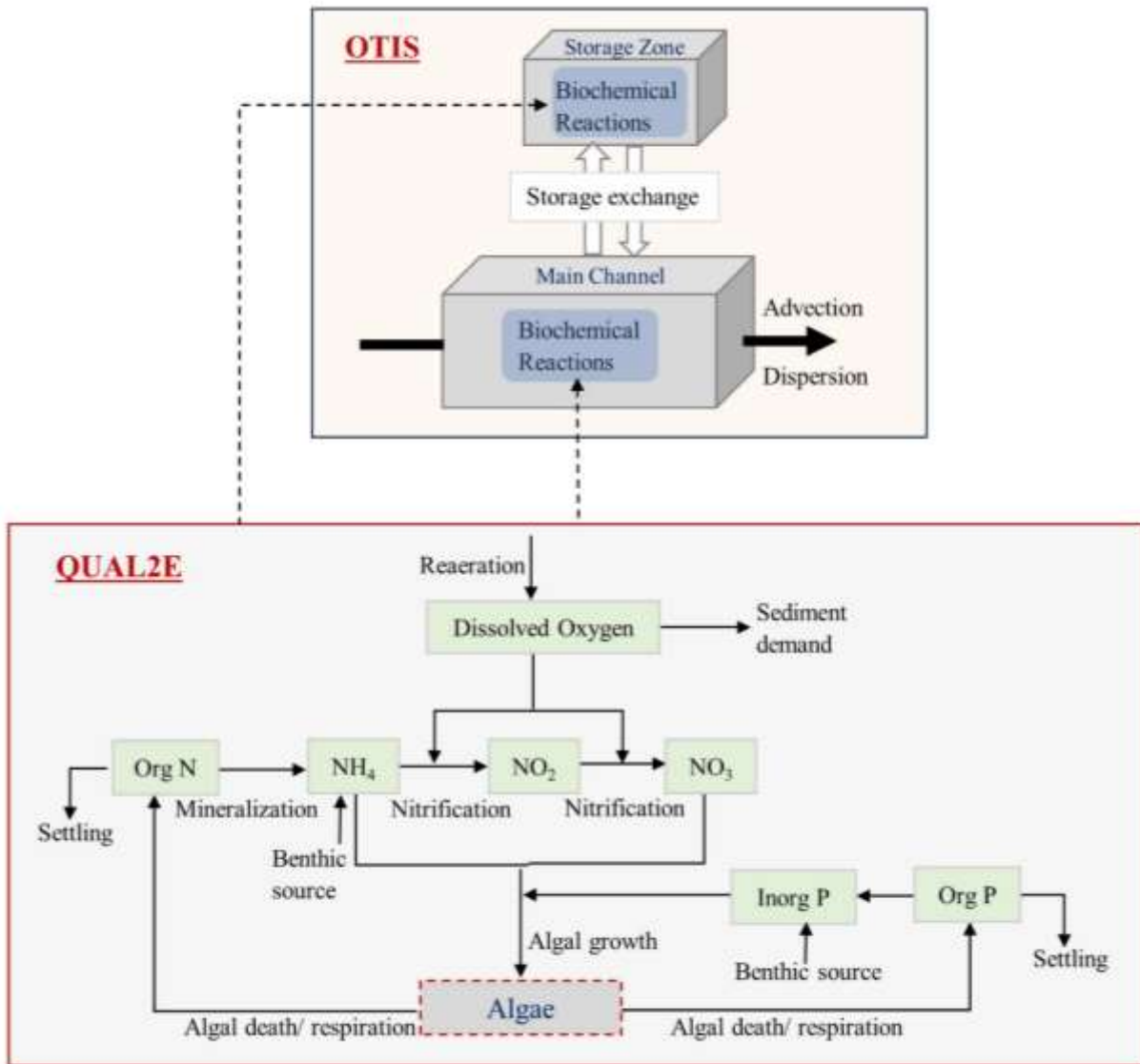


Figure 2.1. Modeling framework showing processes considered in this study.

The improved model replicates OTIS (Runkel and Broshears, 1991), but replaces the first-order reactions in main channel and storage zone with QUAL2E reaction processes (Brown and Barnwell, 1987).

In this study, biochemical reaction equations used in QUAL2E were incorporated into OTIS algorithm using MATLAB™ platform to develop the “Enhanced OTIS” model (Figure 2.1). The biochemical reactions are modeled at the same time step as in OTIS. Instead of the existing first-order-decay-based approach in OTIS, we use QUAL2E equations to estimate the change in solute

concentration. The model has the capability to calibrate the storage parameters using an optimization module when provided with an observed breakthrough curve. Model inputs required are the values of all reaction parameters/constants, stream hydraulic data (such as streamflow, length, cross sectional data) and boundary conditions (such as background and injection concentrations of algae and other water quality variables). Using finite differences, the concentration of all water quality variables can be predicted at any given time and distance.

A fully functional interface was created using MATLAB GUIDE (GUI development environment) in which users can input all data related to the tracer tests, provide upper and lower bounds of calibration parameters and simulate solute transport for both conservative and reactive tracers (Figure 2.2). As an improvement over existing OTIS model, the program will be able to show the observed and modeled breakthrough curves during each iteration of calibration. Users also have the option to choose either first-order decay (as in OTIS) or biochemical reaction-based approach for modeling reactive tracers. Additional options to run and plot breakthrough curves (concentration-distance and concentration-time plots) and to save data files are also provided in this Enhanced OTIS model.

### **2.3.2 Study Area and Data**

The Enhanced OTIS model was calibrated and validated using two different sets of data- (a) field data collected in two separate stream sections in Kielstau catchment (Fohrer and Schmalz, 2012, Schmalz and Fohrer, 2010, Wagner et al. 2018), located in northern Germany (Figure 2.3), and (b) literature data gathered from 5 published studies for a total of 32 sets of experimental data. Nutrient uptake was modeled for all the data and compared with measured uptake to validate the model.

Among the different uptake metrics available, in this study we use the longitudinal nutrient uptake rate ( $k_x$ ) which is measured as the decrease of nutrient concentration per unit length.

**Enhanced OTIS model**

Input Reach Data

**TSM+Reaction Calibration**

Calibration Parameter  
Algae (mg/L) or decay rate (mg/L/day)

Initial Value: 5  
Lower Bound: 1  
Upper Bound: 10

Model Type: Process-based (N/P)  
Tracer Type: Nitrate  
Obs data type: C versus x

Calibrate

**TSM Calibration**

Calibration Parameters

	Initial Value	Lower Bound	Upper Bound
A (m2)	0.6730	0.6000	0.9000
As (m2)	0.1620	0.1000	0.3000
D (m2/s)	0.1900	0.0500	0.3000
Alpha (s-1)	0.0063	1.0000e-03	0.0080

Calibrate

**Run calibrated Model**

Calibrated Parameters

A (m2): 0.673  
As (m2): 0.162  
D (m2/s): 0.19  
Alpha (1/s): 0.00633  
Algae (mg/L) or decay rate (mg/L/day): 5.95

Tracer Type: Conservative  
Plot Type: C versus x  
At time (s): 100  
At location (m): 100

Save data as: Filename.xlsx

Run & Plot

Figure 2.2. Graphical User Interface for Enhanced OTIS Model created using MATLAB with separate sections for calibrating transient storage and reaction modules.

### 2.3.3 Experimental Data

The Kielstau River in Germany is 17 km long and the catchment covers an area of about 50 km<sup>2</sup>. Two instantaneous tracer injections were conducted in two similar order stream reaches towards the outlet of the watershed: (a) a 120 m long reach at Soltfeld gauging station and (b) a 135 m long reach at Freienwill (Figure 2.3, Table 2.1). The experimental locations were chosen considering stream morphology, storage potential, and accessibility for tracer injection and monitoring. A conservative tracer (sodium chloride) and a reactive tracer (potassium phosphate) were used in the study. For phosphate test, a salt solution prepared with 8 kg of NaCl, 250 g of KH<sub>2</sub>PO<sub>4</sub> and 30 L stream water was injected instantaneously at the upstream point of the reach. At the downstream

point, specific conductivity was measured at 5 s intervals using YSI 6600-V2 (YSI Incorporated, USA) water quality probe and salt concentrations calculated based on laboratory calibrations. During the time of experiment, Soltfeld and Freienwill reaches had background  $\text{PO}_4\text{-P}$  concentrations of 0.17 mg/L and 0.27 mg/L respectively. Background algal concentration in the streams were approximately 5.95 mg/L.

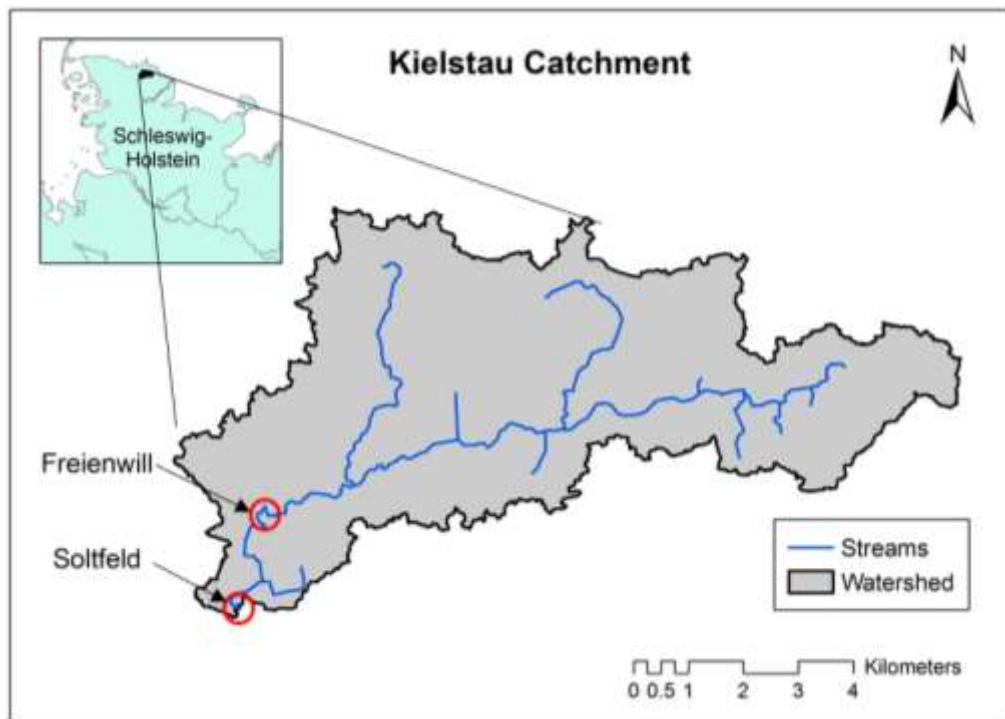


Figure 2.3. Study area (Kielstau Catchment in Northern Germany) with highlighted study reaches at Soltfeld and Freienwill where tracer injections were conducted.

#### 2.3.4 Literature Data

In order to enhance confidence in the developed model, additional model validation was done using data assembled from 5 tracer studies (Table 2.1). Request for data were sent to several

authors who conducted tracer tests in different geologic regions. Among the responses received, we only

Table 2.1. Tracer test details of experimental data from Kielstau catchment (this study) and other published literature data.

\*Conwy stream data was provided by the author separately (not included in Demars, 2008)

<b>Study</b>	<b>Study Area</b>	<b>StreamID</b>	<b>Tracers Used</b>	<b>Type of Injection</b>	<b>Streamflow (L/s)</b>
<i>Demars, 2008</i>	Scotland	Conwy*	NaCl, KH <sub>2</sub> PO <sub>4</sub> , NO <sub>3</sub> -NH <sub>4</sub>	Pulse	43
		Cairn	NaCl, KH <sub>2</sub> PO <sub>4</sub>	Continuous	4.32
<i>Schroer, 2011</i>	Georgia	Protected Stream_25Mar	NaBr, Ca(NO <sub>3</sub> ) <sub>2</sub>	Continuous	22.3
		Protected Stream_21Oct			14.2
		Protected Stream_8Feb			28
		Protected Stream_17Aug			28.6
<i>Baker et al., 2012</i>	Colorado	ShA_X	NaBr, KNO <sub>3</sub>	Continuous	108
		ShC_X			102
		SpR_Y			17
		SpR_Z			21
		SpS_X			133
		SpS_Y			46
		SpS_Z			108
		SpE_X			157
		SpE_Y			72
		SpE_Z			152
<i>Tank et al., 2008</i>	Wyoming	Upper Snake River	NaCl, KNO <sub>3</sub>	Pulse	12000
<i>Burrows et al., 2013</i>	Australia	Arve Loop #1	NaCl, salts of NH <sub>4</sub> and PO <sub>4</sub>	Continuous	0.385
		Arve Loop #2			1.737
		Arve Loop #3			0.29
		PC085A			0.547
		WR15B			0.43
		PC023C			2.29
<i>This study</i>	Germany	Kielstau at Soltfeld	NaCl, KH <sub>2</sub> PO <sub>4</sub>	Pulse	124
		Kielstau at Freienwill	NaCl, KH <sub>2</sub> PO <sub>4</sub>	Pulse	306

selected studies in which both conservative and reactive tracers were used to obtain calibrated transient storage parameters and uptake rates. Two studies (Demars, 2008 and Tank et al., 2008) conducted pulse/instantaneous injections and the remaining three (Schroer, 2011; Baker et al., 2012; Burrows et al., 2013) conducted continuous injections by injecting tracer solution over a period of time. Nitrate, phosphate and ammonium uptake were considered in these studies by injecting salts of these ions along with a conservative tracer. Altogether, literature data provided 32 sets of tracer data for validating our model.

### 2.3.5 Sensitivity Analysis

Using Kielstau experimental data from Freienwill station as a test case, one-at-a-time sensitivity analysis was performed to evaluate the sensitivity of four major parameters affecting N and P uptake: ratio of Chlorophyll-*a* to algal biomass ( $\alpha_0$ ), fraction of algal biomass that is nitrogen ( $\alpha_N$ ), fraction of algal biomass that are phosphorus ( $\alpha_P$ ) and background algal concentration ( $[A]$  in mg/L) were considered for sensitivity analysis. Change in phosphate uptake rate with changing values of  $\alpha_0$ ,  $\alpha_P$  and  $[A]$  was used to determine the sensitivity of these three parameters. Range of typical values for  $\alpha_0$ ,  $\alpha_N$  and  $\alpha_P$ , adopted from Brown and Barnwell (1987) and Bowie et al., (1985) are reported in Table 2.2. However, to study the full extent of parameter sensitivity, the entire feasible range (0.01 to 1 for  $\alpha_0$  and  $\alpha_P$ ) was considered for sensitivity analysis. We also analyzed nutrient uptake over a wide range of algal concentrations (0-500 mg-A/L which corresponds to 0-5 mg-Chl-*a*/L when  $\alpha_0=10$ ). Since  $\alpha_N$  has no effect on P uptake in Freienwill test case, it was ignored in this analysis.

Table 2.2. Typical ranges and default values for key reaction parameters in the model

Parameter	Description	Units	Range of typical values	Default QUAL2E value
$\alpha_0$	Ratio of Chlorophyll-a to algal biomass	$\mu\text{g-Chla/mg-A}$	10-100	50
$\alpha_N$	Fraction of algal biomass that is nitrogen	$\mu\text{g-N/mg-A}$	0.01-0.5	0.08
$\alpha_P$	Fraction of algal biomass that is phosphorus	$\mu\text{g-P/mg-A}$	0.01-0.2	0.014

The major goal behind adapting the QUAL2E-based reaction model is to improve confidence in the model by employing real-world scenarios and considering all major stream processes. To demonstrate the benefits of using a physically-based model, a further analysis was conducted to visualize the varying pattern of stream uptake simulated by the proposed model. This analysis is expected to show the spatial and temporal differences in stream uptake when using a single value for uptake rate (as in OTIS) versus a dynamic uptake rate (as in our model).

### 2.3.6 Model Calibration, Validation and Generalization

The primary aim of this part of the study was to check if certain generalizations could be drawn in terms of parameter values in order to move towards a general nutrient transport model for future studies. The developed model was run using data collected from Soltfeld and Freienwill stream reaches. Similar model runs were carried out for the 32 sets of data obtained from past tracer studies. The Enhanced OTIS model requires calibration of both transient storage model (TSM) and reaction module. For Soltfeld and Freienwill data, the transient storage parameters were automatically calibrated by the model with the help of observed breakthrough curve of conservative tracer. Best fit parameters were derived by using a MALAB optimization function ('fminsearch') with objective function to minimize root mean square error (RMSE) between observed and modeled points along the breakthrough curves. Calibration was attained when the

RMSE values converge to a local minimum and the change in RMSE between consecutive iterations is less than 0.01. For literature data, TSM calibration was performed with the available conservative tracer breakthrough curves in cases that did not directly report storage parameters values. The same calibrated set of storage parameters were used to run the reaction module for N and P tracers. The reaction parameters were calibrated for one test in each study and validated for the remaining tests in the same study area. For instance, the reaction parameters calibrated for 'Stn1' in Tank et al. (2008) study was validated for the remaining three stations. We started with default values of the four key reaction parameters ( $\alpha_0$ ,  $\alpha_N$ ,  $\alpha_P$ , [A]) and followed with manual calibration of these parameters when default values underperformed. Algal or Chl-*a* concentrations were available for Soltfeld and Freienwill streams and thus were not included in calibration. But for the remaining streams from the literature studies, [A] was not reported and thus calibrated as well. By separately calibrating and validating the model for each tracer study, we were able to examine if a general set of reaction parameters performed well in all cases. We assessed model performance by comparing observed and modeled uptake rate values. Uptake rates for pulse injections (Tank et al., 2008 and Demars, 2008) were calculated by plotting the log ratio of reactive and conservative tracer masses over distance from injection point. For continuous injections, the uptake rate was calculated directly by plotting plateau concentrations versus distance. The slope of the linear regression line in both cases gives the main channel nutrient uptake per unit length ( $k_x$ ), which is the inverse of uptake length. Besides visual interpretation, performance indicators such as  $R^2$ , Nash-Sutcliffe Efficiency (NSE) and Percent Bias were evaluated for better assessment.

## 2.4 Results and Discussions

### 2.4.1 Experimental Tracer Test

Nutrient transport in Soltfeld and Freienwill stream reaches were modeled using the developed model and calibrated for the tracer injections carried out in these reaches.  $A$ ,  $A_s$ ,  $D$  and  $\alpha$  values were calibrated for both reaches using conservative tracer data (Table A.1, Appendix A) and the same parameter values were applied to phosphate breakthrough curves. In both streams, the model predicted  $\text{PO}_4\text{-P}$  concentrations with high accuracy (Figure 2.4). Kolmogorov-Smirnov test indicated very close match between the curves with a test statistic of 0.13 for Soltfeld and 0.11 for Freienwill. At 1% significance level, null hypothesis was accepted, indicating that the difference between modeled and observed curves was not significant in either case. Comparing individual data points along the breakthrough curves, both reaches demonstrated a very high  $R^2$  (0.99 for Soltfeld and 0.95 for Freienwill). Using mass balance, measured phosphate uptake rates in Soltfeld and Freienwill were computed as  $0.00054 \text{ m}^{-1}$  and  $0.00029 \text{ m}^{-1}$ . Corresponding uptake rates obtained from our model were  $0.00076 \text{ m}^{-1}$  and  $0.00024 \text{ m}^{-1}$ .

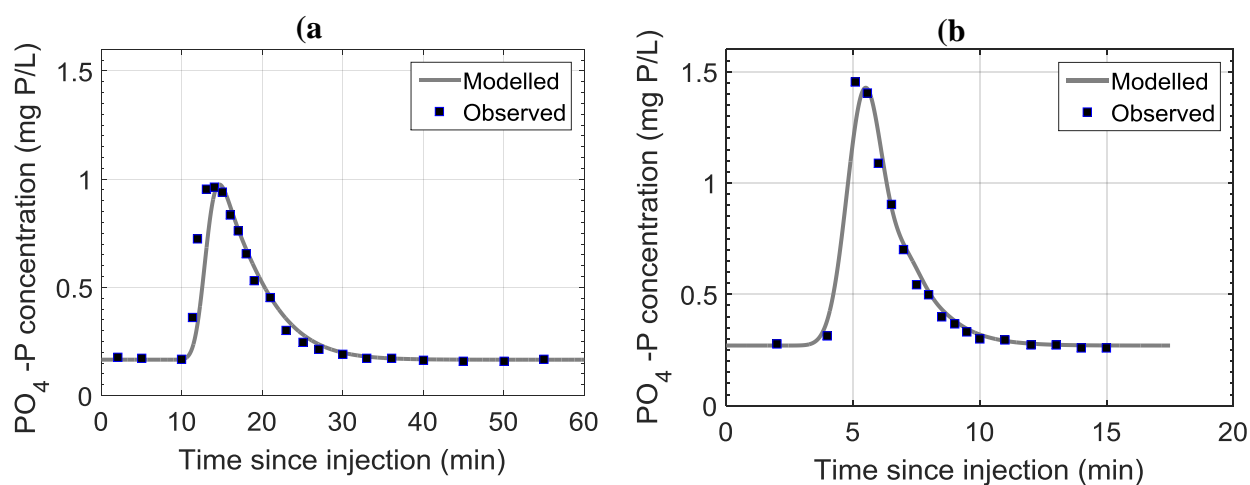


Figure 2.4. Observed and modeled breakthrough curves for Kielstau phosphate tracer tests conducted at (a) Soltfeld and (b) Freienwill.

The ability of our model to simulate “dynamic” uptake was demonstrated by running the model for Freienwill data and estimating uptake in terms of decrease in PO<sub>4</sub>-P concentration ( $\Delta P$ ).

According to the finite difference approach used in the model (Equation 2.1),  $\frac{\partial C}{\partial t}$  and  $\frac{\partial C_s}{\partial t}$  change with  $C$  and  $C_s$ , respectively. In other words, solute concentration and consequently nutrient uptake varies at every time step in both main channel and storage zone (Figure 2.5) showing greater  $\Delta P$  as PO<sub>4</sub>-P concentration increases. This is also in agreement with experimental work done by Bernot et al. (2006) which reported an increase in phosphorus uptake with higher concentrations. A slight lag can be observed between main channel and storage zone uptake curve which is expected in reality where solute entry to storage zones is delayed compared to the main channel (Figure 2.5a). First-order decay approach in OTIS also simulates uptake as a function of solute concentration ( $\frac{\partial C}{\partial t} = kC$ ), however with the enhanced model,  $\frac{\partial C}{\partial t}$  is not just a function of  $C$  but other interactions and factors affecting algal growth and uptake (such as light and nutrient limitations) are also considered. While OTIS and many other solute transport models represents uptake rate by a single value ( $\lambda$  or  $\lambda_s$ ), the enhanced model utilizes a dynamic uptake rate that gets updated during each time and distance step of the model (Figure 2.5b). For steady-state studies in streams with minimal solute interactions, a single uptake rate may be sufficient. However, for real world scenarios where different types of pollutants are fed to streams and where pollutant input

varies over time and distance, the enhanced model provides better and more realistic options to model nutrient transport.

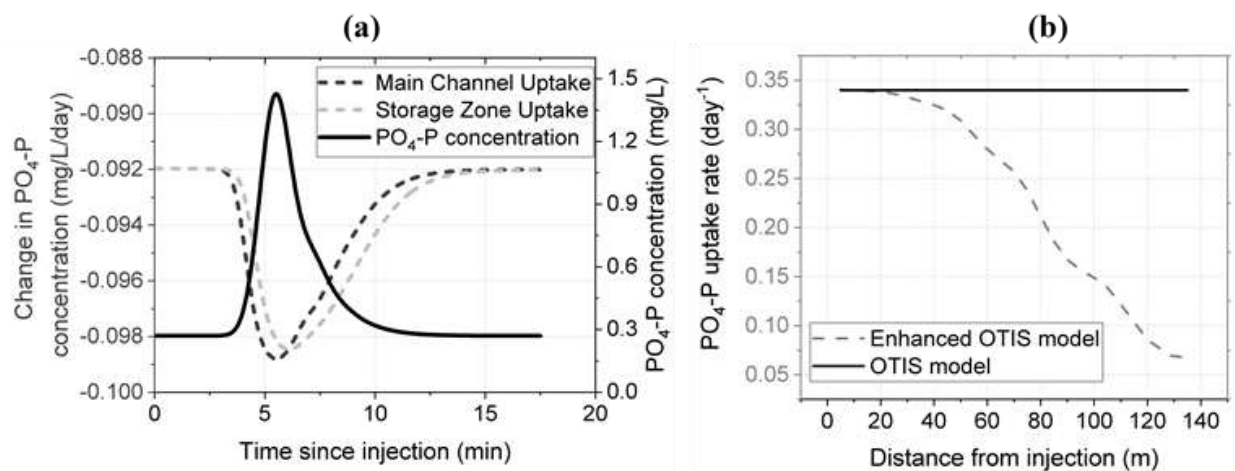


Figure 2.5. PO<sub>4</sub>-P concentration in main channel and change in PO<sub>4</sub>-P concentration in main channel and storage zone as simulated by new model for Freienwill data.

(a) represents model results over time at downstream monitoring station ( $x=135$  m) and (b) represents phosphate uptake rates with OTIS and Enhanced OTIS models 5 minutes after injection

## 2.4.2 Sensitivity Analysis

To understand the influence of background algal concentration on sensitivity of other parameters, the model was run with two levels of algal concentration. The phosphate tracer test at Freienwill was used as the test case for sensitivity analysis. P uptake rate changed from  $0.00023 \text{ m}^{-1}$  to  $0.00028 \text{ m}^{-1}$  when algal concentration was changed from 0 to 500 mg/L (Figure 2.6c). At low algal concentration (1 mg/L), stream uptake rate showed negligible change (-0.13%) when  $\alpha_0$  was increased from 10 to 100 (Figure 2.6a). Similarly, within the considered range of  $\alpha_P$  (0.1-1), uptake rate showed only 5.4% increase at low algal concentration. At high algal concentration, both  $\alpha_0$  and  $\alpha_P$  demonstrated high sensitivity with -10.5% and 114.5 % change in uptake rate, respectively.

These results show the significance of background algal concentration on phosphate uptake. Although similar behavior is expected for  $\alpha_N$  when studying N uptake, nitrate removal in stream is a much more complicated process owing to other factors like denitrification and algal preference for ammonia (Kemp and Dodds, 2002; Bernhardt et al., 2002).

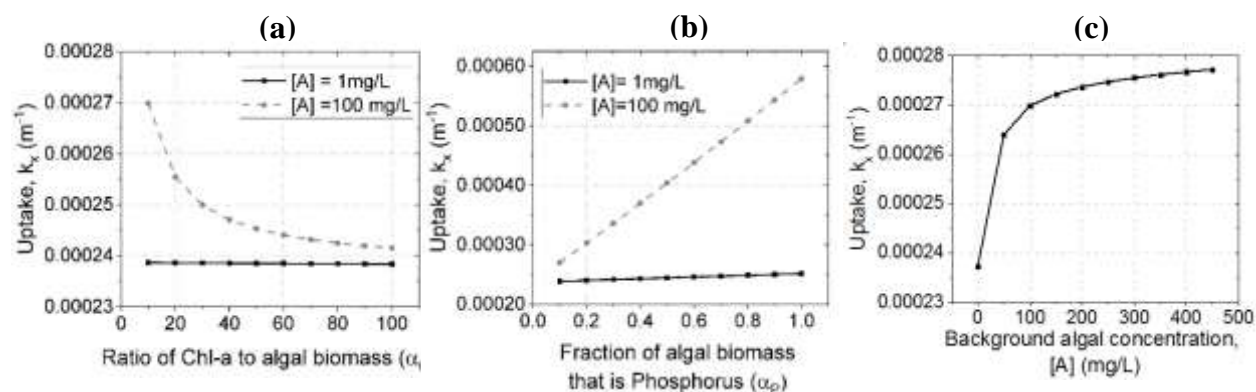


Figure 2.6. Sensitivity analysis plots for Freienwill test data, showing change in phosphate uptake rate with changing values of  $\alpha_0$ ,  $\alpha_P$  and  $[A]$ .

Both  $\alpha_0$  and  $\alpha_P$  are not sensitive to uptake rate at a low value of  $[A]$  but shows higher sensitivity at high background algal concentration.

### 2.4.3 Model Validation for Literature Data

The values of  $\alpha_0$ ,  $\alpha_N$  and  $\alpha_P$  can change according to different types of algae, phytoplankton, periphyton and benthic autotrophs present in the streams. But unlike algal concentration, these parameters are rarely measured in field. Hence, it is most efficient to assume or calibrate their values using tracer test data. In an attempt to avoid extensive calibration and to generalize the values of  $\alpha_0$ ,  $\alpha_N$  and  $\alpha_P$ , further model generalization was carried out with literature data such that background algal concentration remains as the only parameter required for model parameterization that could be derived through calibration or accurate field measurement.

For all of the 32 sets of tracer data obtained from literature, storage parameters-  $A$ ,  $A_s$ ,  $D$  and  $\alpha$ - were either directly fed to the model (in case these were reported in the paper) or calibrated using observed conservative tracer breakthrough curves (Table A.1, Appendix A). Using the derived set of storage parameters, reactive solutes were modeled for each test data. Concentrations of algae were calibrated for all test cases to obtain best fit between observed and modeled breakthrough curves and uptake rates. Chlorophyll-*a* concentration (calculated as  $[A] * \alpha_0$ ) ranged from 0.01 to 5 mg/L for the streams considered.

Manually calibrated values of reaction parameters indicate that values of  $\alpha_0=10$ ,  $\alpha_N=0.2$  and  $\alpha_P=0.1$  were good estimates in predicting nutrient uptake except for the data from Burrows et al. (2013) and Tank et al. (2008). Three stream reaches in Burrows et al. (2013) exhibited high value of  $\alpha_N$  ( $=0.5$ ) suggesting a probable difference in algal species that results in higher fraction of nitrogen in algae in these streams. Value of  $\alpha_P$  remained constant at 0.1 in all test cases. Ratio of Chl-*a* to algal biomass can have a wide range of values from 10-100 according to Bowie et al. (1985). For the tracer tests considered here, 10 was the most suitable estimate for  $\alpha_0$  in 70% of test cases. Models for Tank et al. (2008) and Burrows et al. (2013) had a slightly higher calibrated value for Chl-*a* to algal biomass ratio ( $\alpha_0=20$ ). All tests conducted within a particular stream yielded the same set of reaction parameters. Overall, using the generalized values of the three reaction parameters ( $\alpha_0=10$ ,  $\alpha_N=0.2$  and  $\alpha_P=0.1$ ), the model yielded uptake rates similar to observed values in over 70% of case studies including the experimental data from Kielstau catchment. A two-sample t-test showed no significant difference between observed and modeled uptake rates for these selected cases ( $t$ -statistic <  $t$ -critical at 0.05 significance level). We also conducted additional tests to examine the performance of generalized values for Burrows et al. (2013) and Tank et al.

(2008) data. Even though we obtained a relatively lower  $R^2$  ( $=0.77$ ) between modeled and observed values for these data, it still didn't show significant difference according to the t-test at 0.05 significance level. This reinforces our recommendation that these values would act as approximate estimates of these parameters when field data is unavailable for calibration.

Selected data from Demars (2008), Burrows et al. (2013) and Tank et al. (2008) are shown in Figure 2.7 to demonstrate the capability of developed model to accurately simulate nutrient uptake. For continuous tracer injection conducted in Cairn stream (Demars, 2008) and 'PC023C' stream reach (Burrows et al., 2013), measured plateau concentrations when plotted against distance yielded a phosphate uptake rates of  $0.0033 \text{ m}^{-1}$  and  $0.011 \text{ m}^{-1}$  respectively. Corresponding simulated values were  $0.0034 \text{ m}^{-1}$  and  $0.012 \text{ m}^{-1}$  indicating a very close prediction. For pulse injection conducted in Upper Snake River (Tank et al., 2008), log ratio of reactive and conservative tracer masses at different downstream locations when plotted against distance to estimate nitrate uptake rates. In this case, with generalized parameters, we obtained a slightly higher simulated uptake rate of  $0.0023 \text{ m}^{-1}$  when compared to measured value of  $0.0017 \text{ m}^{-1}$ . It is worth noting that for the same data, calibrated parameters ( $\alpha_0=20$ ,  $\alpha_N=0.2$  and  $\alpha_P=0.1$ ) yielded exact similar values of modeled and measured uptake rates (not shown in Figure 2.7).

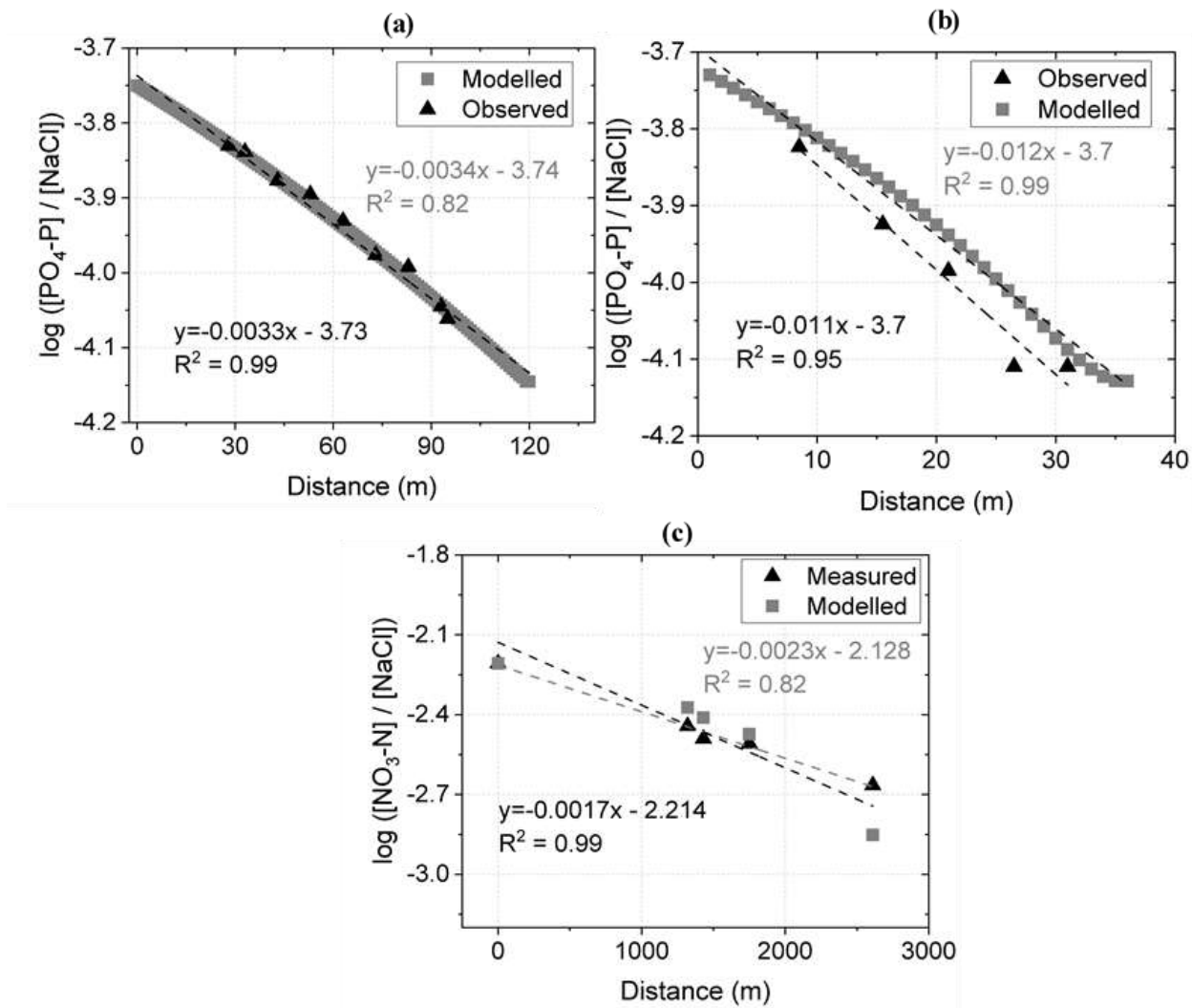


Figure 2.7. Calculation of uptake rates from observed and modeled nutrient concentrations.

(a) shows the phosphate uptake data in Cairn stream from Demars (2008), (b) shows phosphate uptake data from 'PC023C' stream of Burrows et al., (2013) and (c) is nitrate uptake data from Upper Snake River of Tank et al., (2008), all modeled using generalized values of  $\alpha_0=10$ ,  $\alpha_N=0.2$  and  $\alpha_P=0.1$ . Slope of the regression line gives uptake rate.

Overall for the entire dataset, modeled uptake rates for nitrate, phosphate and ammonium closely matched the measured uptake rates (Figure 2.8). A good model performance ( $R^2=0.76$ ,  $NSE=0.47$ , Percent Bias=-4.3%) was thus achieved in terms of nutrient uptake. Most of the inconsistencies between observed and modeled values were observed for 5 streams in Burrows et al. (2013) study (Figure 2.8b). Lack of sufficient breakthrough curve data and relying solely on plateau

concentrations to calibrate storage parameters could be one reason behind this. The only variable in the reactive part of the model that required significant calibration was background algal concentration ( $[A]$ ). Instead of calibrating empirical parameters ( $\lambda$  and  $\lambda_s$ ) in OTIS, the proposed model emphasizes calibrating a physically-based variable ( $[A]$ ) that is expected to affect nutrient uptake. In addition, the process-based nature of our model provides opportunity to feed field-measured values of algal concentration into the model like the example of Kielstau experimental data used in this study. Besides simulating short-term breakthrough curves like the ones from Soltfeld and Freienwill, the developed model also estimated steady state nitrate, ammonium and phosphate uptake rates for multiple stream segments in Scotland, Georgia, Colorado and Australia. Hence, for large-scale studies, this enhancement in nutrient transport representation would assist in realistically predicting water quality without the need for empirical models.

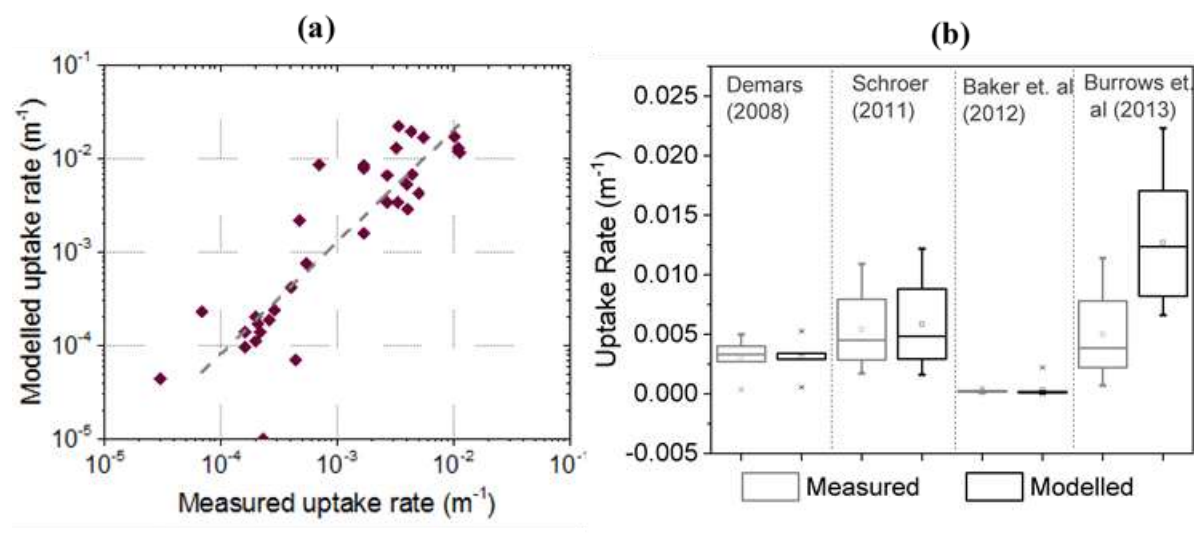


Figure 2.8. (a) Scatter plot showing close match between modeled and measured uptake rates for different parameters from the whole data set (experiment and literature). (b) Box plot showing the range of uptake rates grouped into different studies

## 2.5 Summary and Conclusions

This study presented a modeling framework to simulate stream solute transport by integrating OTIS and QUAL2E models. A finite difference approach was used to model transport and reactions. The Enhanced OTIS model includes an improved user interface with better modeling options and data visualization. The model will enable users to simulate solute transport using existing simple first-order decay approach or using our improved biochemical- reaction-based algorithms. A case study performed with experimental tracer test data (in Kielstau catchment, Germany) showed that with actual biochemical reactions, the new model takes the dynamic nature of uptake rate with changing nutrient concentrations into account. This is an added benefit over existing first-order decay models that calibrate empirical parameters with the help of field-measured tracer data. Sensitivity analysis of a few key model parameters indicated the significance of background algal concentration on nutrient uptake as well as on the sensitivity of other parameters. With high levels of algal concentration in Freienwill stream reach (100 mg/L), the model forecasted a 114.5% increase in uptake rate when  $\alpha_P$  (fraction of algal biomass that is phosphorus) was increased from 0 to 1. A 10.5% decrease in uptake was also observed at this level of algal concentration when  $\alpha_0$  (ratio of Chl-a to algal biomass) increased from 10 to 100.

The developed model calibrated and validated using data from Kielstau and five other published studies gave promising results in terms of ability to predict transport and uptake. Soltfeld and Freienwill breakthrough curves and uptake rates were accurately modeled by using measured algal data. Considering all test data with minimal calibration, the model estimated uptake rates with good accuracy ( $R^2=0.76$ ,  $NSE=0.47$ , Percent Bias=-4.3%). Although the model provides option to calibrate all the parameters, we generalized values of  $\alpha_0$  (=10),  $\alpha_N$  (=0.2) and  $\alpha_P$  (=0.1) to achieve reasonable model performance for more than 70% of the published cases tested here. These values

are thus proposed as reasonable parameter estimates when field-measured data is unavailable for calibration. However, we recommend calibrating or measuring background algal concentration in streams for precise model predictions. Although calibrating first-order-decay rates can provide reasonable estimates of uptake rates in many cases, this study aims to propose a more realistic approach for simulating nutrient transport that is representative of real world scenarios. Recent water quality models like WASP (Di Toro et al., 1983) have the functionality to model different types of algae. Such complex modeling was not included in this study owing to the uncertainty induced by an increased number of parameters in the model. A more comprehensive model could be developed based on the presented findings by incorporating reactions not considered here.

## **2.6 Acknowledgments**

Funding for this study was provided by United State Department of Agriculture – National Institute of Food and Agriculture Regional Research Project S-1063. We would like to thank Dr. Benoit Demars, Dr. Dan Baker, Dr. Jennifer Tank, and Dr. Ryan Burrows for generously sharing tracer test data from their studies. Help provided by Johannes Fischer, Oliver Tank and the lab staff at Kiel University to P.V. Femeena in carrying out the tracer experiments is greatly appreciated.

## **2.7 References**

- Ambrose, R.B., T.A. Wool, J.P. Connolly, and R.W. Schanz. (1988). WASP4, A Hydrodynamic and Water Quality Model—Model Theory, User’s Manual, and Programmer’s Guide. EPA/600/3-87-039, U.S. Environmental Protection Agency, Athens, GA.
- Ani, E., S. Wallis, A. Kraslawski, and P. Serban. (2009). Environmental Modelling & Software Development, calibration and evaluation of two mathematical models for pollutant transport in a small river, 24, 1139–1152. <https://doi.org/10.1016/j.envsoft.2009.03.008>
- Baker, D.W., B.P. Bledsoe, and J. Mueller-Price. (2012). Stream nitrate uptake and transient storage over a gradient of geomorphic complexity, north-central Colorado, USA. *Hydrol. Processes* 26:3241–3252. doi:10.1002/hyp.8385

- Bencala, K.E. and R.A. Walters. (1983). Simulation of solute transport in a mountain pool-and-riffle stream: A transient storage model: *Water Resources Research*, v. 19, no. 3, p. 718-724.
- Bernhardt, E.S., R. O. Hall, G.E. Likens. (2002). Whole-system estimates of nitrification and nitrate uptake in streams of the Hubbard Brook Experimental Forest. *Ecosystems*. 5: 419-430
- Bernot, M.J., J.L. Tank, T.V. Royer, and M.B. David (2006). Nutrient uptake in streams draining agricultural catchments of the midwestern United States. *Freshwater Biol.*
- Bowie, G.L., W.B. Mills, D.B. Porcella, C.L. Campbell, J.R. Pagenkopf, G.L. Rupp, K.M. Johnson, P.W.H. Chan, S.A. Gherini, C.E. Chamberlin. (1985). Rates, Constants, and Kinetics Formulations in Surface Water Quality Modeling U.S. Environmental Protection Agency, EPA/600/3-85/040
- Brown, L.C. and T.O. Barnwell. (1987). The Enhanced Stream Water Quality Model QUAL2E and QUAL2E-UNCAS: Documentatin and User's Manual, EPA/600/3- 87/039, U.S. Environmental Protection Agency, Athens, GA.
- Burrows, R.M., J. B. Fellman, R. H. Magierowski, and L. A. Barmuta. (2013). Greater phosphorus uptake in forested headwater streams modified by clearfell forestry. *Hydrobiologia* 703:1–14.
- Carpenter, S., N. Caraco, D. Correll, R. W. Howarth., A. Sharpley, & V. Smith. (1998). Nonpoint pollution of surface waters with phosphorus and nitrogen. *Ecological Applications*, 8(3), 559–568.
- Chapra, S.C., Pelletier, G.J. and Tao, H. 2008. QUAL2K: A Modeling Framework for Simulating River and Stream Water Quality, Version 2.11: Documentation and Users Manual.
- Connolly, J. and R. Winfield. (1984). User's guide for WASTOX, a framework for modeling the fate of toxic chemicals in aquatic environments. Part 1. Exposure concentration. U.S. Environmental Protection Agency, Washington, D.C., EPA/600/3-84/077 (NTIS PB85152882).
- Demars B.O.L. (2008). Whole-stream phosphorus cycling: testing methods to assess the effect of saturation of sorption capacity on nutrient uptake length measurements. *Water Research*, 42, 2507-2516.
- Di Toro, D. M., J. J. Fitzpatrick, R. V. Thomann, and I. Hydroscience, (1983). Water Quality Analysis Simulation Program (WASP) and Model Verification Program (MVP) - Documentation. Technical Report EPA-600/3-81-044, Hydroscience, Inc., Westwood, NJ. for USEPA, Duluth, MN, Contract No. 68-01-3872, 156 pp.
- Femeena, P. V., K. P. Sudheer, R. Cibin, I. Chaubey. (2018). Spatial optimization of cropping pattern for sustainable food and biofuel production with minimal downstream pollution. *sJ Environ Manage.* 2018 Apr 15;212:198-209. doi: 10.1016/j.jenvman.2018.01.060. Epub 2018 Feb 22.

- Fischer, H.B., E.J. List, R.C.Y. Koh, J. Imberger and N.H. Brooks (1979). *Mixing in Inland and Coastal Waters*, Academic Press, San Diego.
- Fohrer, N. & B. Schmalz. (2012). Das UNESCO Ökohydrologie-Referenzprojekt Kielstau-Einzugsgebiet - nachhaltiges Wasserressourcenmanagement und Ausbildung im ländlichen Raum. *Hydrologie und Wasserbewirtschaftung* 56(4): 160-168.
- Gassman, P. W., M. Reyes, C. H. Green, and J. G. Arnold. (2007). The Soil and Water Assessment Tool: Historical development, applications, and future directions. *Trans. ASABE* 50(4): 1211-1250.
- Hall, R. O. and others. (2009). Nitrate removal in stream ecosystems measured by 15N addition experiments: Total uptake. *Limnology and Oceanography* 54:653-665.
- Harvey, J. W., B. J. Wagner, and K. E. Bencala (1996). Evaluating the reliability of the stream tracer approach to characterize stream-subsurface water exchange, *Water Resour. Res.*, 32(8), 2441–2451, doi:199610.1029/ 96WR01268.
- Johnson, L. B., C. Richards, G. E. Host, and J. W. Arthur (1997). Landscape influences on water chemistry in Midwestern stream ecosystems. *Freshwater Biology* 37:193–208.
- Kemp, M.J. and W. K. Dodds. (2002) The Influence of Ammonium, Nitrate, and Dissolved Oxygen Concentrations on Uptake, Nitrification, and Denitrification Rates Associated with Prairie Stream Substrata. *Limnology and Oceanography*, 47, 1380-1393.  
<http://dx.doi.org/10.4319/lo.2002.47.5.1380>
- Marsalek J., Sztruhar D., Giulianelli M., Urbonas B. (2003). *Enhancing Urban Environment by Environmental Upgrading and Restoration*. Nato Science Series: IV: Earth and Environmental Sciences, vol 43. Springer, Dordrecht
- Mueller Price, J. S., B. P. Bledsoe, and D. W. Baker. (2014). Influences of sudden changes in discharge and physical stream characteristics on transient storage and nitrate uptake in an urban stream. *Hydrological Process*, 29(6), 1466-1479.
- Mueller Price, J. S., D. W. Baker, B. P. Bledsoe (2016). Effects of passive and structural stream restoration approaches on transient storage and nitrate uptake. *River Research and Applications* 32: 1542--1554. DOI: 10.1002/rra.3013.
- Mulholland, P. J., and others. (2008). Stream denitrification across biomes and its response to anthropogenic nitrate loading. *Nature* 452: 202–205
- Mulholland, P. J., and others. (2009). Nitrate removal in stream ecosystems measured by 15N addition experiments: Denitrification. *Limnol. Oceanogr.* 54: 666–680.
- O'Brien, J. M., W. K. Dodds, K. C. Wilson, J. N. Murdock, and J. Eichmiller. (2007). The saturation of N cycling in Central Plains streams: 15N experiments across a broad gradient of nitrate concentrations. *Biogeochemistry* 84: 31–49.

- O'Connor, B. L., M. Hondzo, and J. W. Harvey. (2010). Predictive modeling of transient storage and nutrient uptake: Implications for stream restoration, *J. Hydraul. Eng.*, 136(12), 1018–1032.
- Potter, J. D., W. H. McDowell, J. L. Merriam, B. J. Peterson, and S. M. Thomas. (2010). Denitrification and total nitrate uptake in streams of a tropical landscape, *Ecol. Appl.*, 20(8), 2104–2115, doi:10.1890/09-1110.1.
- Runkel, R. L., and R. E. Broshears. (1991). One dimensional transport with inflow and storage (OTIS): A solute transport model for small streams, Tech. Rep. 91-01, Cent. for Adv. Dec. Support for Water and Environ. Sys., Univ. of Colo., Boulder.
- Runkel, R.L. (1998), One-Dimensional Transport with Inflow and Storage (OTIS): A Solute Transport Model for Streams and Rivers: U.S. Geological Survey Water-Resources Investigations Report 98-4018, 73 p.
- Schmalz, B. & N. Fohrer. (2010). Ecohydrological research in the German lowland catchment Kielstau. *IAHS Publ.* 336. 115-120.
- Schroer, K. L. (2011). Controls on nitrate degradation in two adjacent wetland streams with different geochemistry and flow-source streams, Watkinsville, GA. PhD Dissertation, University of Georgia, Athens, GA.
- Sheibley, R.W., J.H. Duff, and A.J. Tesoriero. (2014). Low transient storage and uptake efficiencies in seven agricultural streams: Implications for nutrient demand. *J. Environ. Qual.* 43:1980–1990. doi:10.2134/jeq2014.01.0034
- Stream Solute Workshop (1990). Concepts and methods for assessing solute dynamics in stream ecosystems, *J. North Am. Benthol. Soc.*, 9(2), 95– 119, doi:10.2307/1467445.
- Tank, J. L., E. J. Rosi-Marshall, M. A. Baker, And R. O. Hall. (2008). Are rivers just big streams? A pulse method to quantify nitrogen demand in a large river. *Ecology* 89: 2935–2945.
- Tank, J.L, M. J. Bernot and E. J. Rosi-Marshall (2017). Nitrogen limitation and uptake. In: *Methods in Stream Ecology* (Eds F.R.Hauer & G.A.Lamberti), Academic Press, New York
- Wagner, P.D., Hörmann, G., Schmalz, B., Fohrer, N. (2018). Characterisation of the water and nutrient balance in the rural lowland catchment of the Kielstau [in German]. *Hydrologie und Wasserbewirtschaftung* 62(3), 145-158.
- Ward, A. S., Kelleher, C. A., Mason, S. J. K., Wagener, T., McIntyre, N., McGlynn, B., Runkel, R. L., Payn, R. A. (2017). A software tool to assess uncertainty in transient-storage model parameters using Monte Carlo simulations. *Freshwater Science* 2017 36:1, 195-217.

### 3. SIMPLE REGRESSION MODELS CAN ACT AS CALIBRATION-SUBSTITUTE TO APPROXIMATE TRANSIENT STORAGE PARAMETERS IN STREAMS

*A version of this chapter has been published in Advances in Water Resources Journal (DOI: 10.1016/j.advwatres.2018.11.010)*

#### 3.1 Abstract

Transient storage models in combination with tracer tests are widely used to study solute transport dynamics in streams. Storage parameters included in such models are typically calibrated for one or more study reaches by monitoring solute concentrations and fitting breakthrough curve data. Since stream characteristics vary spatially and temporally, it is challenging to generalize these calibrated parameters for another stream reach. This study investigates the ability of simple regression models to predict transient storage parameters such as dispersion coefficient ( $D$ ), transient storage area ( $A_s$ ) and storage exchange coefficient ( $\alpha$ ). A meta-analysis of 834 tracer studies from 67 published papers was used to develop parsimonious non-linear regression models that relate storage parameters to easily available stream parameters such as discharge, velocity, flow width and flow depth. Correlation analysis showed moderate correlation of  $D$  with velocity, depth and width; and high correlation of  $A_s$  with the ratio of discharge to depth. Exchange coefficient ( $\alpha$ ) did not show significant correlation with available stream parameters. The models were tested using a subset of meta-analysis data and experimental tracer data from Hubbard Brook Experimental Forest located in the US and Kielstau Catchment located in Germany. We predicted storage and breakthrough curves with reasonable accuracy ( $R^2 > 0.5$ ) by using new regression equations and incorporating it into an advection-dispersion-storage model. These equations provide a viable alternative to parameter calibration by avoiding computationally intensive reach-

specific calibration, and reducing time and cost associated with tracer experiments. Therefore, such regression-based estimates of storage parameters can also form an integral part of larger watershed scale models by predicting solute transport and storage in stream reaches.

### **3.2 Introduction**

Streams are heterogeneous systems with complex hydrological and ecological dynamics. Natural and anthropogenic activities may cause pollutants to enter the streams and result in deteriorated water quality. These pollutants interact with streambed and streambanks as they get transported downstream. Understanding solute transport is thus essential for predicting water quality and the associated risks. Transport models are widely used to forecast the timing and extent of contaminant spills, simulate flood responses, and characterize export of pollutants during extreme events (Mueller Price et al., 2014; Ani et al., 2009). Transient storage models (TSM) simulate solute transport in streams and rivers (Bencala and Walters, 1983 ; Runkel, 1998 ; Gooseff et al., 2003; Kelleher et al., 2013; Ward et al., 2017). Besides predicting conservative solute transport, these models can also quantify reactive transport, which is critical for nutrients and other pollutants (Edwardson et al., 2003; Harvey et al., 1996; Chen et al., 2014; Garcia et al., 2017). The simplest TSM uses a one-dimensional advection-dispersion-reaction equation to route stream solutes along the main channel while exchanging mass with a single transient storage zone. The behavior of reactive solutes can then be simulated within the transient storage zone, which is a conceptual representation of the immobile zones in a channel, including zones associated with slow flow such as pools, hyporheic flows, boundary layers, vegetation etc. (Runkel and Broshears, 1991).

The **One-dimensional Transport with Inflow and Storage** model (OTIS, Runkel 1998) is one of the most commonly used implementations of TSMs that uses finite differences to solve the model

equations (Crank 1979; Bencala and Walters, 1983; Sheibley et al., 2014; Mueller Price et al., 2016). Conservative tracers that do not undergo biochemical reactions are modeled solely using advection, dispersion and transient storage exchange processes, while reactive solutes are modeled by adding first order decay and sorption parameters. This study focuses on transport of all stream solutes and is applicable to both conservative and reactive solutes. The four major parameters in the hydraulic OTIS model (dispersion coefficient ( $D$ ), stream cross-sectional area ( $A$ ), storage zone area ( $A_s$ ) and storage exchange coefficient ( $\alpha$ )) are either user-defined or specifically calibrated for any given stream reach. Cross-sectional area of the stream is usually a known or measured parameter. However, since it is difficult to directly measure the remaining three parameters, tracer experiments are generally conducted to estimate their values (Wagner and Gupta, 2005). A nonreactive tracer is injected in a stream and its concentration is measured over time at one or more downstream locations. Traditionally, tracer tests are conducted by injecting a tracer in a stream and measuring a breakthrough curve (solute concentration versus time curve) downstream for fitting model parameters (Stream Solute Workshop, 1990, Aris 1956). This can be done manually or using the calibration module in OTIS (OTIS-P). Both of these approaches may result in highly correlated parameter values, practically infeasible values and/or lead to equifinality issue where other different sets of parameters may yield similar or better fit (Scott et al., 2002; Ward et al., 2017). Therefore, it is important to further analyze the model and parameter values for optimality. Another limitation associated with OTIS-P is that when it does not converge (referred to as 'false convergence') due to initial model inputs or lack of sufficient measured data, the resulting parameter values are unreliable (Kelleher et al., 2013).

Considering that TSMs are simple models used to represent complex stream processes, past studies have recommended the need for major improvements to these models (Choi et al., 2000; Runkel

2000). Moreover, parameter values obtained using TSMs usually reflect the magnitude of processes for a given stream reach and may not be applicable to a different reach or even the same reach under different ecohydrologic conditions (Kelleher et al., 2013). In this context, alternate metrics such as  $F_{\text{med}}$  (fraction of median travel time due to transient storage) and Damkohler number,  $Dal$  were used to quantify and characterize the variability in transient storage exchange across different streams (Runkel, 2002; Wagner and Harvey, 1997). Nevertheless, for many applications that do not require precise process representation of complex biogeochemical reactions, a simple one-storage transient storage model like OTIS can reliably characterize the dominant physical processes (Choi et al., 2000). The primary limitation of using OTIS for a large-scale watershed study with multiple streams is that it requires extensive field experiments and calibration, which results in more time and cost associated with these studies. Alternate methods to estimate transient storage parameters would avoid the need for reach-specific calibration. Past efforts have tried to develop equations and relationships for predicting these parameters. Most of these studies were focused on developing equations for  $D$  using stream parameters like velocity, shear velocity, flow width and flow depth (Taylor 1954, Elder 1959, Fischer, 1975; Seo and Cheong, 1998; Kashefipour and Falconer, 2002; Deng et al., 2001; McQuivey and Keefer, 1974; Disley et al., 2015). Among these equations, Fischer's equation is one of the most popular and is used in many water quality models such as QUAL2E/K (Brown and Barnwell, 1987; Chapra et al., 2008). Jobson (1996) proposed a method to predict tracer response functions by using prediction equations that relate travel time and dispersion to river characteristics such as unit-peak concentration, reach slope, discharge and drainage area. This study attempts to adopt a similar methodology to develop regression equations for all transient storage parameters except cross-sectional area, which is typically a measured parameter. To the best of our knowledge, regression-

based estimates for all storage parameters have not been developed or applied to TSMs. Because of the unique formulation of TSMs, we must also consider predictive capability for other parameters ( $A_s$  and  $\alpha$ ), but very little research has been done in this regard. Harvey and Wagner (2000) have reported that a non-linear relationship exists between  $A_s$  and the friction factor based on several tracer studies. Estimating both friction factor and shear velocity requires precise knowledge of channel slope and bed material, which is not often known or measured. Approximation of channel slope (for instance- using Digital Elevation Models (DEM)) introduces further uncertainty and may result in inaccurate prediction of dispersion coefficient and storage zone area using these methods. The value of  $\alpha$  is typically small ( $10^{-2} - 10^{-7} \text{ s}^{-1}$ ) and it is difficult to estimate its value from correlations (Harvey and Wagner, 2000).

Expressing transient storage parameters in terms of readily available stream characteristics will provide modeling opportunities to users who are unable to conduct tracer tests for OTIS model calibration. This can further enhance options to incorporate TSMs in larger watershed scale models without the need for extensive calibration. In addition, regression-based estimates of transient storage parameters are expected to overcome ‘false convergence’ issues in OTIS-P since regression modeling is based on actual stream variables and does not involve optimization of parameter values. In this study, we propose new regression equations for transient storage parameters based on a meta-analysis of published values. Parsimonious regression models were developed for predicting transient storage parameters with the minimum number of independent and easily available stream variables. Specific goals of this study were (1) to develop regression equations for three transient storage parameters -  $D$ ,  $A_s$ , and  $\alpha$  - using readily available stream characteristics based on a meta-analysis approach, (2) to test their effectiveness in predicting

parameter values and modeling solute breakthrough curves, and (3) determine the accuracy and sensitivity of the parameter values based on expected ranges in stream characteristics. The overarching goal of this study is thus to propose a complete solute transport model similar to OTIS but with no calibration required. The objective was to provide approximate estimates of storage parameters in cases of data scarcity and help generalize TSMs to all stream types.

### 3.3 Methodology

We used literature reported OTIS fitted transient storage parameters to develop regression relationships. Additionally, we validated the relationships using breakthrough curves and fitted parameter sets from 13 stream reaches in a forested catchment (Hubbard Brook Experimental Forest [HBEF], USA, Hall et al., 2002) and two stream reaches in an agricultural catchment (Kielstau, Germany, this study, Fohrer and Schmalz, 2012). All analyses were completed by replicating the OTIS algorithm in MATLAB™.

#### 3.3.1 The OTIS Model

The OTIS model simulates solute transport in two zones- the main stream channel and the storage zone (Runkel and Broshears, 1991). A solute is transported in the main stream channel using advection, dispersion, lateral inflow, transient storage and first order decay (Figure 3.1). It uses a finite-difference approach to calculate concentration of solute at different times along the stream. Governing equations (ignoring decay and lateral flow components) are given in equations 3.1 and 3.2. Equation 3.1 represents the change in solute concentration and processes within the main channel and equation 3.2 represents the transient storage zone dynamics.

$$\frac{\partial C}{\partial t} = D \frac{\partial^2 C}{\partial x^2} - u \frac{\partial C}{\partial x} + \alpha(C_s - C) \quad (3.1)$$

$$\frac{\partial C_s}{\partial t} = -\alpha \frac{A}{A_s} (C_s - C) \quad (3.2)$$

where

$A$  = stream channel cross-sectional area [ $\text{m}^2$ ]

$A_s$  = storage zone cross-sectional area [ $\text{m}^2$ ]

$C$  = in-stream solute concentration [ $\text{mass}/\text{m}^3$ ]

$C_s$  = storage zone solute concentration [ $\text{mass}/\text{m}^3$ ]

$D$  = dispersion coefficient [ $\text{m}^2/\text{s}$ ]

$Q$  = volumetric flowrate [ $\text{m}^3/\text{s}$ ]

$u$  = average flow velocity (m/s)

$\alpha$  = storage zone exchange coefficient [1/s]

We used a MATLAB™ replica of calibration module in OTIS (known as OTIS-P) to calibrate  $D$ ,  $A$ ,  $A_s$ , and  $\alpha$  based on an observed breakthrough curve obtained using tracer tests.

### Main Channel and Transient Storage

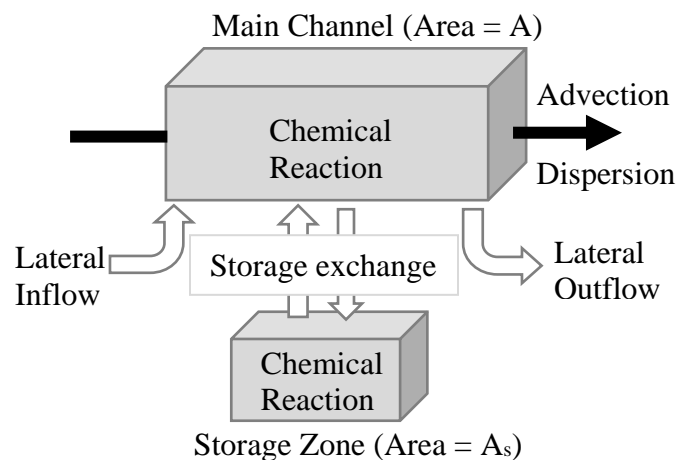


Figure 3.1. Conceptual representation of OTIS model showing main channel and transient storage zone processes (Runkel and Broshears, 1991).

Calibration parameters in the model include main channel cross-sectional area ( $A$ ), storage zone area ( $A_s$ ), storage exchange coefficient ( $\alpha$ ) and dispersion coefficient ( $D$ )

### 3.3.2 Meta-Analysis

Many tracer tests have been conducted in the past using both conservative and reactive tracers. A meta-analysis was done with 67 papers that reported calibrated or measured transient storage parameters based on tracer tests conducted around the world. All the papers used for this meta-analysis are listed in Appendix B. Overall, 834 individual parameter sets were logged into a database, along with available ancillary data. A wide range of parameter values from streams varying in hydrological and geomorphological characteristics were included (Figure 3.2). The storage parameters reported in the papers were obtained either using OTIS-P or by using trial-and-error approach and not necessarily evaluated for optimal models. This meta-analysis is based on the assumption that the reported values are the best set of parameters for the particular reach in question. Furthermore, the effect of different measurement methods used for measuring hydraulic variables was assumed to be negligible.

The dataset involves calibrated storage parameters from both pulse and constant-rate tracer injection studies. Storage parameters typically show different sensitivities to these two experiment types, with  $D$  showing higher sensitivity for pulse injection data and  $A_s$  showing higher sensitivity for constant rate injection data (Wlostowski et al., 2013). However, both types of injections were considered in the study to have a reasonable number of data points for both calibration and validation, and to propose regression equations that are applicable to both experiment types, similar to the OTIS model. We mined the dataset to develop relationships connecting  $A_s$ ,  $D$  and  $\alpha$  with independent variables, including flow width ( $w$ ), flow depth ( $d$ ), velocity ( $u$ ), discharge ( $Q$ ) and several combinations of these parameters. Existing equations to estimate storage parameters indicate that these parameters are rarely linear functions of hydraulic variables (Fischer, 1975; Harvey and Wagner, 2000). Therefore, transformed variables, such as log, exponential, and inverse,

were also included in the analysis. Correlations of  $D$ ,  $A_s$  and  $\alpha$  were tested with these independent variables and variables were eliminated if the absolute value of correlation coefficients were  $<0.1$ . Although shear velocity is frequently reported as an important variable in predicting  $D$ , it was ignored in our study due to (1) lack of data and (2) uncertainty induced by inaccurate channel slope measurement. Other channel metrics such as channel roughness or friction factor, sinuosity and channel slope were also omitted from the analysis since these variables are not always readily available for many streams, especially for large-scale studies. For each relationship developed, only those studies were used which reported all relevant variables. We kept the most parsimonious models without compromising on model performance.

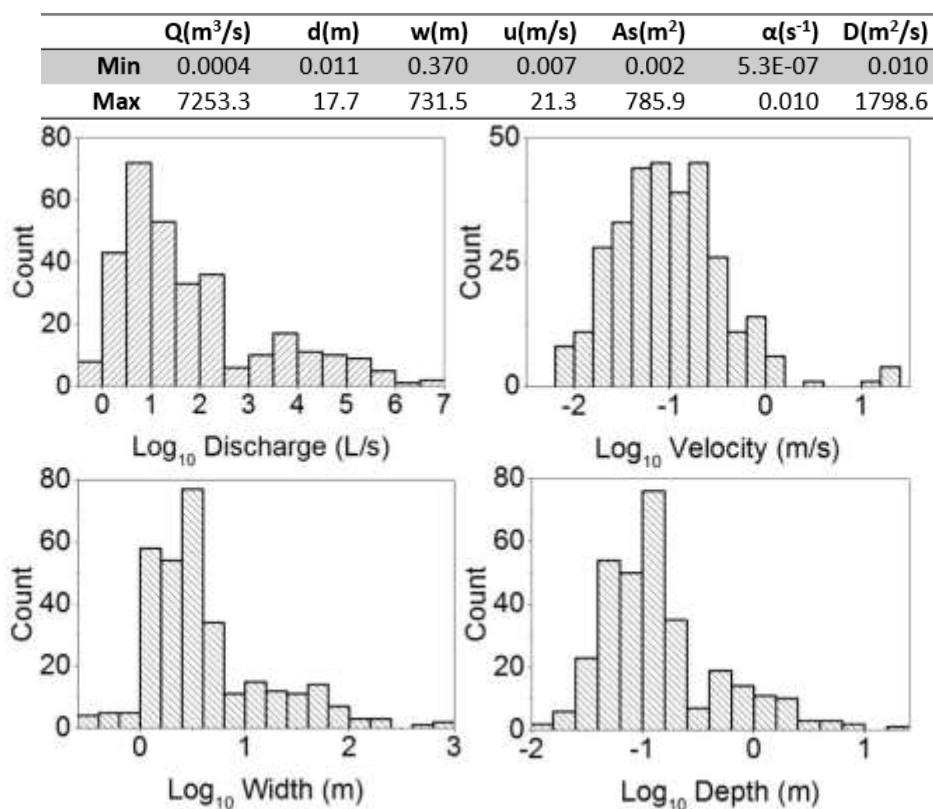


Figure 3.2. Frequency distribution of discharge, velocity, width and depth values used in regression analysis on a log scale.

Range (minimum and maximum) of actual parameter values used are given in the table above the figure.

Instead of using the entire data for regression analysis, the dataset was split randomly into two sets each for calibration and validation. Equations were first developed using calibration data and then validated for the remaining data. Our dataset included 309 data points for  $D$ , 316 points for  $A_s$  and 280 points for  $\alpha$ . We randomly selected 200 data points for calibrating  $D$  and the remaining 109 points were used for validation. Similarly, for  $A_s$  and  $\alpha$ , the number of calibration points were 200 and 180 respectively, and 116 and 100 respectively for validation. Pearson's correlation coefficients between storage parameters and independent variables were used for approximating initial structure of equations. Subsequently, a manual trial and error method was adopted to optimize the constants in the regression equations using the calibration data set for each storage parameter. The widely used performance indicators,  $R^2$ , Nash Sutcliffe Efficiency (NSE) and percent bias (PBIAS), were used to choose models with optimum performance. Past studies that developed regression equations for dispersion coefficient yielded  $R^2$  in the range of 0.06-0.86, with Fisher Equation yielding an  $R^2$  of 0.44 (Disley et al., 2015; Seo and Cheong, 1998). Power law fit between friction factor and  $A_s$  resulted in an  $R^2$  of 0.72 (Harvey and Wagener, 2000). Considering these statistics, we selected our models such that  $R^2$  and NSE between observed and modeled values were  $\geq 0.5$ . Using these indicators would result in multiple equations with similar performance due to equifinality issues. Hence, an additional criterion was utilized by visually inspecting scatter plots (between observed and modeled parameter values). Among the best models obtained using performance indicators, models that closely matches 1:1 regression line was chosen as the best fitted model.

In order to test the model for different geographical locations, the developed regression models were also validated using two additional sets of tracer test data, including breakthrough curves and

fitted storage parameters from: (1) streams draining forested catchments in the Hubbard Brook Experimental Forest (HBEF, Hall et al. 2002) and (2) streams draining the agricultural Kielstau catchment (this study). Hall et al. (2002) data was considered suitable for this study since it provided 35 sets of calibrated storage parameters and breakthrough curves generated from tracer experiments conducted in 13 different streams of the HBEF in New Hampshire, USA. Besides, this data would help validate the model for constant rate (1-3 hr) tracer injection tests. Experimental data collected from Kielstau catchment in Germany yielded 4 sets of breakthrough curves and storage parameters from two separate stream reaches. Detailed explanation of this experimental data is provided in section 3.3.3. Data from HBEF and Kielstau were used to validate the regression models developed during the meta-analysis phase of our study. All the observed breakthrough curves were compared to the regression equations predictions.

We also compared our newly developed regression models for each of the three storage parameters ( $A_s$ ,  $D$ , and  $\alpha$ ) to relationships commonly reported in the literature. For  $A_s$ , we used a relationship using a friction factor (Harvey and Wagner (2000), see Figure 3.3) and the widely used Fischer equation for  $D$  (Fischer et al., 1975; see equation 3.3). Shear velocity and friction factor are necessary inputs and were calculated using channel slope approximated from the DEMs of the corresponding watersheds since field-measured values were unavailable.

$$\frac{D}{du^*} = 0.011 \left(\frac{w}{d}\right)^2 \left(\frac{u}{u^*}\right)^2 \quad (3.3)$$

where  $D$  is dispersion coefficient ( $\text{m}^2/\text{s}$ ),  $d$  is average depth of flow (m),  $u^*$  is shear velocity (m/s),  $w$  is average stream width (m) and  $u$  is average stream velocity (m/s).

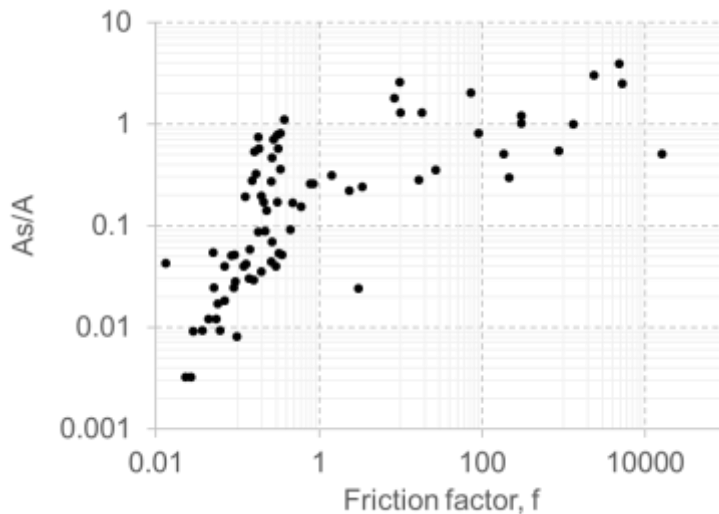


Figure 3.3. Ratio of storage zone area and stream cross-sectional area versus friction factor for tracer tests done on US reaches (Harvey and Wagner, 2000)

Since the variability in values of  $\alpha$  is very small (Harvey and Wagner, 2000), it was hypothesized that a constant value of  $\alpha$  will be a reasonable approximation. With the available literature data,  $\alpha$  was normally distributed with a mean value of  $-3.6$  and standard deviation of  $0.82$  on logarithmic scale (Figure 3.4). Based on this distribution, a value of  $\alpha = 2.5 \times 10^{-4} \text{ s}^{-1}$  was used to test the hypothesis by replacing the regression equation for  $\alpha$  with this constant value.

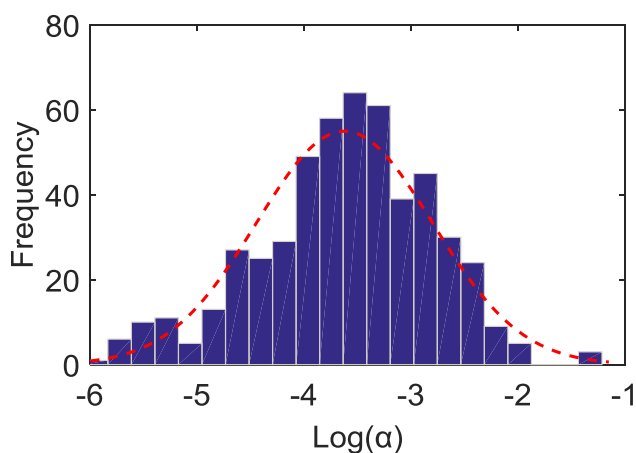


Figure 3.4. Frequency distribution of  $\log(\alpha)$  values for all meta-analysis data ( $n=517$ ) shows an approximate normal distribution with a mean value of  $\alpha = 2.5 \times 10^{-4} \text{ s}^{-1}$

Besides graphical interpretation of observed and modeled breakthrough curves, model performance was evaluated using multiple indicators such as  $R^2$ , NSE and percent bias (PBIAS). Because parameters are broadly distributed, we evaluated the model performance using logarithmic scales of predicted and measured values for better visualization and to avoid large relative error (Disley et al., 2015; Kashefipour and Falconer, 2002).

### **3.3.3 Experimental Instream Tracer Test**

We conducted four pulse tracer tests in the Kielstau catchment (Fohrer and Schmalz, 2012; Schmalz and Fohrer, 2010; Wagner et al., 2018), located in the federal state of Schleswig-Holstein in northern Germany (Figure 3.5). The Kielstau River is 17 km long and the catchment covers an area of about 50 km<sup>2</sup>. The topography is relatively flat and the land use is predominantly agriculture with cropland (64%) and grassland (20%); urban (11%), forest (3%) and water (2%) areas at considerable lower proportion. The outlet of the watershed is located near the gauging station at Soltfeld. Two instantaneous tracer injections were conducted in two similar order stream reaches towards the outlet of the watershed: (a) a 120 m long reach at Soltfeld gauging station and (b) a 135 m long reach at Freienwill (Figure 3.5, Table 3.1). Freienwill and Soltfeld stations have drainage areas of 48 km<sup>2</sup> and 50 km<sup>2</sup> respectively. The experimental locations were chosen considering factors such as storage potential in terms of vegetation, meandering nature of streams and accessibility for tracer injection and monitoring (Figure 3.6).

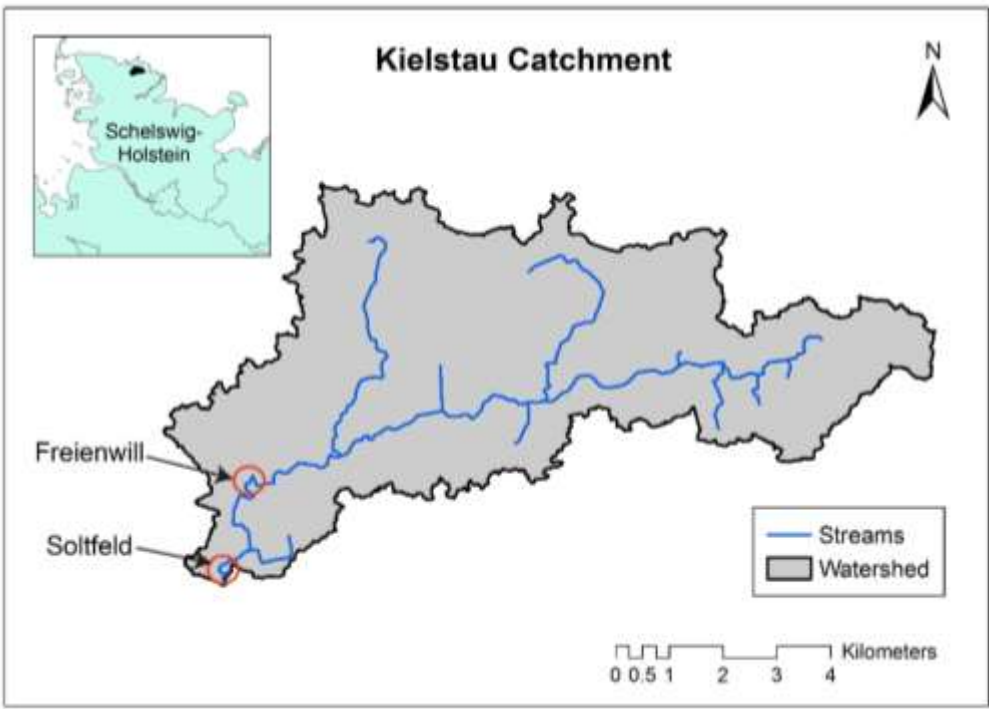


Figure 3.5. Study area (Kielstau Catchment in Northern Germany) with highlighted study reaches at Soltfeld and Freienwill



Figure 3.6. Soltfeld (left) and Freienwill (right) streams showing meandering patterns and transient storage potential with deposited logs and vegetation

Table 3.1. Reach data for tracer tests conducted in Kielstau catchment

Location/Date	Discharge (L/s)	Reach length (m)	D/s flow width (m)	D/s flow depth (m)	Background NaCl concentration (mg/L)
Soltfeld (10/10/2016)	124	120	3.5	0.35	298.2
Soltfeld (10/17/2016)	183	120	3.5	0.4	282
Freienwill (10/14/2016)	306	135	3.7	0.32	262.7
Freienwill (10/14/2016)	306	135	3.7	0.32	263.7

A salt solution was prepared with 8 kg of Sodium Chloride (NaCl) and 30 L stream water, and injected instantaneously at the upstream point of the reach. At the downstream point, specific conductivity was measured at 5 s intervals using YSI6600-V2 water quality sonde and salt concentrations calculated based on laboratory calibrations.

Wetted widths during baseflow conditions at the time of the experiments were 3.5 m and 3.7 m at downstream monitoring stations in Soltfeld and Freienwill respectively. At the same locations, water depths (measured from already installed stream gauges) were 0.35 m and 0.4 m respectively (Table 3.1). The two tracer tests at Freienwill were conducted on the same day during which the measured streamflow was 306 L/s. Tracer tests at Soltfeld were conducted on separate days with streamflows of 124 and 183 L/s. The two tests at Freienwill were conducted for the exact same stream conditions to test our equipment and to verify that the observed tracer data is free from measurement errors. The background NaCl concentrations at Soltfeld were 282 mg/L and 298.2 mg/L for the two test days, and at Freienwill it was 262.7 and 263.7 mg/L. Since there were no observable seeps or concentrated flow paths along the stream reaches, lateral inflow was assumed to be negligible for the short duration of the experiment

We used automatic calibration functionality in OTIS model (OTIS-P) to determine transient storage parameters using the observed breakthrough curves from the two Kielstau river reaches. Four sets of parameters were derived from this experiment. For both HBEF and Kielstau data, the fitted parameter values were compared to parameter estimates obtained using regression equations developed in this study. Besides, breakthrough curves simulated using calibrated and estimated parameter values were also compared. This was vital to evaluate the ability of regression equations to correctly predict key breakthrough curve characteristics such as peak concentration, time to peak and time to return to background.

### **3.4 Results and Discussions**

#### **3.4.1 Meta-Analysis**

Pearson's correlation coefficients between transient storage parameters and variables used for regression analysis show that  $u$ ,  $w$  and  $d$  are significantly correlated with the dispersion coefficient ( $r=0.58$  for  $u$ ,  $0.37$  for  $w$  and  $0.38$  for  $d$ ,  $p<0.001$ , Table 3.2). Storage zone area was highly correlated with  $\frac{Q}{d}$  and moderately correlated with width ( $r=0.85$  for  $\frac{Q}{d}$  and  $0.30$  for  $w$ ,  $p<0.001$ ). Storage exchange coefficient however had relatively smaller positive correlation with  $Q$  ( $r=0.31$ ,  $p<0.001$ ) and insignificant correlation with  $w$  and  $d$  ( $r=-0.11$ ,  $p=0.06$ ). Transformations of variables did not yield better correlation coefficients and hence were ignored for further equation development.

Based on these correlation relationships, non-linear regression analyses were carried out using various combinations of the correlated variables. Even though  $\alpha$  did not appear to be strongly correlated with the selected variables, all the three variables were retained to account for the most

possible variance. We used a trial and error approach to test different forms of equations based on correlation coefficients.

Table 3.2. Pearson's correlation coefficient between storage parameters and streamflow parameters.

Here 'u' is average velocity, 'w' is flow width, 'd' is flow depth, 'Q/d' is ratio of discharge to flow depth, 'D' is dispersion coefficient, 'As' is storage zone area and 'α' is storage exchange coefficient.

	D	As	Alpha
u	0.58	0	0.31
w	0.37	0.3	-0.11
d	0.38	0.19	-0.11
Q/d		0.85	

The formulae and constants were optimized to arrive at best fitting models using  $R^2$ , NSE and trend line in scatter plot as performance indicators. Equations 3.4, 3.5 and 3.6 are the newly proposed equations for D,  $A_s$  and  $\alpha$ .

$$D = 1.5uwd^{0.5} \quad (3.4)$$

$$\alpha = \frac{0.001u}{wd} \quad (3.5)$$

$$A_s = 0.1 \left[ 0.1w + \frac{Q}{d} \right]^{1.2} \quad (3.6)$$

where

u is average velocity (m/s), Q is the average stream flow ( $m^3/s$ ), w is stream width (m) and d is depth of flow (m). Performance of regression models were evaluated using log-log plots of reported parameters versus parameter values using the new equations (Figure 3.7, Table 3.3). For dispersion coefficient,  $R^2$ , NSE and PBIAS values were 0.87, 0.86 and -9.25% respectively in calibration. For validation data, equation for D performed equally well with  $R^2$ , NSE and PBIAS values of 0.86, 0.87 and 4.42% respectively. Regression model for storage zone area yielded a

reasonably fair calibration ( $R^2=0.74$ ,  $NSE=0.64$ ,  $PBIAS=-13.4\%$ ) and validation ( $R^2=0.71$ ,  $NSE=0.67$ ,  $PBIAS=15.9\%$ ). Considering the previously published  $R^2$  values for  $D$  and  $A_s$  (Disley et al., 2015; Harvey and Wagener, 2000), these models account for a large portion of the observed variance and could thus approximate storage parameters well. Equation for  $\alpha$  yielded the lowest values of  $R^2$  (0.52 in calibration; 0.46 in validation) and  $NSE$  (0.39 in calibration; 0.28 in validation) among the three storage parameters. This was expected based on the correlation analysis and supports our hypothesis that  $\alpha$  is not very sensitive to flow and stream geometry. As expected,  $\alpha$  values are clustered around the mean and the regression line is biased towards this value.

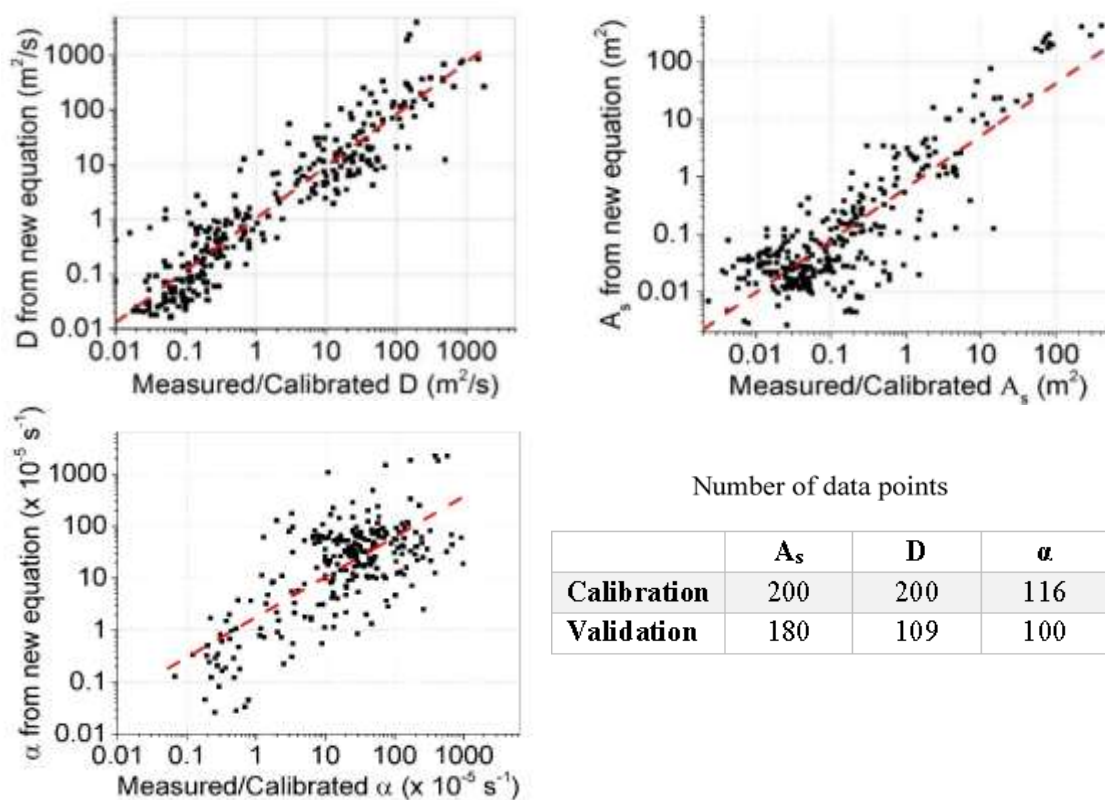


Figure 3.7. Transient storage parameters ( $A_s$ ,  $D$  and  $\alpha$ ) calculated from new regression equations versus measured/calibrated values for the entire calibration and validation data from meta-analysis

Table 3.3. Model performance indicators for newly developed regression equations.

$R^2$ , NSE and PBIAS were calculated on a logarithmic scale separately for calibration and validation data obtained from meta-analysis. 'n' represents the number of data points used in calibration and validation.

Parameter	Calibration				Validation			
	n	$R^2$	NSE	PBIAS	n	$R^2$	NSE	PBIAS
D	200	0.87	0.86	-9.25	109	0.86	0.87	4.42
$A_s$	200	0.74	0.64	-13.4	116	0.71	0.67	15.9
$\alpha$	180	0.52	0.39	-0.011	100	0.46	0.28	-2.21

### 3.4.2 Experimental Instream Tracer Test

Using data collected from tracer tests conducted in Kielstau river, four breakthrough curves were derived (Figure 3.10). The concentration of NaCl reached a peak of 126 and 134 mg/L above background at Soltfeld and 184 and 200 mg/L above background at Freienwill for the first and second tracer tests respectively. The concentrations returned to background conditions in approximately 20-30 mins at Soltfeld and within 15 mins at Freienwill. The parameters calibrated in OTIS-P showed relatively higher dispersion rate and storage exchange for Freienwill compared to the reach at Soltfeld; storage area however was relatively higher for Soltfeld reach (Table 3.4). This could be attributed to more geomorphic complexity (vegetation, large wood) in the Soltfeld reach.

Table 3.4. TSM-calibrated transient storage parameters for tracer tests at Soltfeld and Freienwill

Location/Date	C/S area, A (m <sup>2</sup> )	Storage area, $A_s$ (m <sup>2</sup> )	Dispersion coefficient, D (m <sup>2</sup> /s)	Transient storage coefficient, $\alpha$ (s <sup>-1</sup> )
Soltfeld (10/10/2016)	0.8709	0.2316	0.0830	0.0020
Soltfeld (17/10/2016)	0.9138	0.2309	0.1051	0.0028
Freienwill (14/10/2016)	0.6722	0.1548	0.2817	0.0052
Freienwill (14/10/2016)	0.6765	0.1592	0.1951	0.0061

Data from Hall et al. (2002) and Kielstau experiments were aggregated to get 39 sets of storage parameters. A comparison was done using D values obtained using Fischer equation,  $A_s$  values obtained from friction factor-relationship and a constant- $\alpha$  value (Figure 3.8).

For Kielstau data, our new equations performed relatively well in predicting  $A_s$ , but did not perform well in predicting D and  $\alpha$ . The over-prediction of D and under-prediction of  $\alpha$  with the new equation was possibly due to equifinality of the models as reported by previous researchers (Harvey and Bencala, 1993; Harvey et al., 1996; Harvey and Wagner, 2000; Wagener et al., 2002, Ward et al., 2017). This means that several parameter sets can lead to the same model performance and calibrated storage parameters may not be represent intrinsic characteristic of a given stream. For this study, OTIS-calibrated values for Kielstau were not evaluated in detail and OTIS could have possibly generated a different optimal set of parameters with higher D and lower  $\alpha$  value (as predicted by the new equations). For HBEF data, the new equations resulted in satisfactory prediction of all the three parameters. Considering the entire experimental dataset, our new equation and Fischer's equation behaved rather similarly in calculating D (Figure 3.8a), however the Fischer equation consistently under-predicted the low values of D.  $A_s$  estimated by our new equation was mostly in agreement with observed values, whereas values calculated using the friction factor relationship consistently over-predicted  $A_s$ . Overall, comparing observed and simulated values for both Kielstau and HBEF data, the regression models performed well for D with an  $R^2=0.66$ , NSE=0.36 and PBIAS=17%, compared to Fischer's equation which yielded an  $R^2=0.6$ , NSE=-4.13 and PBIAS=-68%. Slight decrease in  $R^2$  compared to that obtained in calibration is possibly due to the few over-predicted values D in HBEF and Kielstau. For  $A_s$ , with the new equation, percent bias was reduced to -22% as compared to 44% with friction factor

relationship. Estimating  $D$  from Fischer's equation and  $A_s$  from friction factor requires precise knowledge of channel slope and approximating the slope from DEMs may have led to the observed uncertainty. This suggests that in situations when channel slope is not well constrained by field measurements, predicting  $D$  and  $A_s$  using these existing methods may result in over or underestimation.

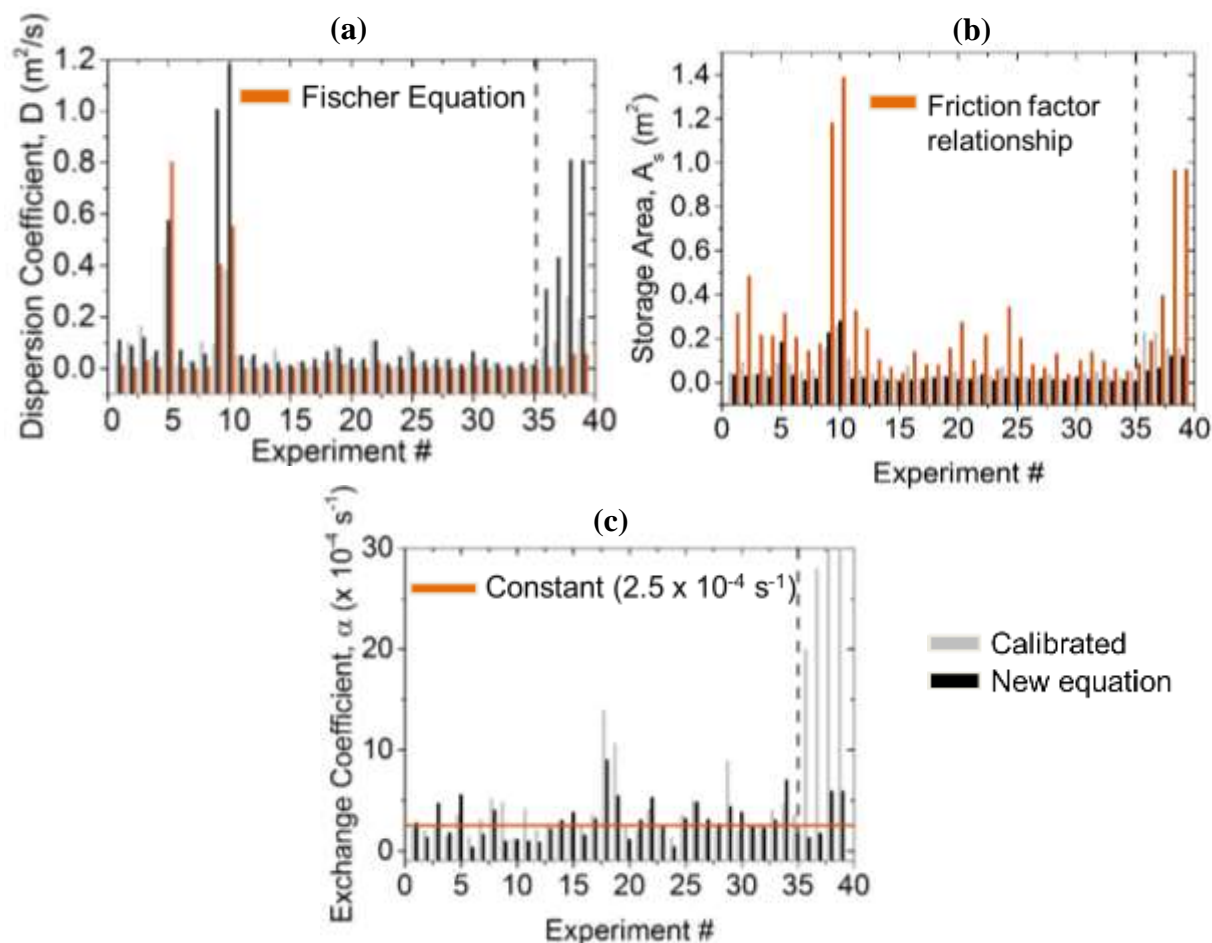


Figure 3.8. Comparison of storage parameters obtained using different equations when compared with calibrated values.

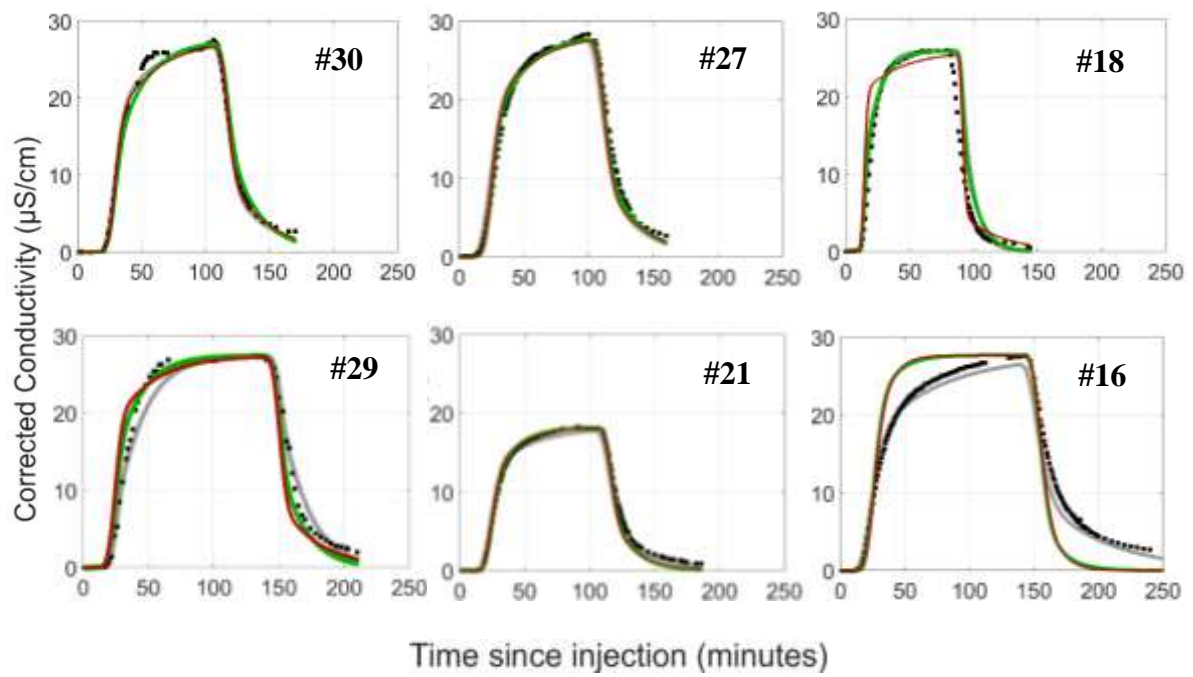
(a)  $D$  calculated using new equation and Fischer equation, (b)  $A_s$  calculated using new equation and friction factor relationship, (c)  $\alpha$  calculated using new equation, all versus calibrated values. The data points plotted are for Hubbard Brook and Kielstau data. Experiment #36-#39 represents Kiel Data. Calibrated values of  $\alpha$  for Freienwill is not plotted due to its high value ( $0.0052$  and  $0.0061 \text{ s}^{-1}$ )

While the new regression equation for  $\alpha$  seemed to have better predictive power than the constant value (Figure 3.8c), both the new equation and constant value yielded similar results in terms of performance indicators (NSE=-0.14 and PBIAS=-5.7% with new equation and NSE=-0.26 and PBIAS=-5.9% with constant value). Low values of NSE indicate that selected regression variables are not sufficient to explain the small variance in  $\alpha$  and additional stream characteristics may influence exchange between main channel and transient storage zone. An alternative explanation is that similar performance using both methods is due to little variation observed in range of  $\alpha$  values selected. Therefore, in scenarios where exchange coefficient does not vary significantly from the mean value, a constant value of  $2.5 \times 10^{-4} \text{ s}^{-1}$  could be used as a fair estimate provided no tracer data is available for precise calibration. This supports our hypothesis that a constant  $\alpha$  value could be sufficient for predicting transient storage for present test cases.

Representative observed and modeled (OTIS-P and new regression equations) breakthrough curves from HBEF and Kielstau catchments show reasonably good prediction (Figure 3.9 and 3.10). In most cases, performance indicators were calculated using data points along observed and modeled breakthrough curves. Out of the 39 cases,  $R^2$  was  $\geq 0.75$  for 97% of cases, NSE was  $\geq 0.75$  for 95% of the cases and PBIAS was within  $\pm 5\%$  of 77% of the cases. Our new models largely captured the peaks and dispersion of breakthrough curves. In a few cases, the curves were not well predicted (experiments #16 in Figure 3.9), which we attribute to under-prediction of  $A_s$ . Even though we saw discrepancy in estimated values of  $\alpha$  in regression plots (Figure 3.7), it does not seem to significantly affect the outcome in terms of breakthrough curves. The curves modeled with constant value of  $\alpha$  performed similarly to the ones predicted with the regression equation. For the 39 test cases,  $R^2$  values using the two  $\alpha$ -estimation methods differed very slightly within  $\pm 0.09$

and difference between NSE values were within  $\pm 0.1$ . Slight deviation of breakthrough curves predicted with constant  $\alpha$  value and regression equation was observed in a few cases (experiments #18 and #29 in Figure 3.9). This small deviation is seen for cases where the constant  $\alpha$  value ( $2.5 \times 10^{-4} \text{ s}^{-1}$ ) is significantly different from the values estimated using the regression equation. The negligible deviation again supports our hypothesis that a mean  $\alpha$  value of  $2.5 \times 10^{-4} \text{ s}^{-1}$  is adequate for predicting breakthrough curves with reasonable accuracy.

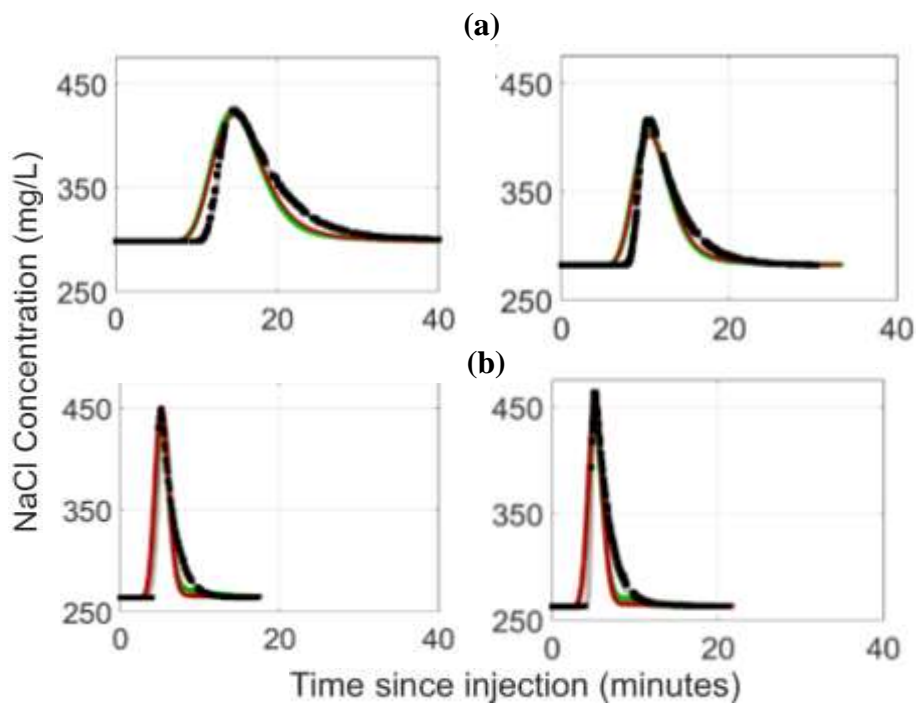
The model was able to capture the peaks well for Soltfeld breakthrough curves based on visual observation of Kielstau data (Figure 3.10). For Freienwill, there was slight under prediction of peak concentration values. The key difference in observed and modeled curves near the recession limb come from low values of exchange coefficient predicted by the regression models. Although predictions of dispersion coefficients and exchange coefficients for Kielstau data by the new equations were not as precise, the observed and modeled breakthrough curves matched reasonably well with  $R^2$  and  $\text{NSE} > 0.87$ , and  $\text{PBIAS}$  within  $\pm 2\%$  for all the four test cases. This validated the equifinality issue explained earlier. Breakthrough curves simulated using calibrated parameter values closely matched the observed curves in all cases due to complete calibration of the model. Since our study objective was to estimate the storage parameters with simple regression models, we did not anticipate perfect fits of observed and modeled breakthrough curves using the new equations. Rather, with our new regression equations, we were able to predict the general behavior of solutes traveling through a diverse array of streams with very simple, easily measurable attributes.



▪ Observed — Model(Hall et al., 2002) — Model(New Eqn) — Model(New Eqn+const alpha)

Figure 3.9. Observed and modelled breakthrough curves for few tracer tests conducted by Hall et al. (2002) at Hubbard Brook Experimental Forest.

Y-axis shows the conductivity values corrected for background concentration. Numbers on each plot represents the experiment number given to each of the 35 tracer tests.



- Observed — Model(OTIS-Calibrated) — Model(New Eqn) — Model(New Eqn+const alpha)

Figure 3.10. Observed and modeled breakthrough curves for Kielstau tracer tests conducted at (a) Soltfeld and (b) Freienwill.

Modeled curves are obtained using parameters that are either OTIS calibrated or estimated from the newly developed regression equations

### 3.5 Summary and Conclusions

Existing equations to calculate dispersion coefficient and storage area require accurate channel slope data and approximating the slope may lead to substantial discrepancies in prediction of  $D$  and  $A_s$  values. The new regression models developed in this study used readily obtainable flow and channel characteristics, including discharge, velocity, flow width and flow depth as independent variables. A meta-analysis of past tracer studies data showed that dispersion coefficient, transient storage area and storage exchange coefficients have significant correlation with few of these stream parameters. We used our regression equations to do forward modeling of breakthrough curves and show generally good agreement between modeled and observed data,

except for Kielstau Data when the exchange rate was particularly high ( $\alpha \geq 0.002$ ). Performance indicators showed that our newly developed equations can predict  $D$ ,  $A_s$  and  $\alpha$  better than other equations and with reasonable accuracy. Storage exchange coefficient was challenging to model with the available stream parameters indicating that it is either influenced by other factors or ill constrained during optimization. A constant mean value of  $\alpha$  when used in the TSM predicted the breakthrough curves similarly to the results obtained with the new equations. This supported our hypothesis that since variation of  $\alpha$  is small, a mean value should be a good approximation to model breakthrough curves. The fit between observed and a priori modeled breakthrough curves demonstrated that our equations could provide satisfactory approximation of storage parameters in many cases and that our method could thus be used where and when tracer data are not available. In predicting storage parameters, it is challenging to achieve high level of accuracy using simple regression models. The goal of this study hence was to provide preliminary estimates of these parameters for conducting modeling studies where field experiments are impossible. The equations proposed in this study is not intended to replace experiments and calibration and may not yield satisfactory results in studies that require precise estimation of transient storage parameters. In addition, we did not essentially attempt to predict ‘optimal’ storage parameters due to lack of sufficient studies reporting the same. However, these equations can prove useful for research that involves large scale solute transport modeling where parameter approximations are necessary. The parsimony of our regression models makes it easy to apply to any existing water quality models where transport with storage is desired.

### **3.6 Acknowledgments**

Funding for this study was provided by United State Department of Agriculture – National Institute of Food and Agriculture Regional Research Project S-1063. We would like to thank Dr. Robert

Hall for generously sharing the data of tracer tests conducted at Hubbard Brook Experimental Forest. We would also like to thank Johannes Fischer, Oliver Tank and the lab staff at Kiel University for their help in carrying out the tracer experiments.

### 3.7 References

- Ani, E., S. Wallis, A. Kraslawski, and P. Serban. (2009). Environmental Modelling & Software Development, calibration and evaluation of two mathematical models for pollutant transport in a small river, 24, 1139–1152. <https://doi.org/10.1016/j.envsoft.2009.03.008>
- Aris, R. (1956). On the dispersion of a solute in a fluid flowing through a tube. Proceedings of the Royal Society of London A: mathematical, physical and engineering sciences. Vol. 235. No. 1200.
- Bencala, K.E. and R.A. Walters. (1983). Simulation of solute transport in a mountain pool-and-riffle stream: A transient storage model: Water Resources Research, v. 19, no. 3, p. 718-724.
- Crank, J. The mathematics of diffusion. Oxford university press, 1979.
- Chen, D., M. Hu, R. A. Dahlgren. (2014). A dynamic watershed model for determining the effects of transient storage on nitrogen export to rivers. Water Resour Res.50: 7714–7730.
- Choi, J., J. W. Harvey & M. H. Conklin. (2000). Characterizing multiple timescales of stream and storage zone interaction that affect solute fate and transport in streams. Water Resources Research, 36(6), 1511–1518.
- Deng, Z. Q., L. Bengtsson, V. P. Singh, D. D. Adrian. (2001). Longitudinal dispersion coefficient in single-channel streams. Journal of Hydraulic Engineering 128(10): 901–916.
- Disley, T., B. Gharabaghi, A. Mahboubi, E. McBena (2015). Predictive equation for longitudinal dispersion coefficient Hydrol. Process., 29 (2) (2015), pp. 161-172, 10.1002/hyp.10139
- Elder, J. W. (1959). The dispersion of marked fluid in turbulent shear flow. Journal of fluid mechanics 5.4 (1959): 544-560.
- Fischer, H.B. (1975). Simple method for predicting dispersion in streams. Discussion by R.S. McQuivey and T.N. Keefer. Journal of Environmental Engineering Division, ASCE. 101(3): 453 – 455.
- Fohrer, N. & B. Schmalz. (2012). Das UNESCO Ökohydrologie-Referenzprojekt Kielstau-Einzugsgebiet - nachhaltiges Wasserressourcenmanagement und Ausbildung im ländlichen Raum. Hydrologie und Wasserbewirtschaftung 56(4): 160-168.

- Gooseff, M. N., D. M. McKnight, R. L. Runkel, and B. H. Vaughn (2003a), Determining long time-scale hyporheic zone flow paths in Antarctic streams, *Hydrol. Processes*, 17(9), 1691–1710, doi:10.1002/hyp.1210.
- Messetta, M.L., Hegoburu, C., Casas-Ruiz, J.P., Butturini, A., Feijoó, C. (2017). Characterization and qualitative changes in DOM chemical characteristics related to hydrologic conditions in a Pampean stream. *Hydrobiologia*, pp. 1-17. Article in Press.
- Gooseff, M. N., D. M. McKnight, R. L. Runkel, and B. H. Vaughn (2003). Determining long time-scale hyporheic zone flow paths in Antarctic streams, *Hydrol. Processes*, 17(9), 1691–1710, doi:10.1002/hyp.1210.
- Hall, R.O., E. S. Bernhardt, G. E. Likens. (2002). Relating nutrient uptake with transient storage in forested mountain streams. *Journal of the North American Benthological Society* 47:255–265.
- Harvey, J. W., and K. E. Bencala (1993). The effect of streambed topography on surface-subsurface water exchange in mountain catchments, *Water Resour. Res.*, 29(1), 89–98, doi:199310.1029/92WR01960.
- Harvey, J. W., B. J. Wagner, and K. E. Bencala (1996). Evaluating the reliability of the stream tracer approach to characterize stream-subsurface water exchange, *Water Resour. Res.*, 32(8), 2441–2451, doi:199610.1029/96WR01268.
- Harvey, J. W., and B. J. Wagner (2000). “Quantifying hydrologic interactions between streams and their subsurface hyporheic zones,” in *Streams and Groundwaters*, J. B. Jones and P. J. Mulholland (eds.), Academic Press, San Diego
- Jobson, H. E. (1996). Prediction of travel time and longitudinal dispersion in rivers and streams. Reston, VA: U.S. Geological Survey.
- Kashefipour, S. M. and R. A. Falconer RA (2002). Longitudinal dispersion coefficients in natural channels. *Water Research* 36: 1596–1608.
- Kelleher, C., T. Wagener, B. McGlynn, A. S. Ward, M. N. Gooseff, and R. A. Payn (2013). Identifiability of transient storage model parameters along a mountain stream, *Water Resour. Res.*, 49, 5290–5306, doi:10.1002/wrcr.20413.
- McQuivey, R. S. and T. N. Keefer. (1974). Simple method for predicting dispersion in streams. *Journal of Environmental Engineering Division ASCE* 100(4): 997–1011.
- Mueller Price, J. S., D. W. Baker, B. P. Bledsoe (2016). Effects of passive and structural stream restoration approaches on transient storage and nitrate uptake. *River Research and Applications* 32: 1542--1554. DOI: 10.1002/rra.3013.
- Mueller Price, J. S., B. P. Bledsoe, and D. W. Baker. (2014). Influences of sudden changes in discharge and physical stream characteristics on transient storage and nitrate uptake in an urban stream. *Hydrological Process*, 29(6), 1466-1479.

- Runkel, R.L. (1998), One-Dimensional Transport with Inflow and Storage (OTIS): A Solute Transport Model for Streams and Rivers: U.S. Geological Survey Water-Resources Investigations Report 98-4018, 73 p.
- Runkel, R. L., and R. E. Broshears. (1991). One dimensional transport with inflow and storage (OTIS): A solute transport model for small streams, Tech. Rep. 91-01, Cent. for Adv. Dec. Support for Water and Environ. Sys., Univ. of Colo., Boulder.
- Runkel, R. L. (2002). A new metric for determining the importance of transient storage. *Journal of the North American Benthological Society*, 21(4), 529–543.
- Schmalz, B. & N. Fohrer. (2010). Ecohydrological research in the German lowland catchment Kielstau. *IAHS Publ.* 336. 115-120.
- Scott, D. T., M. N. Gooseff, K. E. Bencala, & R. L. Runkel. (2002). Automated calibration of a stream solute transport model : implications for interpretation of biogeochemical parameters, 22(4), 492–510.
- Seo, I. W and T. S. Cheong. (1998). Predicting longitudinal dispersion coefficient in natural streams. *Journal of Hydraulic Engineering* 124(1): 25–32.
- Sheibley, R.W., J.H. Duff, and A.J. Tesoriero. (2014). Low transient storage and uptake efficiencies in seven agricultural streams: Implications for nutrient demand. *J. Environ. Qual.* 43:1980–1990. doi:10.2134/jeq2014.01.0034
- Stream Solute Workshop (1990). Concepts and methods for assessing solute dynamics in stream ecosystems, *J. North Am. Benthol. Soc.*, 9(2), 95– 119, doi:10.2307/1467445.
- Taylor, G. I. (1954). Diffusion and mass transport in tubes. *Proceedings of the Physical Society. Section B* 67.12: 857.
- Wagener, T., L. A. Camacho, and H. S. Wheater (2002). Dynamic identifiability analysis of the transient storage model for solute transport in rivers, *J. Hydroinformatics*, 94(3), 199–211, doi:10.1073/pnas.94.17.9171.
- Wagener, T., and H. Gupta (2005). Model identification for hydrological forecasting under uncertainty, *Stochastic Environ. Res. Risk Assess.*, 19(6), 378–387, doi:10.1007/s00477-005-0006-5.
- Wagner, B. J., & J. W. Harvey. (1997). Experimental design for estimating parameters of rate-limited mass transfer: Analysis of stream tracer studies. *Water Resources Research*, 33(7), 1731–1741.
- Wagner, P.D., Hörmann, G., Schmalz, B., Fohrer, N. (2018). Charakterisierung des Wasser- und Nährstoffhaushalts im ländlichen Tieflandeinzugsgebiet der Kielstau. *Hydrologie & Wasserbewirtschaftung*, 62(3), 145-158.

- Ward, A. S., Kelleher, C. A., Mason, S. J. K., Wagener, T., McIntyre, N., McGlynn, B., Runkel, R. L., Payn, R. A. (2017). A software tool to assess uncertainty in transient-storage model parameters using Monte Carlo simulations. *Freshwater Science* 2017 36:1, 195-217.
- Wlostowski, A. N., M. N. Gooseff, M. N., & T. Wagener. (2013). Influence of constant rate versus slug injection experiment type on parameter identifiability in a 1-D transient storage model for stream solute transport. *Water Resources Research*, 49(2), 1184–1188.

## 4. AN IMPROVED PROCESS-BASED REPRESENTATION OF STREAM SOLUTE TRANSPORT IN THE SWAT MODEL

### 4.1 Abstract

Hydrological models have long been used to study the interactions between land, surface and groundwater systems, and to predict and manage water quantity and quality. The Soil and Water Assessment Tool (SWAT) is often regarded as one of the most widely used hydrological models and can simulate various ecohydrological processes on land and subsequently route the water quality constituents through surface and subsurface waters. So far, in-stream solute transport algorithms of the SWAT model have only been minimally revised, even though it has been acknowledged that an improvement of in-stream process representation can contribute to better model performance with respect to water quality. In this study, we aim to incorporate a new and improved solute transport model into the SWAT model framework. The new process-based model was developed using in-stream process equations from two well established models - the One-dimensional Transport with Inflow and Storage (OTIS) model and the Enhanced Stream Water Quality Model (QUAL2E). The modified SWAT model (Mir-SWAT) was tested in a study area in Germany and the accuracy of its water quality predictions was evaluated. Compared to the standard SWAT model, Mir-SWAT improved dissolved oxygen (DO) predictions by removing extreme low values of DO (<6 mg/L) simulated by SWAT. Although no major change was observed for predicted nitrate loads, phosphate concentration peaks were reduced during high flows and a better match of daily predicted and measured values was attained using the Mir-SWAT model ( $R^2=0.17$ ,  $NSE=-0.65$ ,  $RSR=1.29$  with SWAT;  $R^2=0.28$ ,  $NSE=-0.04$ ,  $RSR=1.02$  with Mir-SWAT). In addition, Mir-SWAT performed better than the SWAT model in terms of Chlorophyll-*a* content particularly during winter months, improving the NSE and RSR for monthly average

Chl-*a* by 74% and 42% respectively. A single reach-scale analysis and a case study based on hypothetical point source loads were conducted to demonstrate the effectiveness of Mir-SWAT model for small-scale applications that require a precise representation of in-stream processes. With the new model improvements, we aim to increase confidence in the stream solute transport component of the model, improve the understanding of nutrient dynamics in the stream, and to extend the applicability of SWAT for reach-scale analysis and management.

## **4.2 Introduction**

Pollution of surface waters is viewed as a major environmental concern and is known to cause severe health problems for humans and aquatic life alike (Schwarzenbach, 2006; European Public Health Alliance, 2009; Geissen et al., 2015). Countries around the world continue to pass regulations and adopt resource management strategies to reduce water pollution. In the United States, over \$1 trillion has already been invested since the 1972 U.S Clean Water Act, but nearly half of the U.S streams and rivers still do not meet the required pollution standards (Keiser and Shapiro, 2018). Similarly, the European Water Framework Directive which was launched in 2000 with the goal of achieving good qualitative and quantitative status of all water bodies in the European Union is yet to meet its target with nearly 47 % of the water bodies failing to achieve the aim (European Commission, 2012). Besides industrial and domestic contaminants, nutrients from agricultural lands can impair freshwaters by accelerating eutrophication and subsequent growth of harmful algal blooms like the ones seen in Lake Erie and the Gulf of Mexico. Hydrological models are used to predict water quality conditions of streams and rivers by simulating various terrestrial and in-stream biogeochemical processes. These models are especially useful as a decision-making tool by helping simulate scenarios and assessing potential impacts of land use, land management, climate change (Chiang et al., 2010; Cibin et al., 2012; Hoque et al.,

2014; Wagner et al. 2015; Haas et al., 2017) on stream ecosystems. Accurate simulation of in-stream solute transport can not only help take timely measures in case of accidental spills, but also help stakeholders take necessary actions to alleviate long-term water quality impacts.

The Soil and Water Assessment Tool (SWAT) is a widely applied hydrological model developed by the U.S. Department of Agriculture's Agricultural Research Service and has been used to evaluate impacts of land use and climate change on hydrology and water quality (Arnold et al., 1998; Neitsch et al., 2011). Although several researchers have contributed to improving the model in the past, to the best of our knowledge, no significant efforts have been made to improve the in-stream water quality module in SWAT since the release of its first version. Additionally, previous studies have suggested the need to refine water quality algorithms in SWAT considering that the model's capability to predict water quality variables is relatively poor when compared to hydrological variables such as streamflow (Gassman et al., 2007; Migliaccio et al., 2007). The SWAT model uses equations from an existing water quality model known as The Enhanced Stream Water Quality Model (QUAL2E) for simulating the biochemical processes pertaining to water quality in stream reaches (Brown and Barnwell, 1987). Conventionally, QUAL2E is used as a reach-scale model that simulates sub-daily scale physical processes such as advection and dispersion as well as biochemical reactions using a finite difference approach. However, a modified version of QUAL2E is implemented in SWAT where advection and dispersion processes are ignored and only the biochemical reactions are simulated on a daily scale. Another key process affecting stream solute transport known as the transient storage exchange, which deals with the exchange of solutes between the slow-moving zones in the stream and the main channel, is also neglected in SWAT's in-stream water quality modeling. This process is proven to have significant

influence on the fate and transport of stream solutes and is a major component of many solute transport models including the popular One-dimensional Transport with Inflow and Storage (OTIS, Bencala and Walters, 1983; Runkel, 1998). Unlike the SWAT model which considers a stream reach as a single segment, the finite difference solution technique used in QUAL2E and OTIS divides the reaches into smaller segments and executes the algorithms at sub-daily scale. This approach is especially beneficial in feeding temporally and spatially distributed pollutant input to the model. To closely replicate the actual solute transport processes and to capture the fine structure of in-stream nutrient dynamics, it is therefore required to modify the SWAT model to include advection, dispersion, transient storage exchange and biochemical reaction processes, all at a finer scale both in terms of time and space.

Studies have been conducted in which the SWAT model was coupled with hydrodynamic models like Water Quality Analysis Simulation Program (WASP; Ambrose et al., 1988) and CE-QUAL-W2 (Cole and Wells, 2003) to model water quality in lakes and reservoirs (Debele et al., 2008; Park et al., 2013; Shabani et al., 2017). Such applications were mostly confined to external model coupling in which outputs from the SWAT model were directly fed into the water quality model with little or no changes made to the actual SWAT model. In this study, we propose a comprehensive refinement of the algorithms within the SWAT model so that the newly modified model will be user-ready for all SWAT model users.

Incorporating additional in-stream processes and reactions to any model essentially increases the number of model parameters and consequently the uncertainty associated with those parameters may also increase. Advection, dispersion and transient storage exchange processes are generally

modelled by calibrating stream parameters such as dispersion coefficient ( $D$ ), channel cross-sectional area ( $A$ ), storage zone area ( $A_s$ ) and storage exchange coefficient ( $\alpha$ ) with the help of tracer studies. Since these parameters are channel-specific and alter with changing hydrogeologic conditions, large-scale models often ignore these processes when used for simulating water quality in multiple streams over long time periods. Therefore, to include these processes in the SWAT model without having to perform additional parameter calibration, an alternative approach to estimate these parameters from easily obtainable stream channel metrics (Femeena et al., 2019a) is also considered in this study.

To address the research gaps mentioned above, the overall goal of this study is to improve in-stream solute transport process representation in the SWAT model. Specific objectives of the study are (1) to incorporate a newly developed physically based in-stream water quality model into SWAT, (2) to analyze the modified model's capability to predict water quality variables in streams and (3) to compare the model performances with and without the changes incorporated. By conducting validation studies on a study watershed in Germany, we envisage that an improvement in the in-stream solute transport representation is possible with simultaneous improvement in water quality predictions of SWAT model.

### **4.3 Methodology**

Equations representing solute transport processes such as advection, dispersion, transient storage exchange and biochemical reactions were combined from two models- OTIS and QUAL2E. The new and improved solute transport model was developed by solving these equations using a finite difference solution approach. In the earlier phase of this study, the model was validated at reach scale using (1) experimental data in two streams in northern Germany and (2) literature data

covering 15 stream reaches in different watersheds around the world (Femeena et al., 2019b). This paper focuses on incorporating the developed model into SWAT for modifying solute transport dynamics and for subsequent analysis of model performance on watershed scale.

#### **4.3.1 Study Area and Data**

The SWAT model was set up for the Kielstau watershed (Schmalz and Fohrer, 2010; Wagner et al., 2018) located in lowland area of Schleswig-Holstein in northern Germany (Figure 4.1). The 50 km<sup>2</sup> watershed is primarily dominated by arable (61%) and pasture land (21%) and the tile drainage fraction of agricultural area is estimated at 38% (Fohrer et al., 2007; Lie et al., 2019). A gauging station is located near the watershed outlet at Soltfeld where streamflow and water quality measurements are recorded at a daily resolution. For the SWAT model setup, daily streamflow data at this station from 2007 to 2016 were used. Water quality data comprising of sediment, dissolved oxygen (DO), nitrate (NO<sub>3</sub>-N), nitrite (NO<sub>2</sub>-N), ammonium (NH<sub>4</sub>-N), phosphate (PO<sub>4</sub>-P), Total-N, and Total-P concentrations for the years 2006 to 2016 were also available. Missing water quality data during the model simulation period (2010-2016) amounts to 5-8% of total days during this period. To validate the new water quality model developed in the initial part of the study, instantaneous tracer injections were conducted in two similar order stream reaches towards the outlet of the watershed: (a) a 120 m long reach at Soltfeld gauging station, and (b) a 135 m long reach at Freienwill (Figure 4.1).

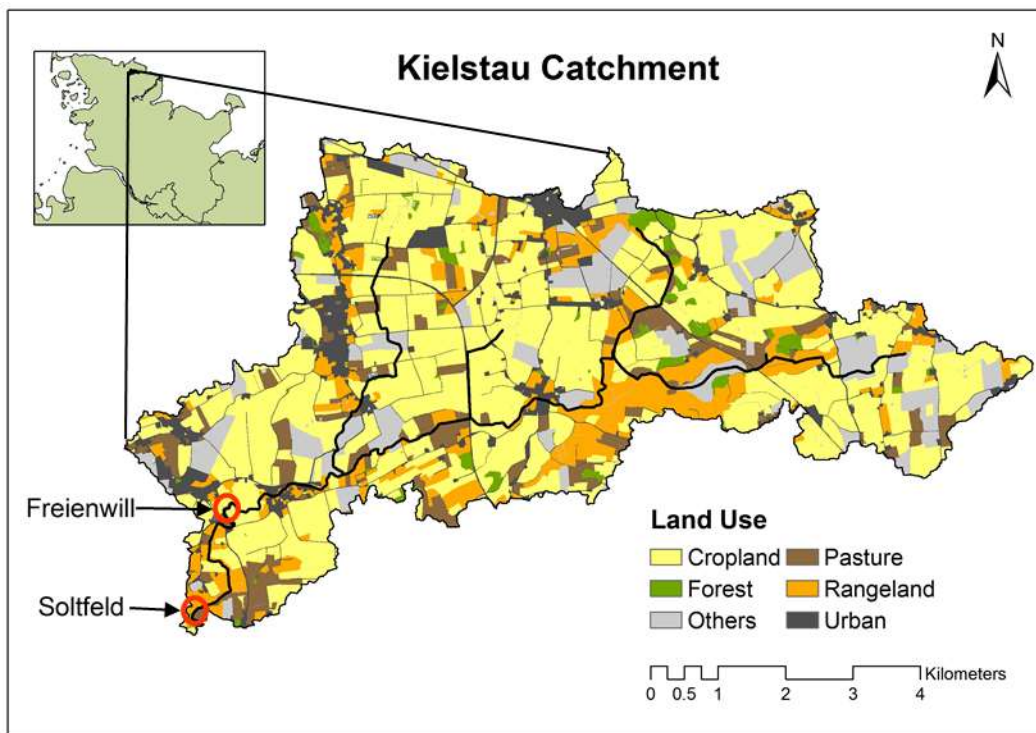


Figure 4.1. Study area: Kielstau Catchment in Northern Germany with highlighted study reaches at Soltfeld and Freienwill where tracer injections were conducted.

#### 4.3.2 SWAT Model Calibration and Validation

The SWAT model for the Kielstau watershed was set up using soil map with a resolution of 1:200 (BGR, 1999) and a 5m x 5m digital elevation model (LVerMA, 1995). Land use data was generated from a mapping campaign conducted in 2011/2012 and based on that, 13 different crop rotations were implemented in the model (Pfannerstill et al., 2014). Auto fertilization option in SWAT model was used in the cropped areas of the catchment. Precipitation data was obtained through measurements taken at Moorau gauging station by Department of Hydrology and Water Resources Management in Kiel University (Wagner et al., 2018). Remaining climate data such as temperature, wind speed and solar radiation were obtained from DWD (German Meteorological Office). The model divides the watershed into smaller subbasins, which are further divided into a

number of homogeneous units known as Hydrologic Response Units (HRU) based on unique combinations of soil, slope, and land use. Watershed delineation resulted in 9 subbasins and 709 HRUs with stream reaches ranging from 137 m to 5400 m in length. The model was run for 10 years from 2007 to 2016 with the first three years as warm up period model and calibrated using the available streamflow and water quality data. The parameters needed for model calibration were selected based on previous SWAT model studies in the same watershed and using the recommended list provided in the user's manual (Kiesel et al., 2010; Pfannerstill et al., 2014; Schmalz and Fohrer, 2010). The complete list of calibration parameters is given in Table C.1 (Appendix C). Streamflow calibration was carried out using daily results at the watershed outlet for five years from 2010-2014 and subsequently validated for 2 years from 2015-2016. Sediment, nitrate, and phosphate were also calibrated and validated for the same years. Since the major focus of this study was not to obtain a well-calibrated model, but to compare a reasonably performing model's effect on modified in-stream algorithm, water quality calibration was only carried out on a monthly scale. Performance metrics such as  $R^2$ , Nash Sutcliffe Efficiency (NSE) and ratio of root mean squared error to standard deviation (RSR) were used to evaluate the calibrated model's performance. Best performing models typically have  $R^2$  and NSE values close to 1 and RSR close to 0. All the calibration was done on Purdue University's high performance computing cluster using an effective optimization algorithm known as Multi-Objective Genetically Adaptive Method (AMALGAM; Vrugt and Robinson, 2007), that uses multiple optimization algorithms in parallel to produce the best optimal parameter set. Basin level parameters that have a single value throughout the watershed as well as HRU-specific and subbasin-specific parameters were used for calibration. NSE was used as the objective function for calibration and the best set of parameters

were obtained when AMALGAM converged to a point where NSE did not show any improvement between consequent iterations.

### 4.3.3 Modified SWAT Model (Mir-SWAT)

The newly developed stream solute transport model combines OTIS and QUAL2E algorithms based on the governing equations given below with equation 4.1 representing main channel dynamics and equation 4.2 representing storage zone dynamics. These two models were specifically chosen due to their long-term popularity in solute transport and water quality modeling applications. Most of the other existing models use various combinations of processes included in these two models.

$$\frac{\partial C}{\partial t} = D \frac{\partial^2 C}{\partial x^2} - u \frac{\partial C}{\partial x} + \alpha(C_s - C) - \frac{dC}{dt} \quad (4.1)$$

$$\frac{\partial C_s}{\partial t} = -\alpha \frac{A}{A_s} (C_s - C) - \frac{dC_s}{dt} \quad (4.2)$$

where  $\frac{\partial C}{\partial t}$  = total change in main channel solute concentration [mg/L/s],  $\frac{\partial C_s}{\partial t}$  = total change in storage zone solute concentration [mg/L/s],  $A$  = stream channel cross-sectional area [m<sup>2</sup>],  $A_s$  = storage zone cross-sectional area [m<sup>2</sup>],  $C$  = in-stream solute concentration [mg/L],  $C_s$  = storage zone solute concentration [mg/L],  $D$  = dispersion coefficient [m<sup>2</sup>/s],  $u$  = average flow velocity [m/s],  $\alpha$  = storage zone exchange coefficient [s<sup>-1</sup>],  $\frac{dC}{dt}$  = change in main channel solute concentration due to growth and decay [mg/L/s] and  $\frac{dC_s}{dt}$  = change in storage zone solute concentration due to growth and decay [mg/L/s].

The above two equations are derived from the original OTIS model except that the first-order decay process in OTIS is substituted with  $\frac{dC}{dt}$  and  $\frac{dC_s}{dt}$  which represents all the biochemical reactions from QUAL2E. The solutions to these equations are derived through a finite-difference approach in which each stream reach is divided into finer stream segments ( $\Delta x$ ) and concentrations are determined in these segments at each time step ( $\Delta t$ ). The solution approach used in our model is the Forward Difference Centered Space (FTCS) scheme, in which concentrations at any location for a future time step ( $C$  at  $x_i, t_{j+1}$ ) are calculated from concentrations at adjacent locations for current time step ( $C$  at  $(x_{i-1}, t_j)$ ,  $(x_i, t_j)$  and  $(x_{i+1}, t_j)$ ) (Equation 4.3)

$$C_{i,j+1} = \left( \frac{u\Delta t}{2\Delta x} + \frac{D\Delta t}{\Delta x^2} \right) C_{i-1,j} + \left( 1 - 2 \frac{D\Delta t}{\Delta x^2} - \right) C_{i,j} + \left( -\frac{u\Delta t}{2\Delta x} + \frac{D\Delta t}{\Delta x^2} \right) C_{i+1,j} + \frac{dC}{dt} + \alpha(C_{s,i,j} - C_{i,j}) \quad (4.3)$$

where  $\Delta x = x_{i+1} - x_i$  and  $\Delta t = t_{i+1} - t_i$

This solution is only stable for the conditions:  $0 \leq \frac{D\Delta t}{\Delta x^2} \leq 2$  and  $0 \leq \frac{u\Delta t}{\Delta x} \leq 2(1 - \frac{D\Delta t}{\Delta x^2})$

Conventionally, parameters  $A_s$ ,  $\alpha$  and  $D$  are calibrated for any given reach by conducting tracer experiments and monitoring the movement of tracers at downstream locations over a period of time. For watershed scale studies, such reach-specific calibration is not feasible due to the number of streams under consideration. Therefore, previously tested regression equations to estimate these parameters were included in our model (Equations 4.4, 4.5 and 4.6; see also Femeena et al., 2019a). These equations rely on stream geometry and streamflow to get approximate values of  $A_s$ ,  $\alpha$  and  $D$  for any given stream.

$$D = 1.5uwd^{0.5} \quad (4.4)$$

$$\alpha = \frac{0.001u}{wd} \quad (4.5)$$

$$A_s = 0.1 \left[ 0.1w + \frac{Q}{d} \right]^{1.2} \quad (4.6)$$

where  $u$  is average velocity (m/s),  $Q$  is the average stream flow ( $\text{m}^3/\text{s}$ ),  $w$  is stream width (m) and  $d$  is depth of flow (m).

Computer code for SWAT model is written in FORTRAN programming language in which several inland and channel-based modules run and interact with each other. The new solute transport model that we developed on MATLAB platform acts as a stand-alone model that can be run independently or in coupled-form with other models. To account for the syntax changes when transferring between different programming languages, the model code was slightly modified as per FORTRAN syntax rules, incorporated into SWAT and linked to other modules in the model (Fig 4.2). The existing source code file in FORTRAN that serves as the in-stream solute transport module for SWAT model has the name ‘watqual.f’ and it interacts with other terrestrial land modules to route the subbasin loads. This module was replaced with the new ‘watqual\_new.f’ file that includes all the new model improvements. In the following sections, this modified version of SWAT model will be referred to as “Mir-SWAT” for “Modified in-stream routing in SWAT”. Two major changes were made to the existing model- (a) changing values of few QUAL2E parameters and (b) adding advection, dispersion and transient storage processes to the existing algorithms using a finite-difference solution approach. During initial testing of our solute transport model, using information from existing popular water quality models, Femeena et al. (2019b) obtained a generalized set of QUAL2E parameter values that gave reasonable results for most of the test cases studied. Hence, this new set of values were also used in Mir-SWAT for consistency

(Table C.2, Appendix C). We also checked for any change in existing SWAT model results with the old and new parameter sets. When the model runs, nutrient and algal loads from each subbasin is provided as input to 'watqual\_new.f' module on each day. The developed stand-alone solute transport model was completely based on sub-daily input and sub-daily process simulation. But, SWAT model users typically use daily scale results due to lack of sub-daily input data, and hourly simulation feature of SWAT is still under development especially with regard to nutrient loads generated in subbasins. Therefore, this study only used the daily flow and nutrient loads from the subbasin and uniformly distributed it throughout the day. The new version can hence be easily used by users to run SWAT on daily timestep. As an improvement over the existing model which uses the entire subbasin load at the upstream of every reach, subbasin loads are uniformly distributed across the reach in Mir-SWAT to replicate non-point source pollution. Additionally, concentration values within each reach segment remaining at the end of the day are passed on to the next day. Using values of streamflow, flow width and flow depth obtained from other modules in the model, parameters  $A$ ,  $A_s$ ,  $\alpha$ , and  $D$  are computed within 'watqual\_new.f'. In the past, a few changes have been made to the QUAL2E equations in the 'watqual.f' module of SWAT model, especially pertaining to dissolved oxygen. To be consistent with the equations used in our in-stream water quality model, these changes were ignored and all equations for N, P,  $O_2$  and algal dynamics have instead been adopted from the original QUAL2E model. The time and distance discretization for each reach was determined based on the stability conditions for FTCS scheme with timesteps ranging from 30 s to 360 s and reach segments of 100 m or 200 m length. Finite-difference solution approach used in Mir-SWAT requires each water quality variable to be represented in matrix form with time represented in columns and distance represented in rows, which is different from the existing SWAT model framework that has a single value of each

variable for any given day. The new code thus has the feature to output the matrix form of concentrations for any water quality variable in the model, so that users have the option to see concentrations for any time step in any segment of the reach. This approach however makes Mir-SWAT computationally much more time consuming when compared to the existing model. On average, for the study watershed, a single day simulation took 3 sec to run with SWAT and 3 minutes with Mir-SWAT. The entire set of modified parameter values along with complete code changes are provided Appendix C. No further calibration of the model was done for parameters used in Mir-SWAT.

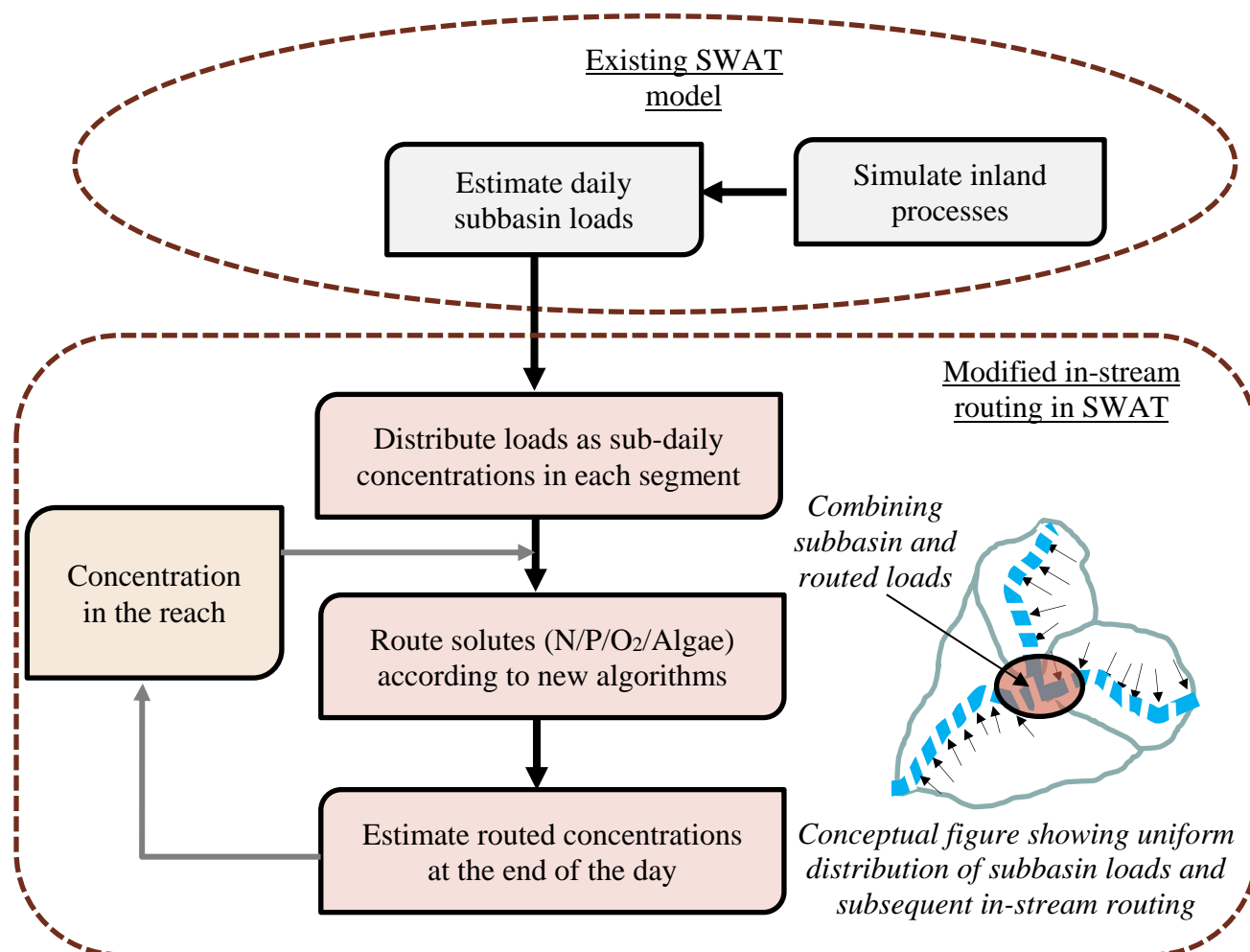


Figure 4.2. Flowchart showing the Mir-SWAT model framework and modified routing algorithms

Results of SWAT model and Mir-SWAT model for both uncalibrated and calibrated model simulations of Kielstau watershed were obtained in this study. Focus of this study was on the calibrated model performance and all the data provided in the results section are from the calibrated model. Studying calibrated model results enables us to comprehend whether the new modified model performs better or worse than the existing one when compared to measured data. Concentrations/loads of various water quality variables such like DO, PO<sub>4</sub>-P, NO<sub>3</sub>-N and Chl-*a* (chlorophyll-*a*) were separately evaluated for the last two years of study (2015-2016). A shorter duration of two years was used in this part of the study due to the high computational time associated with Mir-SWAT runs. For Chl-*a*, measured data from field samples collected at the watershed outlet from July 2009 to December 2010 were used to qualitatively assess the model's performance (Wu et al., 2014). These data were used for qualitative analysis assuming that the summary statistics of Chl-*a* concentrations will not show significant change over a period of a few years. Reach-based analysis at a finer time scale was also carried out in an upstream stream reach of subbasin 1 (length = 2,677 m), in which changes in concentrations of nutrients, oxygen, and algae were studied by running the model for few days of the year 2013. This analysis also considered how varying subbasin nutrient loads for each day affect the biogeochemical processes and subsequently the reach solute concentrations. Matrix output of each water quality variable was used to understand the change in concentrations along the reach for each hour of the day. QUAL2E has long been used to study the effect of such pollutants on downstream waters but since the SWAT version of QUAL2E runs on daily scale and ignores the sub-daily processes such as advection, dispersion and transient storage, it is difficult to use it to study impacts of sub-daily scale point-source loads. In many cases, point source discharge take place for few hours of the day and this detail cannot be incorporated into exiting SWAT model since it takes only daily or monthly

average point-source loads. As a case study, we therefore created a hypothetical scenario where a point source load of 5 mg/L NO<sub>3</sub>-N is injected for 2 hours in the upstream-most point of same reach. This specific study intends to demonstrate that the Mir-SWAT can precisely model solute transport and help study sub-daily reach dynamics if there are point source loads within the watershed.

#### **4.4 Results and Discussions**

The SWAT model for the Kielstau watershed was calibrated for streamflow, sediment, nitrate, and phosphate in the given order using model parameters listed in Table C.1 (Appendix C). Daily streamflow statistics and monthly statistics for sediment and nutrients at the watershed outlet demonstrate a good calibrated model with R<sup>2</sup> values well above 0.5 during both calibration and validation periods (Table 1). Except for few extreme storm events, streamflow was very well predicted by the model, and sediment, nitrate and phosphate also showed reasonable agreement with measured data, with phosphate performing the lowest amongst all (Figure 4.3). Although the extent of SWAT calibration and number of parameters used varies across studies, we used a reasonably calibrated model in this study to check if model improvements could relatively increase the performance of the model. To understand how the new QUAL2E parameter set affects the SWAT model, time series plots of water quality variables obtained with default and new set of QUAL2E parameter values are given in Appendix C (Figure C.1 and C.2). The new Mir-SWAT model included various other code changes in addition to this change in parameter values. Subsequent analysis in this study is therefore based on Mir-SWAT model runs with all code modifications included.

Table 4.1. Performance statistics of calibrated SWAT model for Kielstau catchment during calibration (2010-2014) and validation (2015-2016) periods.

Scale of calibration is given in the variable column.

Variable	2010-2014			2015-2016		
	R <sup>2</sup>	NSE	RSR	R <sup>2</sup>	NSE	RSR
<b>Streamflow-Daily</b>	0.83	0.81	0.43	0.81	0.78	0.46
<b>Sediment-Monthly</b>	0.77	0.70	0.55	0.69	0.62	0.61
<b>NO<sub>3</sub>-Monthly</b>	0.76	0.64	0.60	0.85	0.77	0.48
<b>PO<sub>4</sub>-P-Monthly</b>	0.70	0.31	0.89	0.79	0.68	0.88

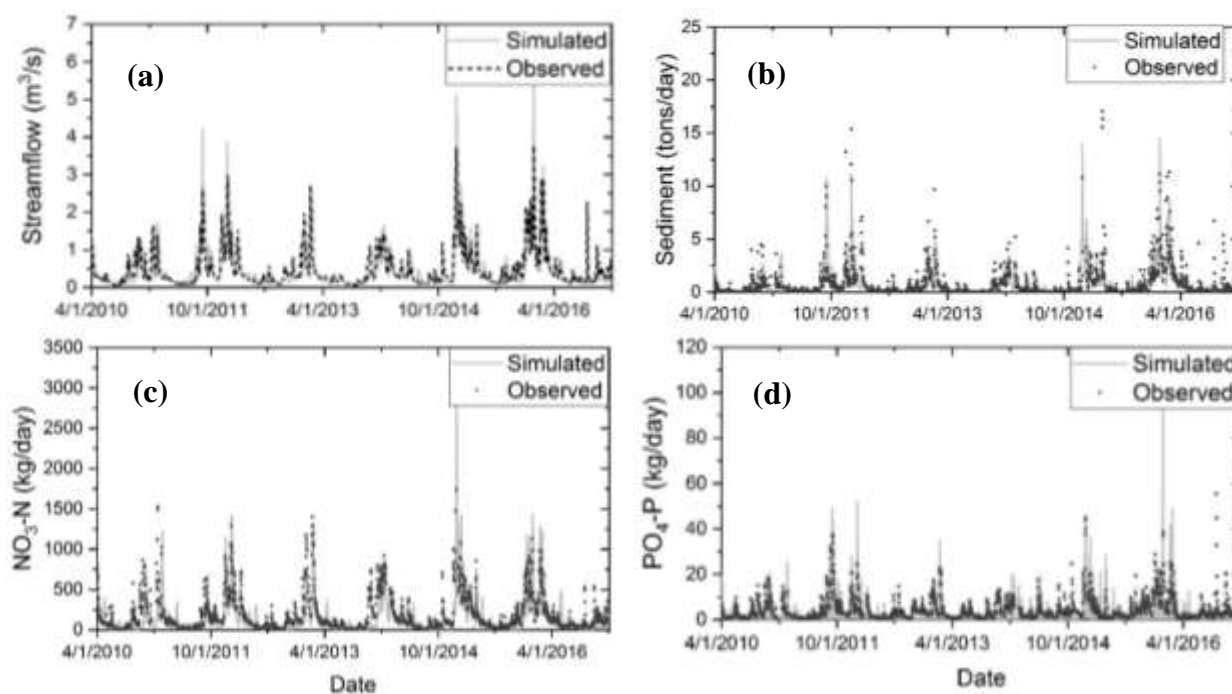


Figure 4.3. Simulated and observed time series data for (a) streamflow , (b) sediment, (c) nitrate and (d) phosphate at Soltfeld station (watershed outlet).

Due to gaps in measured water quality data, values are given as points instead of line in (b), (c) and (d).

#### 4.4.1 Time Series Analysis

Evaluation of SWAT and Mir-SWAT model predictions were carried out by plotting daily concentration/loads of different water quality variables at the watershed outlet for years 2015-2016 after running the model from 2012 to 2016 with initial 3 years as warm up period. Algae, nitrogen, and phosphorus dynamics are highly influenced by the amount of dissolved oxygen in the streams and hence DO predictions play a critical role in representing in-stream biochemical processes. Using existing calibrated SWAT model simulation, dissolved oxygen concentrations showed very high daily fluctuations in the range of 0-14 mg/L, with values less than 6 mg/L during 12% of the days (Figure 4.4). For the same time period, measured DO concentrations varied between 5.8 and 14.8 mg/L. Although, higher values of DO follow the trend in measured DO, the extreme low values during several days show significant deviation of up to 10 mg/L from the measured values. With Mir-SWAT, we were able to eliminate these low values without affecting the overall seasonal trend in concentrations. By using the simulated values for days during which observed data was available, coefficient of determination between measured and modelled values was 0.07 with SWAT and 0.28 with Mir-SWAT (NSE reduced from -2.41 to -0.66 and RSR reduced from 2.16 to 1.51). Since DO is not typically calibrated for SWAT studies, a high value of  $R^2$  and NSE was not expected for the calibrated SWAT model, but an improvement in the metrics with the Mir-SWAT model shows that the new model representation enhances the DO prediction accuracy. Changes made to DO and CBOD (carbonaceous biological oxygen demand) equations of 'watqual.f' module as well as better representation of solute dynamics in our new model is expected to have contributed to this difference in model performances. The reaeration rate parameter (rk2) used in existing 'watqual.f' module has a value of  $1 \text{ day}^{-1}$  within the source code which overwrites the value of  $50 \text{ day}^{-1}$  used in the water quality input file ('basins.wwq'). To examine whether the change in this parameter value caused the large deviations in simulated values,

we used  $rk2=50 \text{ day}^{-1}$  inside the source code and found that DO predictions were only slightly improved with higher  $rk2$  value. In this case, the minimum DO value was 4 mg/L, but  $R^2$  value showed only a very small increase from 0.07 to 0.13. From figure 4.4, it is clear that the simulated DO values from Mir-SWAT follow the same trend as observed values, but have slightly higher values. Calibrating QUAL2E parameters related to reaeration and deoxygenation may result in better match between observed and modeled values. However, without testing Mir-SWAT for other watersheds, it is difficult to conclude whether this DO behavior is consistent across different watersheds and if additional QUAL2E parameter changes are necessary. Compared to the existing model, the new Mir-SWAT model with original QUAL2E equations predicts stream conditions that are closer to reality and could further be used in the study with reasonable confidence.

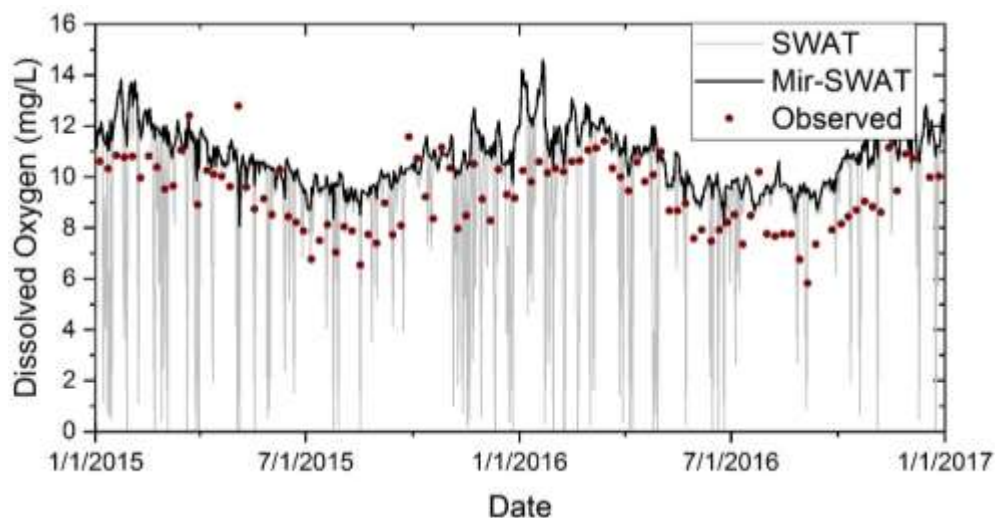


Figure 4.4. Dissolved oxygen concentrations at the watershed outlet with SWAT and Mir-SWAT models along with discrete measured values during 2015-2016.

The calibrated SWAT model reasonably simulates phosphate loads in the outlet reach during low flows, but also overpredicts the values during high flows (Figure 4.5). With the new Mir-SWAT model, daily  $R^2$  statistic between observed and modelled values was only marginally increased

from 0.17 to 0.28 and daily RSR was only reduced from 1.28 to 1.02, but it is critical to note that the simulated peak values of  $\text{PO}_4\text{-P}$  were lowered for high flow events, in some cases even decreasing it by 20-50 kg/day, as shown in Figure 4.5 for two storm events in 2015 and 2016. Since fresh water systems are mostly phosphorus limited, several other processes such as algal growth are largely affected by the concentration of phosphate in streams. Bringing the phosphate values within the measured data range thus enhances the confidence in the overall model. Nitrate loads in the outlet reach did not show any major change after running with calibrated SWAT and Mir-SWAT models similar to our findings when only the parameter values were changed in the SWAT model (Figure C.3., Appendix C). This suggests that reach nitrate concentrations are largely influenced by subbasin loads and streamflow, and unlike phosphate, once the model is well calibrated for streamflow and subbasin loads, in-stream water quality parameters have very little effect on nitrate concentrations. Another possible reason is that with relatively higher values of  $\text{NO}_3\text{-N}$  compared to  $\text{PO}_4\text{-P}$ , algae prefers phosphate over nitrate (phosphate limiting conditions), resulting in very low or negligible nitrate uptake.

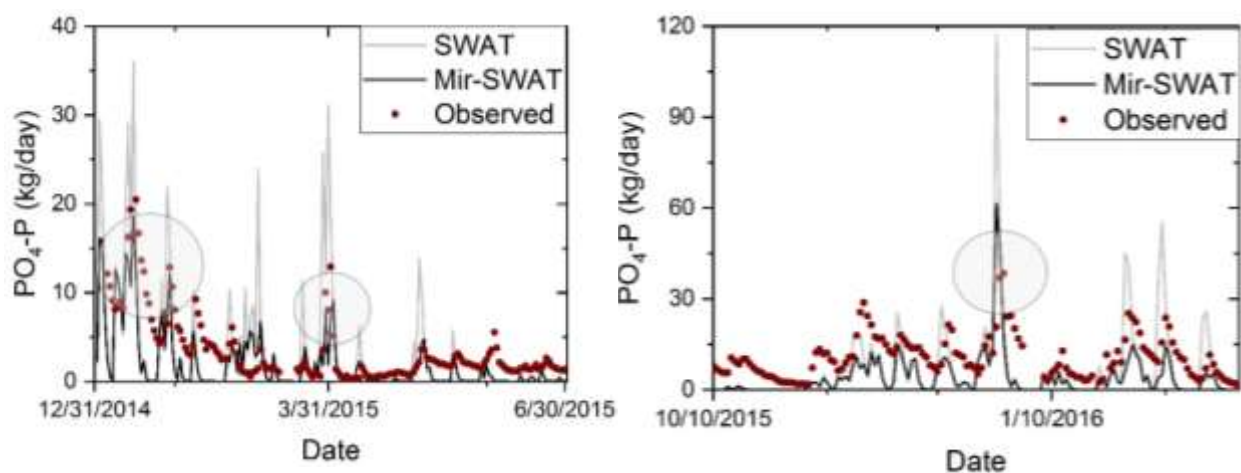


Figure 4.5.  $\text{PO}_4\text{-P}$  concentrations at the watershed outlet with SWAT and Mir-SWAT models along with discrete measured values, enlarged to show the results during two storm events in 2015 and 2016.

Algal growth dynamics in the model was evaluated based on qualitative analysis of Chl-*a* concentrations at the outlet. Observed monthly average and maximum Chl-*a* concentrations for the years 2009-2010 fall in the range of 1-7  $\mu\text{g/L}$  and 5-22  $\mu\text{g/L}$ , respectively (Figure 4.6). The existing SWAT model simulates high concentrations of average Chl-*a* of up to 15  $\mu\text{g/L}$  especially during winter months. Similarly, maximum Chl-*a* values go up to 220  $\mu\text{g/L}$  with SWAT model. The new Mir-SWAT model simulates Chl-*a* values that better resemble the observed summary data (Avg: 0-3.5  $\mu\text{g/L}$  and Max: 0-64  $\mu\text{g/L}$ ). For the months of November-February, NSE for average monthly Chl-*a* increased from -16.39 to -0.89 and RSR decreased from 4.17 to 1.37 with the Mir-SWAT model improvements. Similarly, for the same winter months, NSE for maximum Chl-*a* increased from -404.14 to -31.06 and RSR decreased from 20.12 to 5.66. Although both SWAT and Mir-SWAT fail to accurately predict average Chl-*a* values for many months, Mir-SWAT helps to eliminate extremely high concentrations of Chl-*a* that can have an impact on nutrient uptake and other biochemical reactions in the stream.

Besides evaluating water quality variables, Mir-SWAT provides an opportunity to study time-series analysis of transient storage parameters such as dispersion coefficient ( $D$ ), storage zone area ( $A_s$ ) and storage exchange coefficient ( $\alpha$ ). When exact calibration of these parameters with tracer experiments is unfeasible or if it is required to determine their approximate values for past or futuristic scenarios, by running Mir-SWAT, users will be able to derive a time-series data of  $D$ ,  $A_s$  and  $\alpha$  (Figure C.4, Appendix C). These results may, in turn, open up opportunities for further studies that relate storage parameters to hydrological and water quality variables in streams.

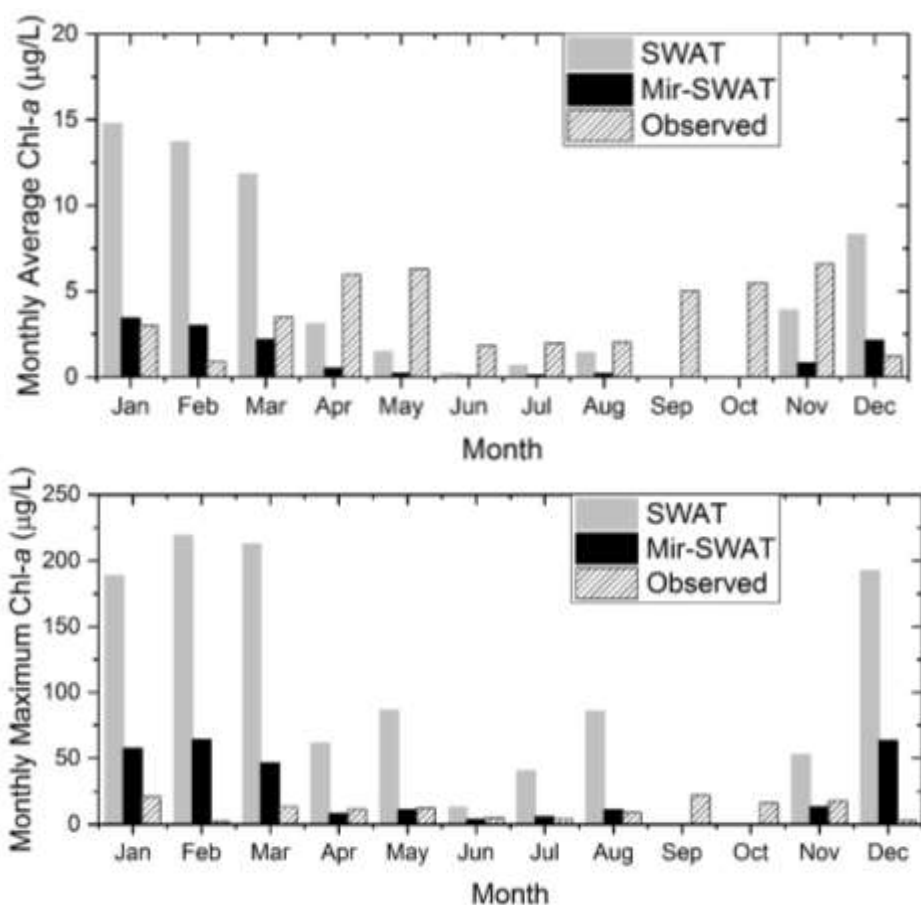


Figure 4.6. Average and maximum concentrations of Chl-a at the watershed outlet with SWAT and Mir-SWAT models for different months during 2015-2016.

Observed values shown are from summary statistics obtained for the years 2009-2010 (Wu et al., 2014).

#### 4.4.2 Reach-Scale Analysis

The developed Mir-SWAT model has advantages over the SWAT model especially in scenarios where reach-scale analysis is required. To demonstrate this and to evaluate the model's ability to represent stream processes on a finer scale, outputs for a single reach in subbasin 1 were extracted after simulating the model for few days of the year 2013. Figure 4.7 illustrates the varying concentrations of algae, nitrate and phosphate along the stream reach and over a 24-hour time period. The SWAT model currently gives the end-of-day concentrations as a single value for the

entire reach as shown in Figure 4.7. As expected from the form of equations used in QUAL2E for algal growth, nitrate and phosphate uptake, these plots follow an exponential/polynomial trend. For this particular case study, we observed 37 mg/L reduction in algal concentration with the Mir-SWAT model compared to 20 mg/L with the SWAT model over a 24-hour duration. Phosphate concentration showed a temporal increasing trend with Mir-SWAT (0.03 to 0.09 mg/L) and decrease in concentration with SWAT (0.03 to 0 mg/L). Reduction in algal concentration may have potentially resulted in lower phosphate uptake by the algae and subsequent increase in PO<sub>4</sub>-P concentration. With the matrix-format output given by the Mir-SWAT model, concentration can be determined for any water quality variable modeled in SWAT during any time and in any reach segment, within the constraints of the time and distance step used in the finite-difference solution. Assessing the reduction in nutrients over a period of time will also allow users to analyze temporally and spatially varying nutrient uptake in the stream, which is a significant metric for ecohydrological studies in streams.

Relationship between daily concentrations of DO and PO<sub>4</sub>-P in the reach reinforces the argument that at extremely low values of DO, PO<sub>4</sub>-P predictions are negatively impacted (Figure 4.8). While the phosphate load input to the reach increases from 0.006 to 0.027 mg/L over a 4-day time period, with existing SWAT model simulations, the end-of-reach phosphate value suddenly decreases from 0.02 mg/L on day 28 to 0 mg/L on day 29 and 30. Such Conversely, the Mir-SWAT model does not show such strong reduction in DO and predicts an increasing trend in phosphate values within the reach similar to the input phosphate values.

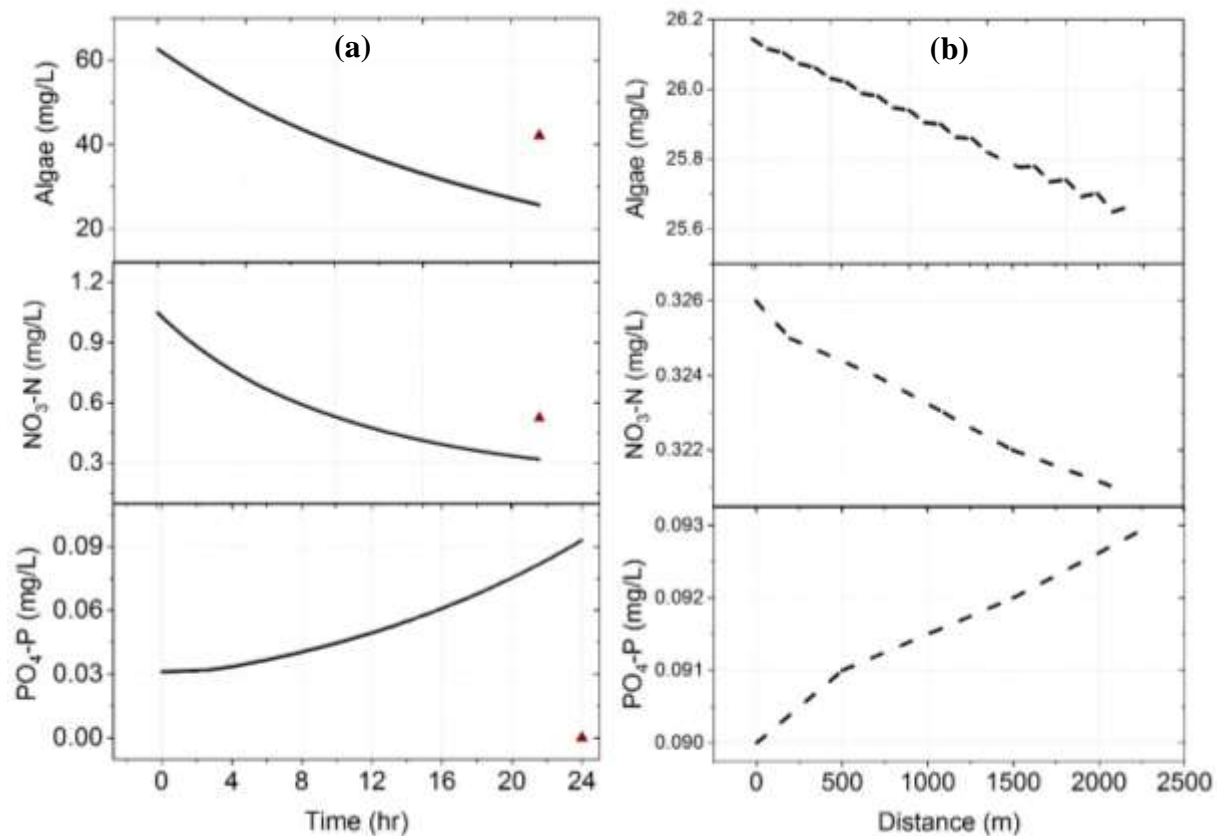


Figure 4.7. Algae, nitrate and phosphate concentrations (a) at the end of the stream reach within subbasin 1 over the 24-hour time period and (b) along the reach at the end of the day, on 01/30/2013 using Mir-SWAT model.

Triangle shaped points represent the end-of-day reach value given by SWAT model.

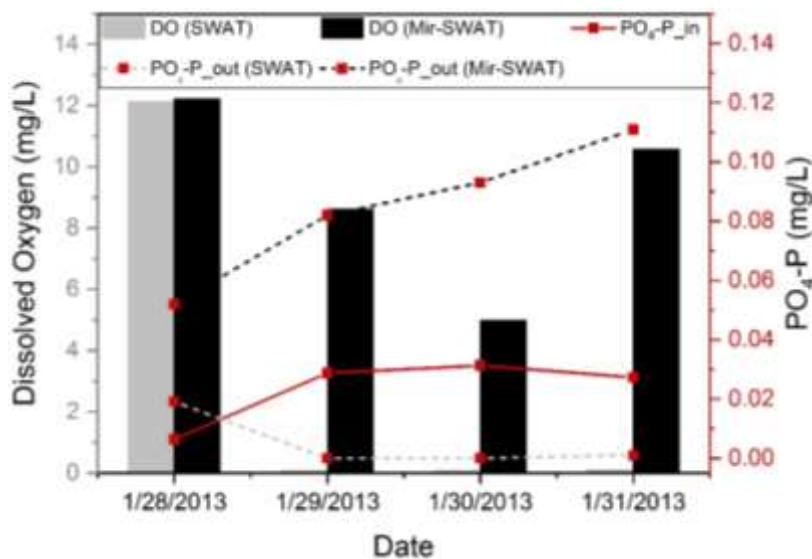


Figure 4.8. Dissolved Oxygen (bars) and PO<sub>4</sub>-P concentrations in the reach for days 28 to 31 of January 2013 using SWAT and Mir-SWAT models.

Solid line represents input PO<sub>4</sub>-P coming from subbasin into the reach and dotted lines represent concentrations at the end of the reach with SWAT and Mir-SWAT respectively

#### 4.4.3 Point Source Load Scenario

Sub-daily simulation of in-stream solute transport can be useful to monitor the transport of point-source loads such as industrial effluents being discharged at certain points in the stream. With Mir-SWAT, point source discharge occurring for <24hr duration can be given as input to the model. After simulating a hypothetical scenario with 2-hr nitrate injection (5 mg/L) and looking at the nitrate concentration at the end of the reach over a 24-hour time period, the breakthrough curve clearly shows the movement of the point source load with peak at 7<sup>th</sup> hour (Figure 4.9). The peak value of 4 mg/L shows the reduction from actual load of 5 mg/L owing to dispersion and transient storage. These outputs can be used to understand the peak concentration and timing of pollutants reaching any specific point in the reach, which can further act as a decision-making tool and help in taking necessary actions. For long-term model simulations, such sub-daily fluctuations may not be of great concern and the existing model may provide approximate results assuming distributed 24-hr point-source discharge. However, with the new model improvements, the aim is to make

SWAT model useful in applications that were earlier not possible. By including the key in-stream sub-daily processes into the SWAT model, we anticipate that the model can be used with higher confidence for both small-scale reach studies as well as for large-scale watershed level studies.

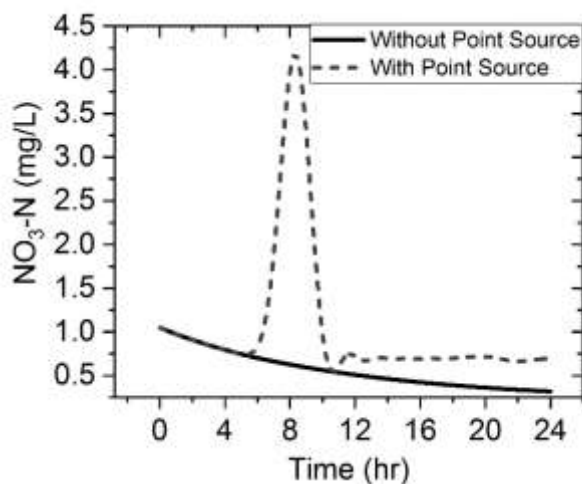


Figure 4.9. Concentration versus time plot for reach within subbasin 1 when a hypothetical point source load of 5 mg/L nitrate was discharge at the beginning of the reach for 2 hours.

#### 4.5 Summary and Conclusions

Since its introduction in 1993, the SWAT model has undergone several improvements in the past to enhance the model representation of processes such as soil dynamics, crop growth, and water and nutrient transport (Arnold et al., 2010; Tuppad et al., 2011; Trybula et al., 2015). Except a few changes made to dissolved oxygen reactions, no major improvements were made to in-stream solute transport processes in the SWAT model which still runs on equations adopted from QUAL2E water quality model. With the aim of improving water quality predictions and to better simulate realistic stream transport processes, this study incorporated a newly developed water quality model into the SWAT framework to replace the existing algorithms. With the inclusion of advection, dispersion and transient storage exchange processes, the modified model (Mir-SWAT) provides users with the option to study sub-daily and reach-scale stream dynamics.

In this paper, we changed the algal-growth based parameter values in the model based on a previous study and additionally incorporated our newly developed model in SWAT source code format. SWAT and Mir-SWAT models exhibited different behaviors in uncalibrated and calibrated models. This study used calibrated model's results to test the reliability of Mir-SWAT and to compare it to SWAT. A major improvement was made for dissolved oxygen predictions, in which extreme low values predicted by SWAT were completely removed with Mir-SWAT. This improvement is further expected to enhance the overall stream nutrient and algal growth dynamics. Based on a qualitative analysis, average and maximum monthly concentrations of Chl-*a* was also better simulated with Mir-SWAT especially for winter months, when SWAT simulated relatively high values of Chl-*a*. While nitrate concentrations did not show any significant changes with the new model improvements, phosphate load peaks were reduced and thus closer to measured values with Mir-SWAT simulations. Reach-scale analysis carried out in this study demonstrated the model's capability to analyze sub-daily concentrations for each reach segment and the potential to evaluate temporally and spatially varying nutrient uptakes which is currently not possible with the SWAT model. A scenario analysis showing the sub-daily and reach-scale variation of nutrient concentrations as a result of a point-source load highlighted that the improved Mir-SWAT model can have extensive applications in small scale and localized studies. The present study did not consider sub-daily changes in flow and nutrient loads generated from subbasins since the hourly N/P simulations in SWAT are still under development stage and hourly climate data may not always be available if users intend to use the new model for other studies. With better quality sub-daily input data that provides the actual amounts of N, P, algae and O<sub>2</sub> flowing into the reach during each hour of the day, reliability of Mir-SWAT model can be further evaluated.

Most watershed scale models ignore the small-scale stream processes due to increased complexity that may increase the computational time without significant improvement in model predictions for long-term simulations. The newly developed Mir-SWAT model enhances the process representation in streams at the cost of increased simulation time. Therefore, using this model to simulate large watersheds for a large number of years may require significant additional time when compared to the default model. By altering the coding configuration, we expect to reduce the simulation time to some extent but finite different solution approach at hourly scale for small reach segments will definitely incur significantly higher computational time. We therefore recommend using this version of Mir-SWAT for smaller watersheds and shorter time periods until further code revisions are made.

#### **4.6 Acknowledgments**

Funding for this study was provided by United State Department of Agriculture – National Institute of Food and Agriculture Regional Research Project S-1063. We would like to thank Jeba Princy and Matthias Pfannerstill for sharing the earlier version of the SWAT model for Kielstau watershed.

#### **4.7 References**

- Ambrose, R., Wool, T., Connolly, J., Schanz, R. (1988). WASP4, A Hydrodynamic and Water Quality Model – Model Theory, User’s Manual, and Programmer’s Guide. URL [https://www.researchgate.net/publication/236507717\\_WASP4\\_A\\_Hydrodynamic\\_and\\_Water\\_Quality\\_Model\\_-\\_Model\\_Theory\\_User's\\_Manual\\_and\\_Programmer's\\_Guide](https://www.researchgate.net/publication/236507717_WASP4_A_Hydrodynamic_and_Water_Quality_Model_-_Model_Theory_User's_Manual_and_Programmer's_Guide) (accessed 1.8.19).
- Anderson, D.M., Glibert, P.M., Burkholder, J.M. (2002). Harmful algal blooms and eutrophication: Nutrient sources, composition, and consequences. *Estuaries* 25, 704–726. <https://doi.org/10.1007/BF02804901>
- Arnold, J.G., Srinivasan, R., Muttiah, R.S., Williams, J.R. (1998). Large Area Hydrologic Modeling and Assessment Part I: Model Development1. *JAWRA J. Am. Water Resour. Assoc.* 34, 73–89. <https://doi.org/10.1111/j.1752-1688.1998.tb05961.x>

- Arnold, J. G., Gassman, P. W., White, M. J. (2010). New Developments in the SWAT Ecohydrology Model. 21st Century Watershed Technology: Improving Water Quality and Environment Conference Proceedings, 21-24 February 2010, Universidad EARTH, Costa Rica 701P0210cd.(doi:10.13031/2013.29393)
- Bencala, K., Walters, R. (1983). Simulation of Solute Transport in a Mountain Pool-and-Riffle Stream: A Transient Storage Model. *Water Resour. Res.* - WATER RESOUR RES 19, 718–724. <https://doi.org/10.1029/WR019i003p00718>
- BGR. (1999). Bundesanstalt für Geowissenschaften und Rohstoffe - Bodenübersichtskarte im Maßstab 1:200.000. Verbreitung der Bodengesellschaften.
- Brown, C. L., Barnwell, T. (1987). The enhanced stream water quality models QUAL2E and QUAL2E-UNCAS: documentation and user manual. Environ. Prot. Agency.
- Chiang, L., Chaubey, I., Gitau, M. W., Arnold, J. G. (2010). Differentiating impacts of land use changes from pasture management in a CEAP watershed using the SWAT model. *Trans. ASABE*, 53 (5), pp. 1569-1584
- Cibin, R., Chaubey, I., Engel, B. (2012). Simulated watershed scale impacts of corn stover removal for biofuel on hydrology and water quality. *Hydrol Process* 26:1629–1641
- Cole, T., Wells, S. (2003). CE-QUAL-W2: A Two-dimensional, Laterally Averaged, Hydrodynamic and Water Quality Model, Version 3.1. Civ. Environ. Eng. Fac. Publ. Present.
- Debele, B., Srinivasan, R., Parlange, J.-Y. (2008). Coupling upland watershed and downstream waterbody hydrodynamic and water quality models (SWAT and CE-QUAL-W2) for better water resources management in complex river basins. *Environ. Model. Assess.* 13, 135–153. <https://doi.org/10.1007/s10666-006-9075-1>
- European Public Health Alliance. (2009). Air, Water Pollution and Health Effects.  
Retrieved from <http://www.who.int/ceah> (accessed 03.21.2019)
- European Commission (2012). Report from the Commission to the European Parliament and the Council on the Implementation of the Water Framework Directive (2000/60/EC) River Basin Management Plans. Retrieved from <https://eur-lex.europa.eu/legal-content/EN/TXT/PDF/?uri=CELEX:52012DC0670&from=EN> (accessed 03.21.2019)
- Femeena, P.V., Chaubey, I., Aubeneau, A., McMillan, S., Wagner, P.D., Fohrer, N. (2019a). Simple regression models can act as calibration-substitute to approximate transient storage parameters in streams. *Adv. Water Resour.* 123, 201–209. <https://doi.org/10.1016/j.advwatres.2018.11.010>
- Femeena, P V., Chaubey, I., Aubeneau, A., Fohrer, N., McMillan, S., Wagner, P. D. (2019b). Merging OTIS and QUAL2E models to develop an enhanced physically-based model for nutrient transport in streams (in peer-review)

- Fohrer, N., Schmalz, B., Tavares, F., Golon, J. (2007). Modelling the landscape water balance of mesoscale lowland catchments considering agricultural drainage systems. *Hydrol. Wasserbewirtschaftung/Hydrology Water Resour. Manag.-Ger.* 51, 164–169.
- Gassman, P., Reyes, M., Green, C., Arnold, J. (2007). The Soil and Water Assessment Tool: Historical Development, Applications, and Future Research Directions. *Trans. ASABE* 1211–1250. <https://doi.org/10.13031/2013.23637>
- Geissen, V., Mol, H., Klumpp, E., Umlauf, G., Nadal, M., van der Ploeg, M., van de Zee, S.E.A.T.M., Ritsema, C. J. (2015). Emerging pollutants in the environment: A challenge for water resource management *ISWCR*, 3 (2015), pp. 57-65, DOI: 10.1016/j.iswcr.2015.03.002
- Haas, M., Guse, B., Fohrer, N (2017). Assessing the impacts of Best Management Practices on nitrate pollution in an agricultural dominated lowland catchment considering environmental protection versus economic development, *J. Environ Manage.* 196, 347-364, doi:10.1016/j.jenvman.2017.02.060.
- Heil, C.A., Steidinger, K.A. (2009). Monitoring, management, and mitigation of *Karenia* blooms in the eastern Gulf of Mexico. *Harmful Algae, Understanding the causes and impacts of the Florida Red Tide and improving management and response* 8, 611–617. <https://doi.org/10.1016/j.hal.2008.11.006>
- Heisler, J., Glibert, P.M., Burkholder, J.M., Anderson, D.M., Cochlan, W., Dennison, W.C., Dortch, Q., Gobler, C.J., Heil, C.A., Humphries, E., Lewitus, A., Magnien, R., Marshall, H.G., Sellner, K., Stockwell, D.A., Stoecker, D.K., Suddleson, M. (2008). Eutrophication and harmful algal blooms: A scientific consensus. *Harmful Algae, HABs and Eutrophication* 8, 3–13. <https://doi.org/10.1016/j.hal.2008.08.006>
- Hoque, Y. M., Cibir, R., Hantush, M. M, Chaubey, I., Govindaraju, R. S. (2014). How do land-use and climate change affect watershed health? A scenario-based analysis *Water Qual. Expo. Health*, 6 , pp. 19-33
- Keiser, D.A., Shapiro, J.S. (2018). Consequences of the Clean Water Act and the Demand for Water Quality. *Q. J. Econ.* <https://doi.org/10.1093/qje/qjy019>
- Kiesel, J., Fohrer, N., Schmalz, B., White, M.J. (2010). Incorporating landscape depressions and tile drainages of a northern German lowland catchment into a semi-distributed model. *Hydrol. Process.* 24, 1472–1486. <https://doi.org/10.1002/hyp.7607>
- Lei, C., Wagner, P.D., Fohrer, N. (2019). Identifying the most important spatially distributed variables for explaining land use patterns in a rural lowland catchment in Germany , *Journal of Geographical Sciences* (accepted)
- LVerma. (1995). Landesvermessungsamt Schleswig-Holstein- Digitales Geländemodell für Schleswig- Holstein. Quelle: TK25. Gitterweite 25 m x 25 m und TK50 Gitterweite 50 m x 50 m sowie ATKIS-DGM2- 1 m x 1 m Gitterweite und DGM 5 m x 5 m Gitterweite, abgeleitet aus LiDAR-Daten.

- Michalak, A.M., Anderson, E.J., Beletsky, D., Boland, S., Bosch, N.S., Bridgeman, T.B., Chaffin, J.D., Cho, K., Confesor, R., Daloğlu, I., DePinto, J.V., Evans, M.A., Fahnenstiel, G.L., He, L., Ho, J.C., Jenkins, L., Johengen, T.H., Kuo, K.C., LaPorte, E., Liu, X., McWilliams, M.R., Moore, M.R., Posselt, D.J., Richards, R.P., Scavia, D., Steiner, A.L., Verhamme, E., Wright, D.M., Zagorski, M.A. (2013). Record-setting algal bloom in Lake Erie caused by agricultural and meteorological trends consistent with expected future conditions. *Proc. Natl. Acad. Sci.* 201216006. <https://doi.org/10.1073/pnas.1216006110>
- Migliaccio, K., Chaubey, I., Haggard, B. (2007). Evaluation of Landscape and Instream Modelling to Predict Watershed Nutrient Yield. *Environ. Model. Softw.* 22, 987–999. <https://doi.org/10.1016/j.envsoft.2006.06.010>
- Neitsch, S., Arbold, J.G., Kinry, J.R., Williams, J.R. (2011). Soil and water assessment tool theoretical documentation. Version.
- Park, J.Y., Park, G.A., Kim, S.J. (2013). Assessment of Future Climate Change Impact on Water Quality of Chungju Lake, South Korea, Using WASP Coupled with SWAT. *JAWRA J. Am. Water Resour. Assoc.* 49, 1225–1238. <https://doi.org/10.1111/jawr.12085>
- Pfannerstill, M., Guse, B., Fohrer, N. (2014). Smart low flow signature metrics for an improved overall performance evaluation of hydrological models. *J. Hydrol.* 510, 447–458. <https://doi.org/10.1016/j.jhydrol.2013.12.044>
- Runkel, R.L. (1998). One-Dimensional Transport with Inflow and Storage (OTIS): A Solute Transport Model for Streams and Rivers (USGS Numbered Series No. 98–4018), Water-Resources Investigations Report. Geological Survey (U.S.).
- Schmalz, F., Fohrer, N. (2010). Ecohydrological research in the German lowland catchment Kielstau. URL: [https://www.researchgate.net/publication/259082577\\_Ecohydrological\\_research\\_in\\_the\\_German\\_lowland\\_catchment\\_Kielstau](https://www.researchgate.net/publication/259082577_Ecohydrological_research_in_the_German_lowland_catchment_Kielstau) (accessed 1.10.19).
- Schwarzenbach, R. P., Escher, B. I., Fenner, K., Hofstetter, T. B., Johnson, C. A., et al. (2006). The challenge of micropollutants in aquatic systems. *Science* 313:1072–77
- Shabani, A., Zhang, X., Ell, M. (2017). Modeling Water Quantity and Sulfate Concentrations in the Devils Lake Watershed Using Coupled SWAT and CE-QUAL-W2. *JAWRA J. Am. Water Resour. Assoc.* 53, 748–760. <https://doi.org/10.1111/1752-1688.12535>
- Tuppad, P., Douglas-Mankin, K. R., Lee, T., Srinivasan, R, Arnold, J. G. (2011). Soil and Water Assessment Tool (SWAT) Hydrologic/Water Quality Model: Extended Capability and Wider Adoption. *Transactions of the ASABE.* 54(5): 1677-1684. (doi: 10.13031/2013.39856)
- Trybula, E.M., Cibin, R., Burks, J.L., Chaubey, I., Brouder, S.M., Volenec, J.J. (2015). Perennial rhizomatous grasses as bioenergy feedstock in SWAT: Parameter development and model improvement. *GCB Bioenergy*, 7, 1185–1202

- Vrugt, J.A., Robinson, B.A. (2007). Improved evolutionary optimization from genetically adaptive multimethod search. *Proc. Natl. Acad. Sci.* 104, 708–711. <https://doi.org/10.1073/pnas.0610471104>
- Wagner, P.D., Reichenau, T.G., Kumar, S., Schneider, K. (2015). Development of a new downscaling method for hydrologic assessment of climate change impacts in data scarce regions and its application in the Western Ghats, India. *Reg. Environ. Change* 15 (3), 435–447. <https://doi.org/10.1007/s10113-013-0481-z>.
- Wagner, P.D., Hörmann, G., Schmalz, B., Fohrer, N. (2018). Characterisation of the water and nutrient balance in the rural lowland catchment of the Kielstau [in German]. URL [https://www.researchgate.net/publication/325465562\\_Charakterisierung\\_des\\_Wasser-\\_und\\_Nahrstoffhaushalts\\_im\\_landlichen\\_Tieflandeinzugsgebiet\\_der\\_Kielstau\\_Characterisation\\_of\\_the\\_water\\_and\\_nutrient\\_balance\\_in\\_the\\_rural\\_lowland\\_catchment\\_of\\_the\\_Kielstau](https://www.researchgate.net/publication/325465562_Charakterisierung_des_Wasser-_und_Nahrstoffhaushalts_im_landlichen_Tieflandeinzugsgebiet_der_Kielstau_Characterisation_of_the_water_and_nutrient_balance_in_the_rural_lowland_catchment_of_the_Kielstau) (accessed 1.10.19).
- Wu, N., Huang, J., Schmalz, B., Fohrer, N. (2014). Modeling daily chlorophyll a dynamics in a German lowland river using artificial neural networks and multiple linear regression approaches. *Limnology* 15, 47–56. <https://doi.org/10.1007/s10201-013-0412-1>

## **5. SUMMARY, CONCLUSIONS AND RECOMMENDATIONS FOR FUTURE RESEARCH**

### **5.1 Research Summary**

Large scale hydrological models often use simplified process representation to reduce computational complexity in simulating in-stream solute transport. Such simplifications are likely the cause of poor water quality predictions in streams. In this study, an improved and generalized process-based solute transport model was developed, and subsequently incorporated into Soil and Water Assessment Tool (SWAT) model. The two main hypotheses tested in the study were that (1) inclusion of additional key stream processes at finer scale can enhance process representation and water quality predictions in SWAT, and (2) simple regression equations used to generalize the new model can be reasonably adapted to approximate transient storage parameters in streams. Experimental tracer tests were conducted in two stream reaches in Kielstau catchment located in Germany using both conservative and reactive tracers to test our model results. Integrating equations from two popular solute transport/water quality models— OTIS and QUAL2E — the new model termed as the ‘Enhanced OTIS’ was developed by including in-stream processes such as advection, dispersion, transient storage exchange and biochemical reactions based on a finite-difference solution approach. A user-friendly interface was also created for ‘Enhanced OTIS’ with the option to model either first-order uptake or QUAL2E reactions-based uptake and to further calibrate and visually interpret the tracer breakthrough curves. Using data from Kielstau catchment and five other published tracer studies, the developed model was tested for reliability and performance. A generalized set of values for three most sensitive QUAL2E parameters were also derived from this study as a recommendation for parameter estimates when field-measured or calibrated values are unavailable.

To apply the newly developed model for large scale studies involving multiple streams, simple regression equations were developed relating transient storage parameters (TSP) with easily available hydraulic variables to get approximate values of these parameters. Meta-analysis conducted on past conservative tracer studies was used to find correlations between TSP (dispersion coefficient ( $D$ ), storage zone area ( $A_s$ ), and exchange coefficient ( $\alpha$ )) and variables like discharge, velocity, flow width and flow depth. Field-monitored breakthrough curves were compared with modeled curves to evaluate whether the regression equations performed well for the test cases studied. The 'Enhanced OTIS' model and associated parameter value changes, together with the developed regression equations for TSP, were incorporated into SWAT model framework to build a new version of SWAT called 'Mir-SWAT'. Kielstau catchment was well calibrated for sediment, flow and nutrients using AMALGAM optimization algorithm. Behavior of Mir-SWAT and SWAT for calibrated model was assessed using time series and reach-scale analyses. Prediction of water quality variables such as nitrate, phosphate, dissolved oxygen and algae (or Chl-*a*) were evaluated in detail to examine whether Mir-SWAT performed similar, better or worse than SWAT model for each test case. Reach-scale analysis demonstrated Mir-SWAT's potential to provide temporally and spatially varying solute concentrations at sub-daily scale. Within this analysis, a hypothetical case study with point-source load was used to show that Mir-SWAT can have wide range of applications in localized studies involving finer-scale nutrient inputs. Based on the study outcomes, the study hypotheses were accepted since the regression equations provided reasonable estimates of transient storage parameters and Mir-SWAT performed better than SWAT in improving dissolved oxygen dynamics and predicting phosphate and Chl-*a* concentrations at the catchment outlet.

## 5.2 Major Research Findings

Key research findings from this study are summarized below.

- Current versions of OTIS and QUAL2E models disregard one or more in-stream processes and lack a good graphical user interface. Combining the processes from these two models and developing an improved physically-based model along with an enhanced user interface will provide better options for modeling and visualizing the results. Specific findings from the newly developed ‘Enhanced OTIS’ model are summarized below:
  - Sensitivity analysis of model parameters showed that background algal concentration ( $[A]$ ), fraction of algae that is nitrogen ( $\alpha_N$ ), fraction of algae that is phosphorus ( $\alpha_P$ ) and ratio of Chl-*a* to algal biomass ( $\alpha_0$ ) are the most sensitive parameters affecting nutrient uptake.
  - With the inclusion of biochemical reactions in the new model, temporally and spatially varying uptake rate corresponding to changing nutrient concentrations can be simulated, which is unfeasible with first-order decay based OTIS model.
  - ‘Enhanced OTIS’ model predicted nutrient uptakes for both experimental Kielstau data and published tracer test data with a good accuracy ( $R^2=0.76$ ,  $NSE=0.47$ ,  $\text{Percent Bias}=-4.3\%$ ).
  - A generalized set of parameters values for  $\alpha_0$  (=10),  $\alpha_N$  (=0.2) and  $\alpha_P$  (=0.1) were derived based on reasonable uptake rate predictions obtained with these values for more than 70% of test cases studied.
  - Replacing first-order decay reactions with actual biochemical reactions may not have considerable effect on small scale tracer uptake rates but may effect stream nutrient dynamics in the long run and improve confidence in the model.

- Calibrating transient storage parameters of OTIS model is challenging when it is impractical to conduct tracer experiments or when the model is applied to relatively larger areas with multiple streams in the watershed. Study to develop simple regression equations to estimate these parameters yielded the following findings:
  - Meta-analysis of published tracer data showed that dispersion coefficient (D) was fairly well correlated to velocity, flow width and flow depth, and storage zone area ( $A_s$ ) was highly correlated to ratio of streamflow and flow depth.
  - Storage exchange coefficient ( $\alpha$ ) is difficult to model with simple hydraulic variables considered in the study suggesting that it may be affected by additional hydrogeological characteristics. A mean value of this coefficient ( $2.5 \times 10^{-4} \text{ s}^{-1}$ ) is often sufficient to model breakthrough curves with reasonable accuracy.
  - New regression equations performed better than few existing equations for D and  $A_s$  for the two experimental data used in this study. Existing equations require channel slope to calculate D and  $A_s$  and approximating these often lead to inaccurate estimates.
  - Comparing 39 modeled and observed breakthrough curves from tracer tests conducted at Kielstau and Hubbard Brook Experimental Forest,  $R^2$  was  $\geq 0.75$  for 97% of cases and NSE was  $\geq 0.75$  for 95% of the cases, showing that a very good fit was obtained with the regression-estimated values of storage parameters.

- Few discrepancies in breakthrough curves were obtained especially due to underprediction of  $A_s$  values, but overall spread and peaks of curves were modelled well.
- New regression models can act as a tool to approximate storage parameters but cannot completely substitute calibration for precise parameter values.
- SWAT model has undergone limited improvements to its in-stream solute transport module in the past and it only considers daily-scale biochemical reactions within the module. ‘Mir-SWAT’ model was developed with the aim of including advection, dispersion and transient storage processes to this module at a finer scale. Specific important findings from this study are summarized below:
  - Use of finite-difference approach at smaller time and distance scale allows model users to study sub-daily and reach-scale solute transport and nutrient dynamics.
  - Calibrated and uncalibrated models behaved differently in terms of water quality predictions when simulated with SWAT and Mir-SWAT. Hence, additional studies in this regard are required to readily evaluate the benefit of Mir-SWAT.
  - For the calibrated Kielstau model, nitrate predictions at the watershed outlet did not show differences when simulated with SWAT and Mir-SWAT showing that it is mostly affected by streamflow and subbasin loads only.
  - Phosphate load peaks during major storm events were reduced and were closer to measured values with the new Mir-SWAT model, simultaneously increasing daily model  $R^2$  value from 0.17 (with existing SWAT) to 0.28.

- Extreme low values of dissolved oxygen (~0 mg/L) predicted with existing SWAT model were completely removed with the Mir-SWAT model (increase in  $R^2$  from 0.07 to 0.28) and predicted DO concentrations fell within the measured range of 6-15 mg/L. This improvement is expected to influence many other biochemical reactions within the stream.
- Qualitative analysis conducted on Chl-*a* concentrations at watershed outlet showed that when compared to SWAT model, Mir-SWAT predicts average and maximum monthly concentrations that are closer to observed values, especially during winter months.
- Hypothetical scenario of point-source load applied to a single reach showed that Mir-SWAT has the capability to study sub-daily scale solute transport and nutrient uptakes, and comes as an added advantage over the existing SWAT model.

### **5.3 Limitations of current study and recommendations for future research**

- The ‘Enhanced OTIS’ model included processes from two popular models-OTIS and QUAL2E. There are many other water quality models that consider complex algal modeling and various other comprehensive biochemical reactions within the stream. These equations have not been included in the study to reduce complexity and parameter/model uncertainty. Further improvements can be made to this model to enhance process representation by including additional processes and reactions.
- The generalized set of certain QUAL2E parameters recommended in the first part of the study should be used with caution since these were tested on only a limited number of

studies. Additional validation with more study data will be required to verify these values or users should use reach-specific values obtained from experts or through measured data.

- Regression equations for transient storage parameters were not developed in this study to completely substitute tracer test calibration technique. These equations should form the basis for making first approximations and should to be applied in case of data scarcity or for large-scale studies. If feasible, comparing the values computed with these equations with those obtained from other existing equations for  $D$ ,  $A_s$  and  $\alpha$  is a good approach to ensure that the parameter values are reasonable.
- When developing Mir-SWAT, sub-daily changes in flow and subbasin nutrient loads were not considered even though the finite difference solution works on a sub-daily scale. Daily values were uniformly distributed throughout the day since the sub-daily routines in SWAT are in developing stages especially with regard to nutrient loads. Additionally, it is difficult to get sub-daily input data to precisely model hourly changes in loads. With better resolution input data and sub-daily scale landscape modeling of nutrients, Mir-SWAT model can be modified to be used for precise fine-scale in-stream solute transport modeling.
- SWAT and Mir-SWAT predictions for Chl-*a* showed extreme seasonal variations between winter and summer months compared to observed variations. This may be attributed to the effect of stream temperature on algal growth. A detailed evaluation of stream temperature calculations in SWAT and its effect on algal growth will be necessary to explain these discrepancies.
- The new Mir-SWAT model was only tested for one catchment (Kielstau). Additional testing on different watersheds will help improve confidence in the model.

- Even though dissolved oxygen predictions improved with Mir-SWAT, this variable was not used in water quality calibration of the model. Modifying model parameters to better calibrate dissolved oxygen could lead to further improvement in DO predictions with Mir-SWAT. At the same time, testing on other watersheds would be required to verify if this model behavior is consistent across different watersheds.
- Since Mir-SWAT runs finite-difference solution on a very fine scale when compared to SWAT's daily scale, it is computationally challenging to run Mir-SWAT for large watersheds and for longer time periods. It is thus currently recommended for small-scale studies until further code revisions are made to reduce the simulation time.

## APPENDIX A. CALIBRATED STORAGE PARAMETERS

Table A. 1 Table A.1. Calibrated or measured transient storage and reaction parameters in the model for all test data. When storage parameters were not reported in the published studies, they were calibrated using available breakthrough curves. Storage parameters (A,  $A_s$ , D and  $\alpha$ ) were automatically calibrated and reaction parameters ( $\alpha_0$ ,  $\alpha_N$ ,  $\alpha_P$  and Chl-a) were manually calibrated in an attempt to generalize the reaction part of the model.

Study	StreamID	A (m <sup>2</sup> )	A <sub>s</sub> (m <sup>2</sup> )	D (m <sup>2</sup> /s)	$\alpha$ (s <sup>-1</sup> )	$\alpha_0$	$\alpha_N$	$\alpha_P$	Chl-a (mg/L)
<i>Demars, 2008</i>	Conwy	0.382	0.2	0.485	0.00063	10	0.2	0.1	2
	Cairn_trial4	0.07	0.001	0.01	0.00001	10	0.2	0.1	0.8
	Cairn_trial5	0.07	0.001	0.01	0.00001	10	0.2	0.1	0.8
	Cairn_trial6	0.07	0.001	0.01	0.00001	10	0.2	0.1	0.8
<i>Schroer, 2011</i>	Protected Stream_25Mar	0.05	0.179	0.014	0.00017	10	0.2	0.1	0.01
	Protected Stream_21Oct	0.049	0.205	0.018	0.00029	10	0.2	0.1	0.01
	Protected Stream_8Feb	0.063	0.164	0.016	0.00014	10	0.2	0.1	1
	Protected Stream_17Aug	0.066	0.166	0.037	0.00014	10	0.2	0.1	2
<i>Baker et al., 2012</i>	ShA_X	0.759	0.113	0.184	0.00424	10	0.2	0.1	5
	ShC_X	0.911	0.167	0.147	0.00421	10	0.2	0.1	5
	SpR_Y	0.166	0.095	0.563	0.009	10	0.2	0.1	0.5
	SpR_Z	0.225	0.044	0.158	0.00082	10	0.2	0.1	5
	SpS_X	1.438	0.501	0.171	0.00191	10	0.2	0.1	2
	SpS_Y	1.041	0.16	0.115	0.00418	10	0.2	0.1	5
	SpS_Z	1.589	0.254	0.19	0.00347	10	0.2	0.1	2
	SpE_X	1.158	0.53	0.26	0.00872	10	0.2	0.1	0.02
	SpE_Y	0.633	0.429	0.119	0.00824	10	0.2	0.1	0.5
SpE_Z	1.092	0.673	0.213	0.00855	10	0.2	0.1	5	
<i>Tank et al., 2008</i>	Stn1	17.697	5.643	9.163	0.0006	20	0.2	0.1	2
	Stn2	23.939	5.715	2.3	0.0007	20	0.2	0.1	2
	Stn3	24.391	5.813	1.429	0.0006	20	0.2	0.1	2
	Stn4	26	7.74	2.027	0.0008	20	0.2	0.1	2

Table A. 1 continued

<i>Burrows et al., 2013</i>	Arve Loop #1	0.01	0.001	0.1	0.0001	20	0.2	0.1	4
	Arve Loop #2	0.029	0.01	0.5	0.0001	20	0.2	0.1	4
	Arve Loop #3	0.007	0.01	0.1	0.0001	20	0.2	0.1	4
	PC085A	0.023	0.01	0.1	0.0001	20	0.5	0.1	2
	WR15B	0.014	0.01	0.1	0.0001	20	0.5	0.1	4
	PC023C	0.077	0.01	0.1	0.0001	20	0.5	0.1	4
<i>Kielstau Data</i>	Soltfeld	0.871	0.232	0.083	0.002	10	0.2	0.1	0.0595
	Freienwill	0.672	0.155	0.282	0.0052	10	0.2	0.1	0.0595

## APPENDIX B. META-ANALYSIS PAPERS

- Arce, M., D. von Schiller, and R. Gómez (2014). Variation in nitrate uptake and denitrification rates across a salinity gradient in Mediterranean and semiarid streams, *Aquat. Sci.*, 76(2), 295–311, doi:10.1007/s00027-014-0336-9.
- Ashkenas, L. R., S. L. Johnson, S. V. Gregory, J. L. Tank, and W. M. Wollheim (2004). A stable isotope tracer study of nitrogen uptake and transformation in an old-growth forest stream. *Ecology* 85:1725–1739.
- Baker, D. W., B. P. Bledsoe, J. S. Mueller Price (2012). Stream nitrate uptake and transient storage over a gradient of geomorphic complexity, north-central Colorado, USA. *Hydrological Processes* 26:3241–3252. DOI:10.1002/hyp.8385.
- Battin, T. J., L. A. Kaplan, S. Findlay, C. S. Hopkinson, E. Marti, A. I. Packman, F. Sabater (2008). Biophysical controls on organic carbon fluxes in fluvial networks. *Nature Geoscience*, 1(2), 95-100. DOI: 10.1038/ngeo101
- Becker, J. F., T. A. Endreny, J. D. Robison (2013). Natural channel design impacts on reach-scale transient storage. *Ecological Engineering* 57: 380–392.
- Bernhardt, E. S., G. E. Likens (2002) Dissolved organic carbon enrichment alters nitrogen dynamics in a forest stream. *Ecology* 83:1689–1700.
- Bernot, M.J., J.L. Tank, T.V. Royer, and M.B. David (2006). Nutrient uptake in streams draining agricultural catchments of the midwestern United States. *Freshwater Biol.* 51:499–509. doi:10.1111/j.1365-2427.2006.01508.

- Bott, T.L. and J. D. Newbold (2013). Ecosystem metabolism and nutrient uptake in Peruvian headwater streams. *International Review of Hydrobiology*, 98(3), 117-131. <http://dx.doi.org/10.1002/iroh.201201612>.
- Bukaveckas, P. A. (2007), Effects of channel restoration on water velocity, transient storage, and nutrient uptake in a channelized stream, *Environ. Sci. Technol.*, 41(5), 1570–1576, doi:10.1021/es061618x.
- Butturini, A., and F. Sabater (1998). Ammonium and phosphate retention in a Mediterranean stream: Hydrological vs. temperature control. *Can. J. Fish. Aquat. Sci.* 55: 1938–1945.
- Cooper, A. and J. G. Cooke (1984). Nitrate loss and transformations in two vegetated headwater streams. *New Zeal. J. Mar. Freshwater Res.* 18: 441–450.
- Cheong, T. S. & I. W. Seo (2003) Parameter estimation of the transient storage model by a routing method for river mixing processes. *Water Resour. Res.* 39(4), 1074–1084.
- Claessens, L., C.L. Tague, P.M. Groffman, and J.M. Melack. (2010). Longitudinal and seasonal variation of stream nitrogen uptake in an urbanizing watershed: Effect of organic matter, stream size, transient storage and debris dams. *Biogeochemistry* 98:45–62. doi:10.1007/s10533-009-9375-z.
- D'angelo, D. J., & J. R. Webster (1991). Phosphorus retention in streams draining pine and hardwood catchments in the southern Appalachian Mountains. *Freshwater Biology*, 26(3), 335–345. <https://doi.org/10.1111/j.1365-2427.1991.tb01401.x>
- Davis, J. C., and G. W. Minshall (1999). Nitrogen and phosphorus uptake in two Idaho (USA) headwater wilderness streams. *Oecologia* 19: 247–255.

- Deng, Z.-Q., L. Bengtsson L., V. P. Singh and D.D. Adrian (2002). Longitudinal dispersion coefficient in single-channel streams. *Journal of Hydraulic Engineering*. 128(10): 901 – 916.
- Dodds, W. K., A. J. Lopez, W. B. Bowden, S. Gregory, N. B. Grimm, S. K. Hamilton, A. E. Hershey, E. Martí, W. H. McDowell, J. L. Meyer, D. Morrall, P.J. Mulholland, B. J. Peterson, J. T. Tank, H. M. Valett, , J. R. Webster, W. Wollheim (2002). N uptake as a function of concentration in streams. *J North Am Benthol Soc* 21:206–220
- Edwardson, K. J., W. B. Bowden, C. Dahm, and J. Morrice (2003), The hydraulic characteristics and geochemistry of hyporheic and parafluvial zones in Arctic tundra streams, north slope, Alaska, *Adv. Water Resour.*, 26, 907 – 923.
- Ensign, S. H. and M.W. Doyle (2006). Nutrient spiraling in streams and river networks. *J Geophys Res—Biogeosci* 111:G04009
- Gooseff, M. N., S. M. Wondzell, R. Haggerty, and J. Anderson (2003). Comparing transient storage modeling and residence time distribution (RTD) analysis in geomorphically varied reaches in the Lookout Creek basin, Oregon, USA, *Adv. Water Resour.*, 26(9), 925–937, doi:10.1016/ s0309-1708(03)00105-2.
- Gooseff, M. N., R. O. Hall, Jr., and J. L. Tank (2007). Relating transient storage to channel complexity in streams of varying land use in Jackson Hole, Wyoming, *Water Resour. Res.*, 43, W01417, doi:10.1029/ 2005WR004626.
- Gooseff, M. N., M. A. Briggs, K. E. Bencala, B. L. McGlynn, D. T. Scott (2013). Do transient storage parameters directly scale in longer, combined stream reaches? Reach length dependence of transient storage interpretations. *J Hydrol* 2013; 483:16–25.

- Grimm, N. B., R. W. Sheibley, C. L. Crenshaw, C. N. Dahm, W. J. Roach, and L. H. Zeglin. (2005). N retention and transformation in urban streams. *Journal of the North American Benthological Society* 24:626–642.
- Gucker, B., and I. G. Boechat (2004). Stream morphology controls ammonium retention in tropical headwaters. *Ecology* 85:2818–2827.
- Haggard, B. E., D. E. Storm, R. D. Tejral, Y. A. Popova, V. G. Keyworth, and E. H. Stanley. (2001). Stream nutrient retention and limitation in three northeastern Oklahoma agricultural catchments. *Trans. ASAE* 44(3): 597-605.
- Haggard, B. E., and D. E. Storm (2003). Effect of leaf litter on phosphorus retention and hydrological properties at a first order stream in Northeast Oklahoma, USA. *J. Freshwater Ecol.* 18: 557–565.
- Hall, R.O., B.J. Peterson, J.L. Meyer (1998). Testing a nitrogen-cycling model of a forest stream by using a nitrogen-15 tracer addition. *Ecosystems* 1:283–298.
- Hall, R. O., J. L. Tank (2003). Ecosystem metabolism controls nitrogen uptake in streams in Grand Teton National Park, Wyoming. *Limnology and Oceanography* 48: 1120–1128.
- Hamilton, S. K., J. L. Tank, D. R. Raikow, W. M. Wollheim, B. J. Peterson, J. R. Webster (2001). Nitrogen uptake and transformation in a midwestern U.S. stream: a stable isotope enrichment study. *Biogeochemistry* 54:297–340.
- Hart, B. T., P. Freeman, I. D. McKelvie, S. Pearse, and D. G. Ross (1991). Phosphorus spiralling in Myrtle Creek, Victoria, Australia. *Int. Ver. Theor. Angew. Limnol. Verh.* 24:2065-2070.

- Hart, B. T., P. Freeman, and I. D. Mciceune (1992). Whole-stream phosphorus release studies: variation in uptake length with initial phosphorus concentration. *Hydrobiologia* 235 / 236:573-584
- Hart, D. R., P. J. Mulholland, E. R. Marzolf, D. L. Deangelis, and S. P. Hendricks (1999). Relationships between hydraulic parameters in a small stream under varying flow and seasonal conditions. *Hydrol. Proc.* 13: 1497–1510.
- Harvey, J. W., M. H. Conklin, and R. S. Koelsch (2003). Predicting changes in hydrologic retention in an evolving semi-arid alluvial stream. *Adv. Water Resour.* 26: 939–950.
- Hoellein, T. J., J. L. Tank, E. J. Rosi-Marshall, S. A. Entrekin, and G. A. Lamberti. (2007). Controls on spatial and temporal variation of nutrient uptake in three Michigan headwater streams. *Limnology and Oceanography* 52: in press.
- Johnson, Z. C., R. Schumer, J. J. Warwick (2014). Factors affecting hyporheic and surface transient storage in a western U.S. river, *Journal of Hydrology*, 510, 325--339, doi: 10.1016/j.jhydrol.2013.12.037
- Johnson, Z. C., J. J. Warwick, R. Schumer (2015). Nitrogen retention in the main channel and two transient storage zones during nutrient addition experiments, *Limnology and Oceanography*, DOI:10.1002/lno.10006, doi: 10.1002/lno.10006
- Kashefipour, S.M. and R. A. Falconer (2002). Longitudinal dispersion coefficients in natural channels. *Water Research.* 36: 1596 – 1608.
- Klockner, C. A., S. S. Kaushal, P. M. Groffman, P. M. Mayer, R. P. Morgan (2009). Nitrogen uptake and denitrification in restored and unrestored streams in urban Maryland, USA. *Aquat Sci* 71(4):411–424.

- Kopacek, J., and P. Blazka (1994). Ammonium uptake in alpine streams in the High Tatra Mountains (Slovakia). *Hydrobiologia* 294:157–165.
- Koussis, A.D. and J. Rodriguez-Mirasol (1998). Hydraulic estimation of dispersion coefficient for streams. *Journal of Hydraulic Engineering*. 124(3): 317 – 320.
- Lautz, L. K., D. I. Siegel, and R. L. Bauer (2006). Impact of debris dams on hyporheic interaction along a semi-arid stream. *Hydrol. Proc.* 20: 183–196.
- Lees, M. J., L. A. Camacho, and S. Chapra (2000). ‘On the relationship of transient-storage and aggregated dead zone models of longitudinal solute transport in streams.’ *Water Resour. Res.*, 36(1), 213–224.
- Lehto, L. L., B. H. Hill (2013). The effect of catchment urbanization on nutrient uptake and biofilm enzyme activity in Lake Superior (USA) tributary streams. *Hydrobiologia* 713:35–51.
- Marti, E., J. Armengol, and R. Sabater (1994). Day and night nutrient uptake differences in a calcareous stream. *Verh. Internat. Verein. Limnol.* 25:1756–1760.
- Marti, E., and F. Sabater (1996). High variability in temporal and spatial nutrient retention in Mediterranean streams. *Ecology* 77:854–869.
- Meals, D.W., J. P. Hoffmann, S. N. Levine, E. A. Cassell, D. Wang, J. C. Drake, D. K. Pelton, H. M. Galarneau and A. B. Brown (1999). Retention of spike additions of soluble phosphorus in a northern eutrophic stream. *J. N. Am. Benthol. Soc.* 18:185-198.
- Merriam, J. L., W. H. McDowell, J. L. Tank, W. M. Wollheim, C. L. Crenshaw, and S. L. Johnson (2002). Characterizing nitrogen dynamics, retention and transport in a tropical rainforest stream using an in situ  $^{15}\text{N}$  addition. *Freshwater Biology* 47:143–160.

- Meyer, J. L., M. J. Paul, and W. K. Taulbee (2005). Stream ecosystem function in urbanizing landscapes. *Journal of the North American Benthological Society* 24:602–612.
- Mueller Price, J. S., D. W. Baker, B. P. Bledsoe (2016). Effects of passive and structural stream restoration approaches on transient storage and nitrate uptake. *River Research and Applications* 32: 1542--1554. DOI: 10.1002/rra.3013
- Newbold, J. D., J. W. Elwood, R. V. O'Neill, and A. L. Sheldon (1983). Phosphorus dynamics in woodland stream ecosystems: A study of nutrient spiraling. *Ecology* 64(5): 1249-1265.
- Niyogi, D. K., K. S. Simon, and C. R. Townsend (2004). Land use and stream ecosystem functioning: nutrient uptake in streams that contrast in agricultural development. *Archiv fur Hydrobiologie* 160:471–486.
- Runkel, R. L. (2002). A new metric for determining the importance of transient storage. *J N Am Bentholl Soc* 2002;21:529–43.
- Schmid, B. H., I. Innocenti, and U. Sanfilippo (2010). Characterizing solute transport with transient storage across a range of flow rates: The evidence of repeated tracer experiments in Austrian and Italian streams, *Adv. Water Resour.*, 33(11), 1340–1346, doi:10.1016/j.advwatres.2010.06.001.
- Sheibley, R.W., J.H. Du, and A.J. Tesoriero (2014). Low transient storage and uptake efficiencies in seven agricultural streams: Implications for nutrient demand. *J. Environ. Qual.* 43:1980–1990. doi:10.2134/jeq2014.01.0034
- Simon, K.S., C.R. Townsend, B.J.F. Biggs, and W.B. Bowden (2005). Temporal variation of N and P uptake in 2 New Zealand streams. *Journal of the North American Benthological Society* 24:1–18.

- Sudduth, E.B., B.A. Hassett, P. Cada and E.S. Bernhardt (2011). Testing the Field of Dreams Hypothesis: Functional Responses to Urbanization and Restoration in Stream Ecosystems. *Ecological Applications* 21: 1972-1988.
- Tank, J. L., J. L. Meyer, D. M. Sanzone, P.J. Mulholland, J. R. Webster, B. J. Peterson, W. M. Wollheim, and N. E. Leonard (2000). Analysis of nitrogen cycling in a forest stream during autumn using a  $^{15}\text{N}$ -tracer addition. *Limnology and Oceanography* 45:1013–1029.
- Thomas, S. A., H. M. Valett, J. R. Webster, and P. J. Mulholland (2003). A regression approach to estimating reactive solute uptake in advective and transient storage zones of stream ecosystems. *Advances in Water Resources* 26:965–976.
- Triska, R. J., V. C. Kennedy, R. J. Avanzino, G. W. Zellweger, and K. E. Bencala (1989). Retention and transport of nutrients in a third-order stream: channel processes. *Ecology* 70:1877–1892.
- Valett, H. M., J. A. Morrice, C. M. Dahm, and M. E. Campana (1996). Parent lithology, surface-groundwater exchange, and nitrate retention in headwater streams. *Limnol. Oceanogr.* 41: 333–345.
- Valett, H. M., C. L. Crenshaw, and P. F. Wagner (2002). Stream nutrient uptake, forest succession, and biogeochemical theory. *Ecology* 83:2888-2901.
- Webster, J. R., P. J. Mulholland, J. L. Tank, H. M. Valett, W. K. Dodds, B. J. Peterson, W. B. Bowden, C. N. Dahm, S. Findlay, S. V. Gregory, N. B. Grimm, S. K. Hamilton, S. L. Johnson, E. Marti, W. H. McDowell, J. L. Meyer, D. D. Morrall, S. A. Thomas, and W. M. Wollheim (2003). Factors affecting ammonium uptake in streams - an interbiome perspective. *Freshwater Biology* 48:1329–1352.

- Weigelhofer, G., J. Fuchsberger, B. Teufel, N. Welti & T. Hein (2012). Effects of riparian forest buffers on in-stream nutrient retention in agricultural catchments. *Journal of Environmental Quality* 41: 373–379.
- Wilcock, R. J., M. R. Scarsbrook, K. J. Costley, and J. W. Nagels (2002). Controlled release experiments to determine the effects of shade and plants on nutrient retention in a lowland stream. *Hydrobiologia* 485:153–162.
- Wollheim, W. M., B. J. Peterson, L. A. Deegan, J. E. Hobbie, B. Hooker, W. B. Bowden, K. J. Edwardson, D. B. Arscott, A. E. Hershey, and J. Finlay (2001). Influence of stream size on ammonium and suspended particulate nitrogen processing. *Limnology and Oceanography* 46:1–13.
- Wondzell, S. M. (2006), Effect of morphology and discharge on hyporheic exchange flows in two small streams in the Cascade Mountains of Oregon, USA, *Hydrological Processes*, 20(2), 267 – 287.
- Zarnetske, J. P., M. N. Gooseff, T. R. Brosten, J. H. Bradford, J. P. McNamara, and W. B. Bowden (2007). Transient storage as a function of geomorphology, discharge, and permafrost active layer conditions in Arctic tundra streams, *Water Resources Research*, 43, W07410, doi:10.1029/2005WR004816.

## APPENDIX C. MODIFIED SWAT MODEL PERFORMANCE

Table C.1 List of calibrated parameters for Kielstau SWAT model categorized according to streamflow, sediment, nitrate and phosphate calibration. Description of each parameter, type of parameter changes (absolute/percentage) and initial values are also provided

<b>1. FLOW</b>					
<b>Parameter</b>	<b>Description</b>	<b>File</b>	<b>Change</b>	<b>Initial Value</b>	<b>Calibrated Value</b>
SFTMP	Snowfall Temperature (oC)	.bsn	Absolute	1	5.00
SURLAG	Surface Runoff Lag Coefficient	.bsn	Absolute	4	3.42
ALPHA_BF	Baseflow alpha factor (1/days)	.gw	Absolute	0.048	0.48
GW_DELAY	Groundwater delay time (days)	.gw	Absolute	31	43.81
GW_REVAP	Groundwater revap coefficient	.gw	Absolute	0.02	0.07
GWQMN	Threshold water depth in shallow aquifer (mm H2O)	.gw	Absolute	1000	5.95
SOL_AWC	Available soil water capacity (mm H2O/mm soil)	.sol	%	Variable	-0.26
SOL_K	Saturated Hydraulic Conductivity (mm/hr)	.sol	%	Variable	0.85
DDRAIN	Depth to sub-surface drain (mm)	.mgt	%	1000	0.18
GDRAIN	Drain tile lag time (hours)	.mgt	%	72	-0.50
TDRAIN	Time to drain soil to field capacity (hours)	.mgt	%	36	0.25
DEP_IMP	Depth to impervious layer (mm)	.hru	%	6000	0.35
<b>2. SEDIMENT</b>					
<b>Parameter</b>	<b>Description</b>	<b>File</b>	<b>Change</b>	<b>Initial Value</b>	<b>Calibrated Value</b>
SPCON	Linear parameter for channel sediment routing	.bsn	Absolute	0.0001	0.0001
SPEXP	Exponent parameter for channel sediment routing	.bsn	Absolute	1.00	1.04
PRF_BSN	Peak rate adjustment factor in main channel	.bsn	Absolute	1.000	0.60
ADJ_PKR	Peak rate adjustment factor in subbasin	.bsn	Absolute	1	2.00
USLE_P	USLE support practice factor	.mgt	Absolute	1.000	0.78
CH_COV1	Channel erodibility factor	.rte	Absolute	0	0.00
CH_K2	Effective hydraulic conductivity in main channel alluvium (mm/hr)	.rte	Absolute	0	70.00
CH_N2	Main channel Manning's n value	.rte	Absolute	0.014	0.04
CH_COV2	Channel cover factor	.rte	Absolute	0.000	0.32

Table C.1. continued

<b>3. Nitrogen and Phosphorus</b>					
<b>Parameter</b>	<b>Description</b>	<b>File</b>	<b>Change</b>	<b>Initial Value</b>	<b>Calibrated Value</b>
NPERCO	Nitrate percolation coefficient	.bsn	Absolute	0.2	0.15
CDN	Denitrification exponential rate coefficient	.bsn	Absolute	1.4	1.66
PPERCO	Phosphorus percolation coefficient (m <sup>3</sup> /Mg)	.bsn	Absolute	10	10.60
RSDCO	Residue decomposition coefficient	.bsn	Absolute	0.05	0.52
RCN	Concentration of nitrogen in rainfall (mg N/L)	.bsn	Absolute	0	1.95
SDNCO	Denitrification threshold water content	.bsn	Absolute	1.1	1.20
N_UPDIS	Nitrate uptake distribution factor	.bsn	Absolute	20	1.00
P_UPDIS	Phosphorus uptake distribution factor	.bsn	Absolute	20	28.41
PHOSKD	Phosphorus soil partitioning coefficient (m <sup>3</sup> /Mg)	.bsn	Absolute	175	100.00
PSP	Phosphorus availability index	.bsn	Absolute	0.4	0.52
SOL_ORGP	Initial organic P concentration in soil layer (mg P/kg soil)	.chm	Absolute	0	50.00
SOL_ORGN	Initial organic N concentration in soil layer (mg N/kg soil)	.chm	Absolute	0	5000.00
SOL_SOLP	Initial soluble P concentration in soil layer (mg P/kg soil)	.chm	Absolute	5	3.21
SOL_NO3	Initial NO <sub>3</sub> concentration in soil layer (mg N/kg soil)	.chm	Absolute	0	5.00
BIOMIX	Biological mixing efficiency	.mgt	Absolute	0.2	0.01
ERORGP	Phosphorus enrichment ratio for loading with sediment	.hru	Absolute	0	1.00

Table C.2 Default and new values of water quality parameters used in SWAT and Mir-SWAT respectively. Note: Only basin level parameter values are changed.

<b>Parameter</b>	<b>Description</b>	<b>Default SWAT value</b>	<b>Mir-SWAT value</b>
lambda0	Non-algal portion of the light extinction coefficient ( $m^{-1}$ )	1	0.581
lambda1	Linear algal self-shading coefficient ( $m^{-1} \cdot (ug\ chl a/L)^{-1}$ )	0.03	0.0088
lambda2	Nonlinear algal self-shading coefficient ( $m^{-1} \cdot (ug\ chl a/L)^{-2/3}$ )	0.054	0.054
ai0	Ratio of chlorophyll-a to algal biomass ( $\mu g\ Chla/mg\ alg$ )	50	10
ai1	Fraction of algal biomass that is nitrogen ( $mg\ N/mg\ alg$ )	0.08	0.2
ai2	Fraction of algal biomass that is phosphorus ( $mg\ P/mg\ alg$ )	0.015	0.1
ai3	Rate of oxygen production per unit of algal photosynthesis ( $mg\ O_2/mg\ alg$ )	1.6	1.6
ai4	Rate of oxygen uptake per unit of algae respiration ( $mg\ O_2/mg\ alg$ )	2	2
ai5	Rate of oxygen uptake per unit of $NH_3$ oxidation ( $mg\ O_2/mg\ NH_3-N$ )	3.5	3.5
ai6	Rate of oxygen uptake per unit of $NO_2$ oxidation ( $mg\ O_2/mg\ NO_2-N$ )	1.07	1.07
mumax	Maximum specific algal growth rate at $20^\circ C$ ( $day^{-1}$ )	2	3
rhoq	Algal respiration rate at $20^\circ C$ ( $day^{-1}$ )	2.5	0.1
tfact	Fraction of solar radiation that is Photosynthetically active radiation	0.3	0.3
k_l	Half saturation coefficient for light ( $KJ/(m^2 \cdot min)$ )	0.75	0.75
k_n	Half saturation constant for nitrogen ( $mg\ N/L$ )	0.02	0.02
k_p	Half saturation constant for phosphorus ( $mg\ P/L$ )	0.25	0.25
p_n	Algal preference factor for ammonia	0.5	0.5

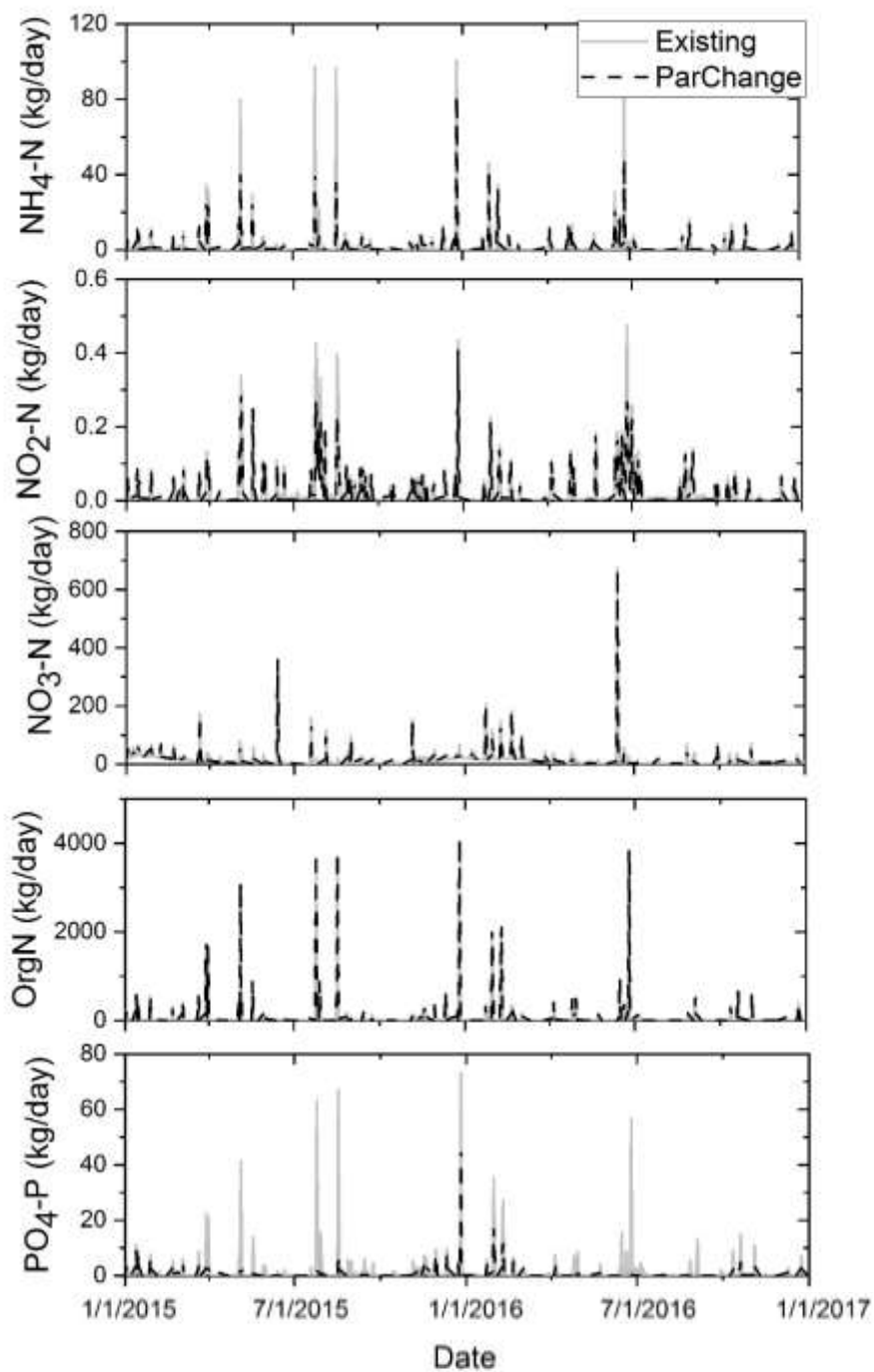


Figure C.1. Time series plots of NH<sub>4</sub>-N, NO<sub>2</sub>-N, NO<sub>3</sub>-N, Organic N and PO<sub>4</sub>-P loads during 2015-2016 simulated with uncalibrated SWAT model using default and new values of water quality parameters.

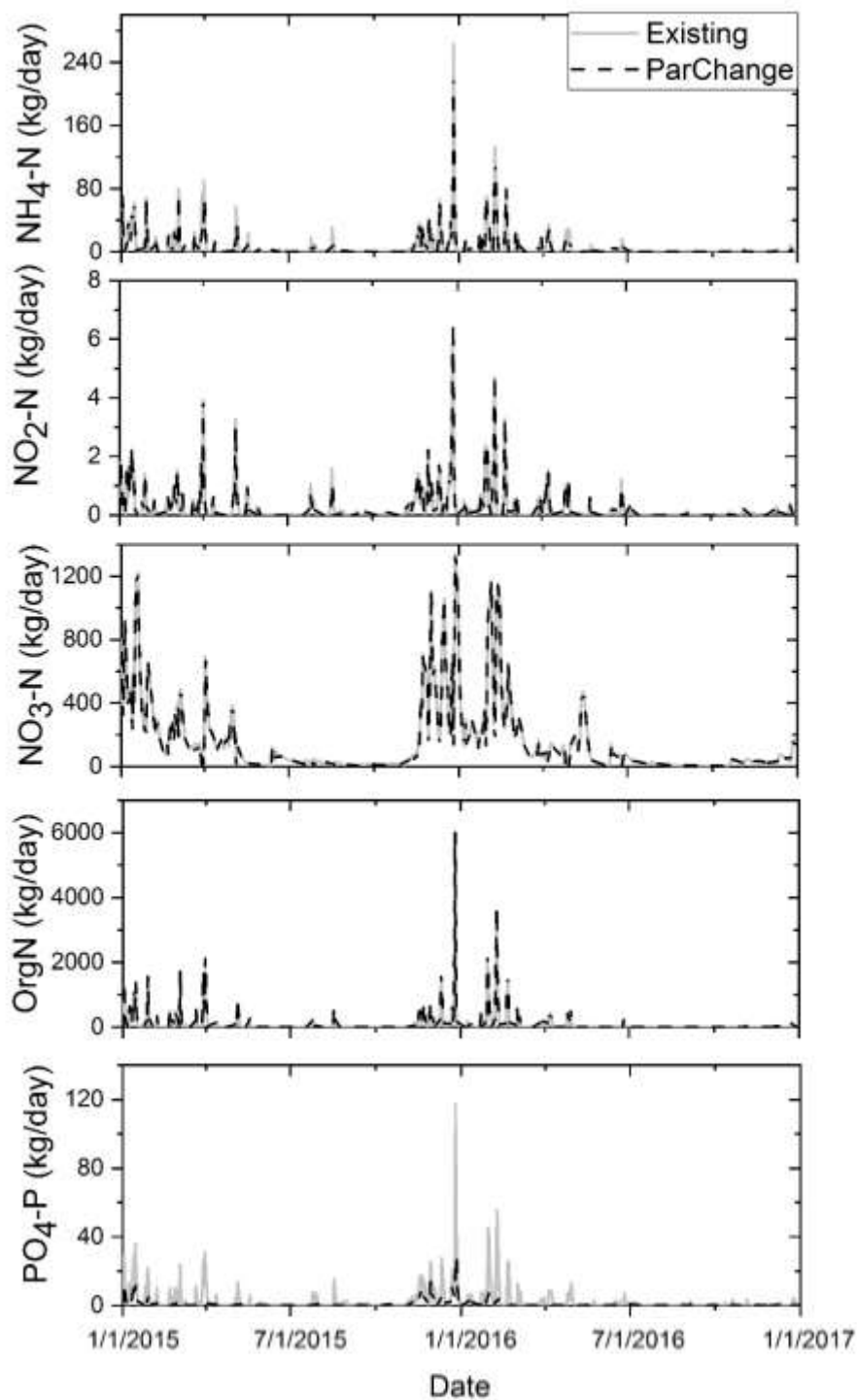


Figure C.2. Time series plots of NH<sub>4</sub>-N, NO<sub>2</sub>-N, NO<sub>3</sub>-N, Organic N and PO<sub>4</sub>-P loads during 2015-2016 simulated with calibrated SWAT model using default and new values of water quality parameters.

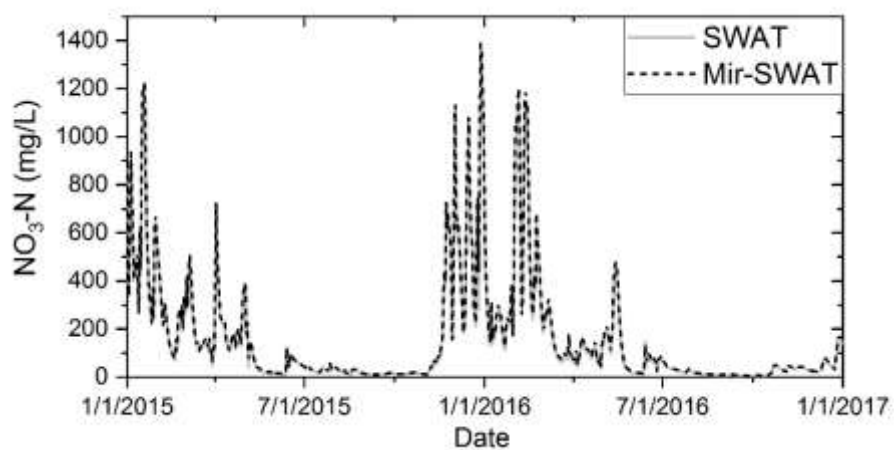


Figure C.3.  $\text{NO}_3\text{-N}$  loads at the watershed outlet with SWAT and Mir-SWAT model runs

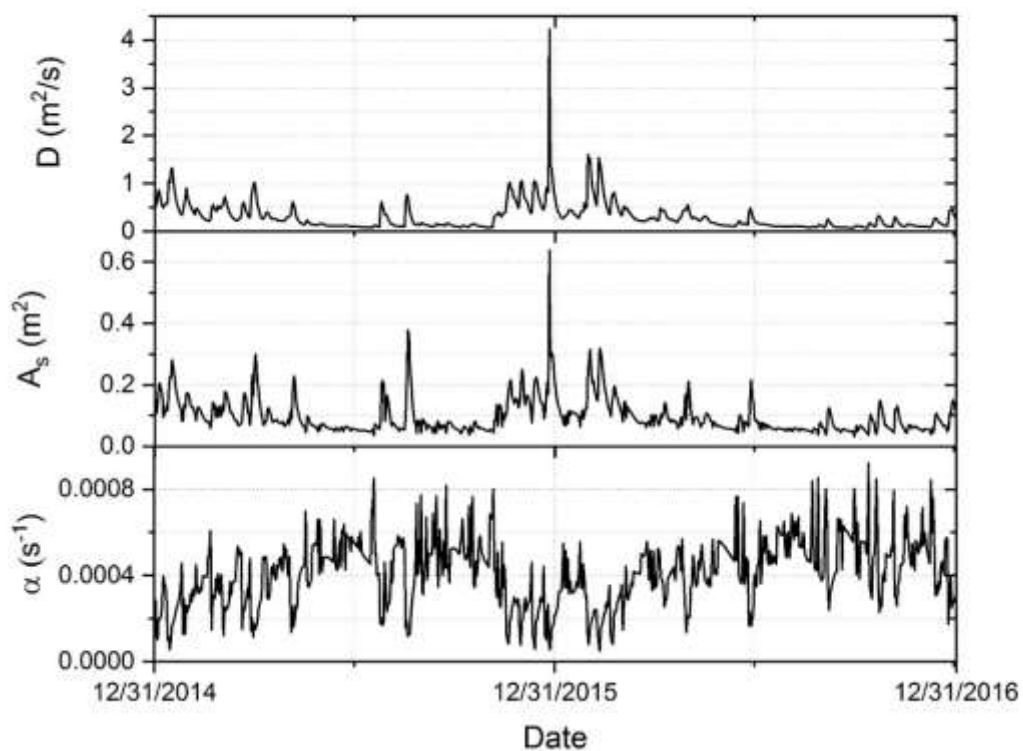


Figure C.4. Time series plots of dispersion coefficient ( $D$ ), storage zone area ( $A_s$ ) and storage exchange coefficient ( $\alpha$ ) in reach 1 of Kielstau SWAT model.









```

real :: orgpin, dispin, cbodin, disoxin, tday, wtmp
real :: algi, xx, yy, zz, ww, cinn, gg
real :: uu, vv, algcon, orgncon, nh3ncon, no2ncon, no3ncon
real :: orgpcon, solpcon, cbodcon, o2con, wrtot
real :: thgra = 1.047, thrho = 1.047, thrs1 = 1.024
real :: thrs2 = 1.074, thrs3 = 1.074, thrs4 = 1.024, thrs5 = 1.024
real :: thbc1 = 1.083, thbc2 = 1.047, thbc3 = 1.047, thbc4 = 1.047
real :: thrk1 = 1.047, thrk2 = 1.024, thrk3 = 1.024, thrk4 = 1.060
real :: area_chan, dispD, alpha, storAs, rchwid
real :: thetarhoq,thetars1,thetars2,thetars3,thetars4
real :: thetarhoq,thetark1,thetark2,thetark3,thetark4
real :: thetabc3,thetabc4

jrch = 0
jrch = inum1
dcoef= 3.
!!new matrix initializations
  dx = 100
  dt = 360
  if (vel_chan(jrch)>0.05) dt=60
  if (vel_chan(jrch)>0.8) dt=30

  ch_lr = int(ch_l2(jrch)*1000)
  if (ch_l2(jrch)<0.2) ch_lr=200
  tottim = 24*3600
  xet=int(2+ch_lr/dx)
  chl_int=(xet-1)*dx
  te = int(1 + tottim / dt)

  k = 1
  do ff = 0, chl_int, dx
    xmat(k) = ff
    k = k + 1
  end do

  k = 1
  do hh = 0, tottim, dt
    tmat(k) = hh
    k = k + 1
  end do

!! initialize water flowing into reach
wtrin = 0.
wtrin = varoute(2,inum2) * (1. - rnum1)

if (wtrin > 1.e-4) then

!! all water quality variables set to zero when no flow
algin = 0.0
chlin = 0.0
orgnin = 0.0
ammoin = 0.0
nitritin = 0.0
nitratin = 0.0
orgpin = 0.0
dispin = 0.0
cbodin = 0.0

```

```

disoxin = 0.0

if (wtrin > 0.001) then
  !! concentrations
  !! initialize inflow concentrations
  chlin = 1000. * varoute(13,inum2) * (1. - rnum1) / wtrin
  algin = 1000. * chlin / ai0      !! QUAL2E equation III-1
  orgnin = 1000. * varoute(4,inum2) * (1. - rnum1) / wtrin
  ammoin = 1000. * varoute(14,inum2) * (1. - rnum1) / wtrin
  nitritin = 1000. * varoute(15,inum2) * (1. - rnum1) / wtrin
  nitratin = 1000. * varoute(6,inum2) * (1. - rnum1) / wtrin
  orgpin = 1000. * varoute(5,inum2) * (1. - rnum1) / wtrin
  dispin = 1000. * varoute(7,inum2) * (1. - rnum1) / wtrin
  cbodin = 1000. * varoute(16,inum2) * (1. - rnum1) / wtrin
  disoxin = 1000. * varoute(17,inum2) * (1. - rnum1) / wtrin
end if

  !! initialize concentration of nutrient in reach
  wtrtot = 0.
  algcon = 0.
  orgncon = 0.
  nh3con = 0.
  no2con = 0.
  no3con = 0.
  orgpcon = 0.
  solpcon = 0.
  cbodcon = 0.
  o2con = 0.
  wtrtot = wtrin + rchwtr

if (curyr == 1.and. iida == 1) then
  rch_cbod(jrch) = amax1(1.e-6,rch_cbod(jrch))
  algcon = (algin * wtrin + algae(jrch) * rchwtr) / wtrtot
  orgncon = (orgnin * wtrin + organicn(jrch) * rchwtr) / wtrtot
  nh3ncon = (ammoin * wtrin + ammonian(jrch) * rchwtr) / wtrtot
  no2ncon = (nitritin * wtrin + nitriten(jrch) * rchwtr) / wtrtot
  no3ncon = (nitratin * wtrin + nitraten(jrch) * rchwtr) / wtrtot
  orgpcon = (orgpin * wtrin + organicp(jrch) * rchwtr) / wtrtot
  solpcon = (dispin * wtrin + disolvp(jrch) * rchwtr) / wtrtot
  cbodcon = (cbodin * wtrin + rch_cbod(jrch) * rchwtr) / wtrtot
  o2con = (disoxin * wtrin + rch_dox(jrch) * rchwtr) / wtrtot
  if (o2con.le.0.001) o2con=0.001
  if (o2con.gt.30.) o2con=30.
  if (orgncon < 1.e-6) orgncon = 0.0
  if (nh3con < 1.e-6) nh3con = 0.0
  if (no2con < 1.e-6) no2con = 0.0
  if (no3con < 1.e-6) no3con = 0.0
  if (orgpcon < 1.e-6) orgpcon = 0.0
  if (solpcon < 1.e-6) solpcon = 0.0
  if (cbodcon < 1.e-6) cbodcon = 0.0
  if (o2con < 1.e-6) o2con = 0.0

!!matrix assignment
  algmat = algcon
  o2mat = o2con
  cbodmat = cbodcon
  orgnmat = orgncon
  no3nmat = no3ncon

```

```

no2nmat = no2ncon
nh3nmat = nh3ncon
orgpmat = orgpcon
solpmat = solpcon
else

do gg=1,xet
  alpmat(gg,1:te)=(algin * wtrin + algaef(gg,jrch)*rchwtr)/wtrtot
  orgnmat(gg,1:te)=(orgnin*wtrin+organicnf(gg,jrch)*rchwtr)/wtrtot
  nh3nmat(gg,1:te)=(amoin*wtrin+ammonianf(gg,jrch)*rchwtr)/wtrtot
  no2nmat(gg,1:te)=(nitritin*wtrin+nitritenf(gg,jrch)*rchwtr)/wtrtot
  no3nmat(gg,1:te)=(nitratin*wtrin+nitratenf(gg,jrch)*rchwtr)/wtrtot
  orgpmat(gg,1:te)=(orgpin*wtrin+organicpf(gg,jrch)*rchwtr)/wtrtot
  solpmat(gg,1:te)=(dispin*wtrin+disolvpf(gg,jrch)*rchwtr)/wtrtot
  cbodmat(gg,1:te)=(cbodin*wtrin+rch_cbodf(gg,jrch)*rchwtr)/wtrtot
  o2mat(gg,1:te)=(disoxin*wtrin+rch_doxf(gg,jrch)*rchwtr) / wtrtot
end do
end if
  cscbod = cbodmat
  csorgn = orgnmat
  csorgp = orgpmat
  csalg = alpmat
  cso2 = o2mat
  csno3n = no3nmat
  csno2n = no2nmat
  csnh3n = nh3nmat
  cssolp = solpmat

!! calculate temperature in stream
  !! Stefan and Preudhomme. 1993. Stream temperature estimation
  !! from air temperature. Water Res. Bull. p. 27-45
  !! SWAT manual equation 2.3.13
  wtmp = 0.
  wtmp = 5.0 + 0.75 * tmpav(jrch)
  if (wtmp <= 0.) wtmp = 0.1

  !! calculate effective concentration of available nitrogen
  !! QUAL2E equation III-15
!!new equations for transient storage parameters
  area_chan = (wtrtot/(24*3600)) / vel_chan(jrch)
  rchwid = area_chan / rchdep
  dispD = 1.5 * vel_chan(jrch) * rchwid * (rchdep**0.5)
  storAs = 0.1*((rchwid*0.1+((wtrtot/(24*3600)) / rchdep))**1.2)
  alpha = 0.001 * vel_chan(jrch) / (rchwid * rchdep)
  write(*,'(3x,I2,a6,F5.3,a6,F5.3,a6,F5.2,a6,F5.2)') jrch,
  & 'vel:',vel_chan(jrch),'K:',dispD,'w:',rchwid,'d:',rchdep
!! calculate daylight average, photosynthetically active,
!! light intensity QUAL2E equation III-8
!! Light Averaging Option # 2
  algi = 0.
  if (dayl(hru1(jrch)) > 0.) then
    algi = hru_ra(hru1(jrch)) * tfact / dayl(hru1(jrch))
  else
    algi = 0.
  end if
!! calculate saturation concentration for dissolved oxygen
!! QUAL2E section 3.6.1 equation III-29
  ww = 0.

```

```

xx = 0.
yy = 0.
zz = 0.
ww = -139.34410 + (1.575701e05 / (wtmp + 273.15))
xx = 6.642308e07 / ((wtmp + 273.15)**2)
yy = 1.243800e10 / ((wtmp + 273.15)**3)
zz = 8.621949e11 / ((wtmp + 273.15)**4)
soxy = Exp(ww - xx + yy - zz)
if (soxy < 1.e-6) soxy = 0.
!! end initialize concentrations
thetarhoq=rhoq*(thrho**(wtmp-20))
thetars1=rs1(jrch)*(thrs1**(wtmp-20))
thetars2=rs2(jrch)*(thrs2**(wtmp-20))
thetars3=rs3(jrch)*(thrs3**(wtmp-20))
thetars4=rs4(jrch)*(thrs4**(wtmp-20))
thetars5=rs5(jrch)*(thrs5**(wtmp-20))
thetark1=rk1(jrch)*(thrk1**(wtmp-20))
thetark2=rk2(jrch)*(thrk2**(wtmp-20))
thetark3=rk3(jrch)*(thrk3**(wtmp-20))
thetark4=rk4(jrch)*(thrk4**(wtmp-20))
thetabc3=bc3(jrch)*(thbc3**(wtmp-20))
thetabc4=bc4(jrch)*(thbc4**(wtmp-20))

xs=xet-1
xp=xet-2
do j=1, te-1

!! calculate light extinction coefficient
!! (algal self shading) QUAL2E equation III-12
!! if (ai0 * algcon > 1.e-6) then
&
&   lambda(1:xp) = lambda0 + (lambda1 * ai0 *
&     algmat(2:xs,j)) + lambda2 *
&       (ai0 * algmat(2:xs,j)) ** (.66667)
!! calculate algal growth limitation factors for nitrogen
!! and phosphorus QUAL2E equations III-13 & III-14
&
&   fnn(1:xp)=(no3nmat(2:xs,j)+no2nmat(2:xs,j) + nh3nmat(2:xs,j)) /
&     ((no3nmat(2:xs,j) + no2nmat(2:xs,j) + nh3nmat(2:xs,j))+ k_n)
&   fpp(1:xp) = solpmat(2:xs,j) / (solpmat(2:xs,j) + k_p)

!! calculate growth attenuation factor for light, based on
!! daylight average light intensity QUAL2E equation III-7b
&
&   fl_1(1:xp) = (1. / (lambda(1:xp) * rchdep)) *
&     Log((k_l + algi) / (k_l + algi*(Exp(-1.*lambda(1:xp)*rchdep))))
&   fll(1:xp) = 0.92 * (dayl(hru1(jrch)) / 24.) * fl_1(1:xp)

!! calculcate local algal growth rate
  algra(1:xp) = mumax * fll(1:xp) * Min(fnn(1:xp), fpp(1:xp))
!! O2 impact calculations
  cordo(1:xp) = 1.0 - Exp(-0.6 * o2mat(2:xs,j))
  bc1mod(1:xp) = bc1(jrch) * cordo(1:xp)
  bc2mod(1:xp) = bc2(jrch) * cordo(1:xp)
!! end O2 impact calculations

!! calculate algal biomass concentration at end of day
!! (phytoplanktonic algae)

```

```

!! QUAL2E equation III-2
!algae(jrch) = 0.
algdt(1:xp) = (algra(1:xp)*(thgra**(wtmp-20)))* algmat(2:xs,j)-
& thetarhoq*algmat(2:xs,j)-(thetars1/rchdep)*algmat(2:xs,j)

!! oxygen calculations
!! calculate carbonaceous biological oxygen demand at end
!! of day QUAL2E section 3.5 equation III-26
!!deoxygenation rate

cboddt(1:xp)=-1*(thetark1*cbodmat(2:xs,j)-thetark3*cbodmat(2:xs,j))

!! calculate dissolved oxygen concentration if reach at
!! end of day QUAL2E section 3.6 equation III-28
o2dt(1:xp)=thetark2 * (soxy - o2mat(2:xs,j)) +
& (ai3*(algra(1:xp)*(thgra**(wtmp-20)))-ai4 *thetarhoq)*
& algmat(2:xs,j)-thetark1*cbodmat(2:xs,j)-thetark4/(rchdep*1000)-
& ai5 *(bc1mod(1:xp) *(thbc1**(wtmp-20))) * nh3nmat(2:xs,j) -
& ai6*(bc2mod(1:xp) * (thbc2**(wtmp-20))) * no2nmat(2:xs,j)

!! end oxygen calculations

!! nitrogen calculations
!! calculate organic N concentration at end of day
!! QUAL2E section 3.3.1 equation III-16
orgndt(1:xp)= ai1*thetarhoq*algmat(2:xs,j)-thetabc3*orgnmat(2:xs,j)-
& thetars4*orgnmat(2:xs,j)

!! calculate fraction of algal nitrogen uptake from ammonia
!! pool QUAL2E equation III-18
if (any(p_n*nh3nmat(2:xs,j)==0)) then
  nf1(1:xp)=0;
else
  nf1(1:xp)=(p_n*nh3nmat(2:xs,j))/(p_n*nh3nmat(2:xs,j)+
& (1-p_n)*no3nmat(2:xs,j));
end if
!! calculate ammonia nitrogen concentration at end of day
!! QUAL2E section 3.3.2 equation III-17

nh3ndt(1:xp)=thetabc3*orgnmat(2:xs,j)-(bc1mod(1:xp)*
& (thbc1**(wtmp-20)))*nh3nmat(2:xs,j)+thetars3/(rchdep*1000)-
& nf1(1:xp)*ai1*algmat(2:xs,j)*(algra(1:xp)*(thgra**(wtmp-20)))

!! calculate concentration of nitrite at end of day
!! QUAL2E section 3.3.3 equation III-19

no2ndt(1:xp)=(bc1mod(1:xp)*(thbc1**(wtmp-20)))*nh3nmat(2:xs,j)-
& (bc2mod(1:xp)*(thbc2**(wtmp-20))) * no2nmat(2:xs,j)

!! calculate nitrate concentration at end of day
!! QUAL2E section 3.3.4 equation III-20
no3ndt(1:xp)=(bc2mod(1:xp)*(thbc2**(wtmp-20)))* no2nmat(2:xs,j)-
& (1-nf1(1:xp))*ai1*algmat(2:xs,j)*(algra(1:xp)*(thgra**(wtmp-20)))

!! end nitrogen calculations

!! phosphorus calculations
!! calculate organic phosphorus concentration at end of

```

```

!! day QUAL2E section 3.3.6 equation III-24
orgpdt(1:xp) = ai2*thetarhoq*alpmat(2:xs,j)-thetabc4*orgpmat(2:xs,j)-
& thetars5*orgpmat(2:xs,j)

!! calculate dissolved phosphorus concentration at end
!! of day QUAL2E section 3.4.2 equation III-25

solpdt(1:xp) =thetabc4*orgpmat(2:xs,j)+(thetars2/(rchdep*1000))-
& ai2*(algra(1:xp)*(thgra**(wtmp-20)))*alpmat(2:xs,j)

!! end phosphorus calculations

!!STORAGE ZONE CALCULATIONS
!! Light extinction coefficient
lambda(1:xp) = lambda0 + (lambda1 * ai0 *
& csalg(2:xs,j)) + lambda2 *
& (ai0 * csalg(2:xs,j)) ** (.66667)

!! algal growth limitation factors
& fnn(1:xp) = (csno3n(2:xs,j) + csno2n(2:xs,j) + csnh3n(2:xs,j))/
((csno3n(2:xs,j) + csno2n(2:xs,j) + csnh3n(2:xs,j))+ k_n)
fpp(1:xp) = cssolp(2:xs,j) / (cssolp(2:xs,j) + k_p)
!! algal growth attenuation factor
& fl_1(1:xp) = (1. / (lambda(1:xp) * rchdep)) *
Log((k_l + algi)/(k_l + algi*(Exp(-1.*lambda(1:xp)*rchdep))))
fll(1:xp) = 0.92 * (dayl(hru1(jrch)) / 24.) * fl_1(1:xp)

algra(1:xp) = mumax * fll(1:xp) * Min(fnn(1:xp), fpp(1:xp))
cordo(1:xp) = 1.0 - Exp(-0.6 * cso2(2:xs,j))
bc1mod(1:xp) = bc1(jrch) * cordo(1:xp)
bc2mod(1:xp) = bc2(jrch) * cordo(1:xp)
!! calculate algal biomass concentration change
& algdt1(1:xp) = (algra(1:xp)*(thgra**(wtmp-20)))* csalg(2:xs,j)-
thetarhoq*csalg(2:xs,j)-(thetars1/rchdep)*csalg(2:xs,j)

!! calculate carbonaceous biological oxygen demand change
cboddt1(1:xp)=-1*(thetark1*cscbod(2:xs,j)-thetark3*cscbod(2:xs,j))

!! calculate dissolved oxygen concentration change
& o2dt1(1:xp)=thetark2 * (soxy - cso2(2:xs,j)) +
& (ai3 *(algra(1:xp)*(thgra**(wtmp-20)))-ai4 *thetarhoq)*
& csalg(2:xs,j)-thetark1*cscbod(2:xs,j) - thetark4/(rchdep*1000)-
& ai5 *(bc1mod(1:xp) *(thbc1**(wtmp-20))) * csnh3n(2:xs,j) -
& ai6*(bc2mod(1:xp) * (thbc2**(wtmp-20))) * csno2n(2:xs,j)

!! calculate organic N concentration change
& orgndt1(1:xp)= ai1*thetarhoq*csalg(2:xs,j)-thetabc3*csorgn(2:xs,j)-
thetars4*csorgn(2:xs,j)

!! calculate fraction of algal nitrogen uptake from ammonia

if (any(p_n*csnh3n(2:xs,j)==0)) then
  nf1(1:xp)=0;
else
  nf1(1:xp)=(p_n*csnh3n(2:xs,j))/(p_n*csnh3n(2:xs,j)+
& (1-p_n)*csno3n(2:xs,j));
end if

```

```

!! calculate ammonia nitrogen concentration change
nh3ndt1(1:xp) = thetabc3 * csorgn(2:xs,j)-(bc1mod(1:xp)*
& (thbc1**(wtmp-20)))*csnh3n(2:xs,j) + thetars3/(rchdep*1000)-
& nf1(1:xp)*ai1*csalg(2:xs,j)*(algra(1:xp)*(thgra**(wtmp-20)))

!! calculate nitrite concentration change
no2ndt1(1:xp)=(bc1mod(1:xp)*(thbc1**(wtmp-20)))*csnh3n(2:xs,j)-
& (bc2mod(1:xp)*(thbc2**(wtmp-20))) * csno2n(2:xs,j)

!! calculate nitrate concentration change
no3ndt1(1:xp)=(bc2mod(1:xp)*(thbc2**(wtmp-20)))*csno2n(2:xs,j)-
& (1-nf1(1:xp))*ai1*csalg(2:xs,j)*(algra(1:xp)*(thgra**(wtmp-20)))

!! calculate organic phosphorus concentration change
orgpdt1(1:xp) = ai2*thetarhoq*csalg(2:xs,j)-thetabc4*csorgp(2:xs,j)-
& thetars5*csorgp(2:xs,j)

!! calculate dissolved phosphorus concentration at end
solpdt1(1:xp) =thetabc4*csorgp(2:xs,j)+(thetars2/(rchdep*1000))-
& ai2*(algra(1:xp)*(thgra**(wtmp-20)))*csalg(2:xs,j)

```

#### !! Advection-Dispersion-Storage Calculations

```

alpmat(xet,j+1)=alpmat(xs,j)
o2mat(xet,j+1)=o2mat(xs,j)
cbodmat(xet,j+1)=cbodmat(xs,j)
orgnmat(xet,j+1)=orgnmat(xs,j)
no3nmat(xet,j+1)=no3nmat(xs,j)
no2nmat(xet,j+1)=no2nmat(xs,j)
nh3nmat(xet,j+1)=nh3nmat(xs,j)
orgpmat(xet,j+1)=orgpmat(xs,j)
solpmat(xet,j+1)=solpmat(xs,j)
no3nmat(xet,j+1)=no3nmat(xs,j)

csalg(xet,j+1)=csalg(xs,j)
cso2(xet,j+1)=cso2(xs,j)
cscbod(xet,j+1)=cscbod(xs,j)
csorgn(xet,j+1)=csorgn(xs,j)
csno3n(xet,j+1)=csno3n(xs,j)
csno2n(xet,j+1)=csno2n(xs,j)
csnh3n(xet,j+1)=csnh3n(xs,j)
csorgp(xet,j+1)=csorgp(xs,j)
cssolp(xet,j+1)=cssolp(xs,j)
csno3n(xet,j+1)=csno3n(xs,j)

csalg(2:xs,j+1)=(-1*alpha*area_chan/storAs)*(csalg(2:xs,j)-
& alpmat(2:xs,j))*dt+csalg(2:xs,j)+algdt1(1:xp)*dt/(24*3600)
cso2(2:xs,j+1)=(-1*alpha*area_chan/storAs)*(cso2(2:xs,j)-
& o2mat(2:xs,j))*dt+cso2(2:xs,j)+o2dt1(1:xp)*dt/(24*3600)
cscbod(2:xs,j+1)=(-1*alpha*area_chan/storAs)*(cscbod(2:xs,j)-
& cbodmat(2:xs,j))*dt+cscbod(2:xs,j)+cboddt1(1:xp)*dt/(24*3600)
csorgn(2:xs,j+1)=(-1*alpha*area_chan/storAs)*(csorgn(2:xs,j)-
& orgnmat(2:xs,j))*dt+csorgn(2:xs,j)+orgndt1(1:xp)*dt/(24*3600)
csno3n(2:xs,j+1)=(-1*alpha*area_chan/storAs)*(csno3n(2:xs,j)-
& no3nmat(2:xs,j))*dt+csno3n(2:xs,j)+no3ndt1(1:xp)*dt/(24*3600)
csno2n(2:xs,j+1)=(-1*alpha*area_chan/storAs)*(csno2n(2:xs,j)-
& no2nmat(2:xs,j))*dt+csno2n(2:xs,j)+no2ndt1(1:xp)*dt/(24*3600)
csnh3n(2:xs,j+1)=(-1*alpha*area_chan/storAs)*(csnh3n(2:xs,j)-
& nh3nmat(2:xs,j))*dt+csnh3n(2:xs,j)+nh3ndt1(1:xp)*dt/(24*3600)

```

```

csorgp(2:xs,j+1)=(-1*alpha*area_chan/storAs)*(csorgp(2:xs,j)-
& orgpmat(2:xs,j))*dt+csorgp(2:xs,j)+orgpdt1(1:xp)*dt/(24*3600)
& cssolp(2:xs,j+1)=(-1*alpha*area_chan/storAs)*(cssolp(2:xs,j)-
& solpmat(2:xs,j))*dt+cssolp(2:xs,j)+solpdt1(1:xp)*dt/(24*3600)

alpmat(2:xs,j+1)=(vel_chan(jrch)*dt/(2*dx)+dispD*dt/(dx**2))*
& alpmat(1:xp,j)+(1-2*dispD*dt/(dx**2))*alpmat(2:xs,j)+
& (-1*vel_chan(jrch)*dt/(2*dx) + dispD*dt/(dx**2))*alpmat(3:xet,j)+
& algdt(1:xp)*dt/(24*3600)+dt*alpha*(cscalg(2:xs,j)-alpmat(2:xs,j))
& o2mat(2:xs,j+1)=(vel_chan(jrch)*dt/(2*dx)+dispD*dt/(dx**2))*
& o2mat(1:xp,j)+(1-2*dispD*dt/(dx**2))*o2mat(2:xs,j)+
& (-1*vel_chan(jrch)*dt/(2*dx) + dispD*dt/(dx**2))*o2mat(3:xet,j)+
& o2dt(1:xp)*dt/(24*3600)+dt*alpha*(cso2(2:xs,j)-o2mat(2:xs,j))
& cbodmat(2:xs,j+1)=(vel_chan(jrch)*dt/(2*dx)+dispD*dt/(dx**2))*
& cbodmat(1:xp,j)+(1-2*dispD*dt/(dx**2))*cbodmat(2:xs,j)+
& (-1*vel_chan(jrch)*dt/(2*dx) + dispD*dt/(dx**2))*cbodmat(3:xet,j)+
& cboddt(1:xp)*dt/(24*3600)+dt*alpha*(cscbod(2:xs,j) -
& cbodmat(2:xs,j))
& orgnmat(2:xs,j+1)=(vel_chan(jrch)*dt/(2*dx)+dispD*dt/(dx**2))*
& orgnmat(1:xp,j)+(1-2*dispD*dt/(dx**2))*orgnmat(2:xs,j)+
& (-1*vel_chan(jrch)*dt/(2*dx) + dispD*dt/(dx**2))*orgnmat(3:xet,j)+
& orgndt(1:xp)*dt/(24*3600)+dt*alpha*(csorgn(2:xs,j) -
& orgnmat(2:xs,j))
& no3nmat(2:xs,j+1)=(vel_chan(jrch)*dt/(2*dx)+dispD*dt/(dx**2))*
& no3nmat(1:xp,j)+(1-2*dispD*dt/(dx**2))*no3nmat(2:xs,j)+
& (-1*vel_chan(jrch)*dt/(2*dx) + dispD*dt/(dx**2))*no3nmat(3:xet,j)+
& no3ndt(1:xp)*dt/(24*3600)+dt*alpha*(csno3n(2:xs,j) -
& no3nmat(2:xs,j))
& no2nmat(2:xs,j+1)=(vel_chan(jrch)*dt/(2*dx)+dispD*dt/(dx**2))*
& no2nmat(1:xp,j)+(1-2*dispD*dt/(dx**2))*no2nmat(2:xs,j)+
& (-1*vel_chan(jrch)*dt/(2*dx) + dispD*dt/(dx**2))*no2nmat(3:xet,j)+
& no2ndt(1:xp)*dt/(24*3600)+dt*alpha*(csno2n(2:xs,j) -
& no2nmat(2:xs,j))
& nh3nmat(2:xs,j+1)=(vel_chan(jrch)*dt/(2*dx)+dispD*dt/(dx**2))*
& nh3nmat(1:xp,j)+(1-2*dispD*dt/(dx**2))*nh3nmat(2:xs,j)+
& (-1*vel_chan(jrch)*dt/(2*dx) + dispD*dt/(dx**2))*nh3nmat(3:xet,j)+
& nh3ndt(1:xp)*dt/(24*3600)+dt*alpha*(csnh3n(2:xs,j) -
& nh3nmat(2:xs,j))
& orgpmat(2:xs,j+1)=(vel_chan(jrch)*dt/(2*dx)+dispD*dt/(dx**2))*
& orgpmat(1:xp,j)+(1-2*dispD*dt/(dx**2))*orgpmat(2:xs,j)+
& (-1*vel_chan(jrch)*dt/(2*dx) + dispD*dt/(dx**2))*orgpmat(3:xet,j)+
& orgpdt(1:xp)*dt/(24*3600)+dt*alpha*(csorgp(2:xs,j) -
& orgpmat(2:xs,j))
& solpmat(2:xs,j+1)=(vel_chan(jrch)*dt/(2*dx)+dispD*dt/(dx**2))*
& solpmat(1:xp,j)+(1-2*dispD*dt/(dx**2))*solpmat(2:xs,j)+
& (-1*vel_chan(jrch)*dt/(2*dx) + dispD*dt/(dx**2))*solpmat(3:xet,j)+
& solpdt(1:xp)*dt/(24*3600)+dt*alpha*(cssolp(2:xs,j) -
& solpmat(2:xs,j))

    if (iida==30.and. jrch==1) then
        if (j>59.and.j<181) then
            no3nmat(1,j+1)=((5*1)+no3nmat(1,j+1)*wtrtot/(24*3600))/
& (1+(wtrtot/(24*3600)))
            end if
        end if

chlormat(1:xet,:) = alpmat(1:xet,:) * ai0 / 1000.

```

```

where (algmtat < 1.e-6) algmtat = 0.0
where (o2mat < 1.e-6) o2mat = 0.0
where (cbodmat < 1.e-6) cbodmat = 0.0
where (orgnmat < 1.e-6) orgnmat = 0.0
where (no3nmat < 1.e-6) no3nmat = 0.0
where (no2nmat < 1.e-6) no2nmat = 0.0
where (nh3nmat < 1.e-6) nh3nmat = 0.0
where (orgpmat < 1.e-6) orgpmat = 0.0
where (solpmat < 1.e-6) solpmat = 0.0
where (csalg < 1.e-6) csalg = 0.0
where (cso2 < 1.e-6) cso2 = 0.0
where (cscbod < 1.e-6) cscbod = 0.0
where (csorgn < 1.e-6) csorgn = 0.0
where (csno3n < 1.e-6) csno3n = 0.0
where (csno2n < 1.e-6) csno2n = 0.0
where (csnh3n < 1.e-6) csnh3n = 0.0
where (csorgp < 1.e-6) csorgp = 0.0
where (cssolp < 1.e-6) cssolp = 0.0
algaef(1:xet,jrch) = algmtat(1:xet, te)
chloraef(1:xet,jrch) = chlormat(1:xet, te)
organicnf(1:xet,jrch) = orgnmat(1:xet, te)
ammonianf(1:xet,jrch) = nh3nmat(1:xet, te)
nitritenf(1:xet,jrch) = no2nmat(1:xet, te)
nitratenf(1:xet,jrch) = no3nmat(1:xet, te)
organicpf(1:xet,jrch) = orgpmat(1:xet, te)
disolvpf(1:xet,jrch) = solpmat(1:xet, te)
rch_cbodf(1:xet,jrch) = cbodmat(1:xet, te)
rch_doxf(1:xet,jrch) = o2mat(1:xet, te)

algaef(jrch) = algmtat(xet, te)
chlora(jrch) = chlormat(xet, te)
organicn(jrch) = orgnmat(xet, te)
ammonian(jrch) = nh3nmat(xet, te)
nitriten(jrch) = no2nmat(xet, te)
nitraten(jrch) = no3nmat(xet, te)
organicp(jrch) = orgpmat(xet, te)
disolvp(jrch) = solpmat(xet, te)
rch_cbod(jrch) = cbodmat(xet, te)
rch_dox(jrch) = o2mat(xet, te)
end do

else
! all water quality variables set to zero when no flow
algin = 0.0
chlin = 0.0
orgnin = 0.0
ammoin = 0.0
nitritin = 0.0
nitratin = 0.0
orgpin = 0.0
dispin = 0.0
cbodin = 0.0
disoxin = 0.0
algmtat = 0.0
o2mat = 0.0
cbodmat = 0.0
orgnmat = 0.0
no3nmat = 0.0

```

```
no2nmat = 0.0  
nh3nmat = 0.0  
orgpmat = 0.0  
solpmat = 0.0  
algae(jrch) = 0.0  
chlora(jrch) = 0.0  
organicn(jrch) = 0.0  
ammonian(jrch) = 0.0  
nitriten(jrch) = 0.0  
nitraten(jrch) = 0.0  
organicp(jrch) = 0.0  
disolvp(jrch) = 0.0  
rch_cbod(jrch) = 0.0  
rch_dox(jrch) = 0.0  
soxy = 0.0  
orgncon = 0.0  
end if  
return  
end
```